Doppler Effect: Analyses and Applications in Wireless Sensing and Communications

Lie-Liang Yang[1]

[1]Lie-Liang Yang is the professor of wireless communications, with the School of Electronics and Computer Science (ECS) in the University of Southampton, UK. This document is a chapter of my next book to be published. If you have any comments, please email: lly@ecs.soton.ac.uk, which is highly appreciated.

Abstract: This chapter is motivated by the need for a rigorous and comprehensive analysis of the Doppler effects encountered by electromagnetic and acoustic signals across a diverse spectrum of modern applications. These include land mobile communications, various Internet of Things (IoT) networks, machine-type communications (MTC), and various radar and satellite-based systems for navigation and sensing, as well as the emerging regime of integrated sensing and communications (ISAC). A wide array of kinematic profiles is investigated, ranging from uniform motion and constant acceleration to more complex general motion. Consequently, the multi-faceted factors influencing the Doppler shift are addressed in detail, encompassing classical kinematics, special and general relativity, atmospheric dynamics, and the properties of the propagation medium. This work is intended to establish a definitive theoretical foundation for both the general enthusiast and the specialized researcher seeking to master the complexities of signal frequency shifts in modern wireless sensing and communications systems.

Keywords: Wireless, acoustic, electromagnetic wave, communications, sensing, navigation, Doppler effect, Doppler shift, land mobile system, satellite system, kinematics, special relativity, general relativity, gravity, atmosphere, ionosphere, troposphere, integrated sensing and communications (ISAC), integrated space-air-ground networks (ISAGN)

Contents

0.1 Introduction

Traditionally, radar and wireless communications are operated in different frequency bands and implemented with different hardware platforms, resulting in the separation of their research and development. Correspondingly, in the majority of textbooks and research-oriented books in wireless communications, such as [1–9], to list a few, the principles of the Doppler effect are mainly presented in association with one to three scenarios. The first one is the non-relativistic uniform motion of signal source or/and receiver, which is the most common scenario considered. The second scenario is the relativistic uniform motion between source and receiver, which is often learned from physics classes. The third scenario is the non-relativistic uniform motion in medium like water. The fact is that, the practical scenarios generating Doppler effect are much richer and their analyses are also more challenging.

This was not an issue in the era when wireless communications was operated in relatively low frequency bands, such as sub-6GHz, and separated from radar, which may more generally be referred to as wireless sensing. This is because the design and operation of traditional wireless communication systems concern mostly about the maximum Doppler shift and Doppler spectrum experienced in a system. However, as wireless communications enter the era of information transmission in millimeter wave (mmWave), terahertz, and even optical bands, especially when communication and sensing functions are jointly implemented in the same system, the knowledge about Doppler effect at the ray level becomes increasingly critical. The reason behind is that in mmWave, terahertz and optical bands, the number of propagation paths from a transmitter to its aimed receiver is very limited, resulting in a sparse channel where signal rays conveyed over different paths are well separated in space and time. In this kind of channels, it is desirable that the Doppler effect experienced by individual rays can be estimated. Moreover, when sensing, such as velocity estimation of environmental moving objects, is implemented with communications, the Doppler shifts induced by the individual environmental objects need to be distinguished and estimated.

For example, in satellite navigation, there are various factors resulting in Doppler effect. The kinematics of satellite and ground device result in not only the classic Doppler shift but also the time-dilation induced Doppler shift. The difference of gravity potentials between satellite and ground device also induces time-dilation, adding another Doppler shift. Furthermore, a satellite navigation signal passing through the atmosphere experiences the path bending resulted from the density increasing air, the ion's dynamics resulted by solar flares, geomagnetic storms, etc., and many other random events, including wind, cloud, rain and varying-pressure. To achieve the most accurate sensing for the velocity of ground device, errors introduced by all the above-mentioned factors, except that by the device itself, must be corrected to a best level, which demands knowledge of the Doppler effects by these different factors.

To bridge this knowledge gap within the wireless communications field, this chapter provides a comprehensive analysis of the Doppler effect across a broad spectrum of scenarios. We transition from conventional models to modern wireless contexts, examining motions ranging from uniform to general, and cases from non-relativistic to relativistic regimes. The analysis further scales from individual Doppler events to the complex interplay of simultaneous multi-event phenomena. Given the movement towards integrated space-air-ground networks (ISAGN) [10–12], we also characterize the specific Doppler effects induced by the Earth's atmosphere. Furthermore, we explore two practical applications to demonstrate the utility of Doppler analysis in wireless sensing. Finally, a comparative study of the acoustic Doppler effect is presented, emphasizing its fundamental physical distinctions from the effects experienced by radio signals.

0.2 Theoretical Basis of the Doppler Effect

In physics, frequency is defined as the number of occurrences of a periodic, such as a harmonic, wave within a unit of time, typically in one second. In electromagnetic (EM) wave based communications, frequency can be measured in different ways, which can be explained from the basic EM wave functions. Specifically, a transverse electric wave propagating in z-direction while polarized in x-direction can be written as

$$\begin{aligned}\boldsymbol{E}_x(z,t) =& A\cos\left(\omega t-\kappa z\right)\boldsymbol{i}\\ =& A\cos\left(2\pi f t-\frac{2\pi}{\lambda}z\right)\boldsymbol{i}\\ =& A\cos\left(2\pi f t-\frac{2\pi}{cT}z\right)\boldsymbol{i}\end{aligned} \tag{1}$$

which is a function of both time t and position z. In (1), A is magnitude, $\boldsymbol{i}$ is a unit vector pointing in x-direction, $\omega = 2\pi f$ is angular frequency representing the rate of phase change with time t, $\kappa = 2\pi/\lambda$ is wave number representing the rate of phase change with distance z, f, λ and T are frequency, wavelength and period, respectively. The wave propagation speed in z-direction is

$$c = \lambda f \tag{2}$$

Furthermore, T and λ are connected via the formula $\lambda = cT$. Substituting it into (2) gives $f = 1/T$. Hence, (1) also has the form of

$$\boldsymbol{E}_x(z,t) = A\cos\left(2\pi ft - \frac{2\pi fz}{c}\right)\boldsymbol{i} \tag{3}$$

Note that in the above formulas, the constant c usually representing by fault the speed of light in vacuum free space is directly used. It will be continuously used in this way in this chapter, provided that it does not generate confusion. However, we should emphasize that most EM-wave based signals propagate in media, such as air, water, where the speed of wave propagation is smaller than the speed of light in vacuum. For example, the speed of light in vacuum is $c = 299,792,458$ meters per second (m/s), while the speed of EM waves, including light, in air is about $c' = 299,702,547$ m/s, giving a difference of about $89,911$ m/s. Hence, in the following contents, when distinction between the speed of wave in media and that in vacuum is needed, c' is used to indicate the speed of wave in media, while c is kept as the constant of speed of light in vacuum.

According to (1) and (3), to estimate frequency f, in addition to directly estimating f, we can instead estimate T. Furthermore, when c is given, we can estimate frequency f via estimating the wavelength λ.

Write the phase in (3) as

$$\phi(z,t) = 2\pi ft - \frac{2\pi fz}{c} \tag{4}$$

Then, f is also given by the formulas

$$f = \frac{1}{2\pi}\frac{\partial\phi(z,t)}{\partial t} = -\frac{c}{2\pi}\frac{\partial\phi(z,t)}{\partial z} \tag{5}$$

Hence, information about frequency f can be obtained via observing the phase change with respect to time or space.

Doppler effect accounts for the phenomenon - first described by an Austrian scientist Christian Doppler in the 19th century - that the wave frequency or period perceived by a receiver or an observer[1] is different from the frequency or period of source wave. Doppler effect occurs when wave source, where wave emits, and wave receiver (observer), where wave is measured, are in relative motion, or/and when the propagation environment between wave source and receiver, such as due to reflectors, is time-varying. For example, if a stationary observer stays at $z = r_0$, the phase of (4) is $\phi(r_0,t) = 2\pi ft - \frac{2\pi fr_0}{c}$ and the frequency f can be ideally recovered by the

[1]Receiver and observer may be alternatively used in the forthcoming analysis of Doppler effect without distinction. Also, transmitter and source may alternatively be used.

first equation in (5). If observer moves by following the equation $z = r_0 + vt$, where v is velocity, the phase varies according to

$$\phi(z,t) = 2\pi f t - \frac{2\pi f(r_0 + vt)}{c} \tag{6}$$

Then, the measured frequency by observer is

$$f' = \frac{1}{2\pi}\frac{\partial\phi(z,t)}{\partial t} = f - \frac{fv}{c} \tag{7}$$

Furthermore, if the motion of observer follows the equation $z = r_0 + v_0 t + \frac{1}{2}at^2$, where v_0 is initial velocity and constant a is acceleration, by following the steps of (6) and (7), we obtain

$$f(t) = f - \frac{f(v_0 + at)}{c} \tag{8}$$

which is time dependent. In both cases of (7) and (8), the frequency measured by observer is different from that emitted by source.

In general, let the geometric propagation path from transmitter to receiver be expressed as $P(t)$. Then, when without considering relativity, and when the propagation path length $r(t) = |P(t)|$ from transmitter via propagation environment to receiver is time-variant, then the frequency measured at the receiver follows the formulas

$$f' = f - \frac{f}{c} \times \frac{dr(t)}{dt} \tag{9a}$$

$$= f - \frac{1}{\lambda} \times \frac{dr(t)}{dt} \tag{9b}$$

$$= f - \frac{fv(t)}{c} \tag{9c}$$

where $v(t) = dr(t)/dt$ is the relative moving speed between transmitter and receiver.

Assume that source emits a harmonic wave within one uniform medium or in free space. Then, the level of Doppler effect can be reflected by either of the ratios expressed as

$$\frac{T}{T'}, \quad \frac{f'}{f} \tag{10}$$

where T and f are respectively the period and frequency of source emitted wave, and correspondingly, T' and f' are the perceived period and frequency by receiver. Hence, for convenience, T/T' and f'/f can either be referred to as the Doppler effect

factor (DEF) or simply Doppler effect. Furthermore,

$$f_D = f' - f \tag{11}$$

represents the direct measurement of the Doppler frequency shift, which is often referred to as Doppler frequency or Doppler shift for short. Following (9), we have the corresponding formulas for Doppler frequency represented as

$$f_D = -\frac{f}{c} \times \frac{dr(t)}{dt} \tag{12a}$$

$$= -\frac{1}{\lambda} \times \frac{dr(t)}{dt} \tag{12b}$$

$$= -\frac{fv(t)}{c} \tag{12c}$$

where positive $v(t) = dr(t)/dt$ explains that the length of propagation path from transmitter to receiver increases with time, hence resulting in negative Doppler shift.

From the above analysis we should emphasize that it is the time-varying distance, i.e., $r(t)$, of the propagation path, i.e., $P(t)$, from transmitter to receiver that generates the Doppler effect. If $r(t) = r_0$ is fixed, there is no Doppler effect. Otherwise, any phenomenas making $P(t)$, and hence $r(t)$, time-dependent generate Doppler effect. To reflect this, $P(t)$ is terminologically referred to as the *phase path* from transmitter to receiver. In further detail, a phase path from transmitter to receiver can be represented as $P(n,t)$ to account for both the physical signal propagation path, expressed as $\mathcal{P}(t)$, and the optical properties of propagation media on the path. Here, $n(p,t)$ is medium's refractive index, which may be a function of p of the points on $\mathcal{P}(t)$, and may also be time-variant. The reason for having such an expression of $P(n,t)$ can be explained with the aid of the z-relied component in (4). Specifically, when transmitting in the media with refractive index $n(t)$ that is independent of $\mathcal{P}(t)$, the phase contributed by this component is

$$-\frac{2\pi f r(t)}{c/n(t)} = -\frac{2\pi f n(t) r(t)}{c} = -\frac{2\pi f P(n,t)}{c} \tag{13}$$

where $c/n(t)$ is the phase velocity of wave in medium and $P(n,t) = n(t)r(t)$. Correspondingly, following (12), the Doppler frequency is

$$f_D = -\frac{f}{c}\frac{dP(n,t)}{dt} = -\frac{f}{c}\left[n(t)\frac{dr(t)}{dt} + r(t)\frac{dn(t)}{dt}\right] \tag{14}$$

demonstrating that Doppler effect may be generated by the dynamics of physical propagation path, propagation medium, or both.

In practice, the refractive index n is often correlated with the physical position

in medium. For example, when a satellites sends a radio signal to a ground station, the refractive index n experienced by a ray of signal increases in the propagation direction, as the result that the density of air increases. In this case, $P(n,t)$ should be represented as[2]

$$\begin{aligned} P(n,t) &= \lim_{\Delta p \to 0} \sum_{m=\text{Tx}}^{\text{Rx}} n(m\Delta p, t)\Delta p \\ &= \int_{\mathcal{P}(t)} n(p,t)dp \end{aligned} \tag{15}$$

where the integration is along the signal's propagation path $\mathcal{P}(t)$ from transmitter to receiver. Here, we should emphasize that the path $\mathcal{P}(t)$ is not necessary a straight line, but may bend due to refraction. Then, corresponding to (14),

$$f_D = -\frac{f}{c}\frac{dP(n,t)}{dt} = -\frac{f}{c}\frac{d}{dt}\int_{\mathcal{P}(t)} n(p,t)dp \tag{16}$$

We will return this issue in Section 0.6 when the Doppler effect by Earth's atmosphere is analyzed.

It is worth noting that although we have the formulas for deriving the Doppler effect from dr/dt, as seen in (9) and (12), or more generally, from dP/dt, as shown in (14) and (16), the results obtained in such ways for some cases may not be accurate. This is because dr/dt (or dP/dt) implies $dt \to 0$. However, Doppler effect is explained by the change of wave's period, which has the minimum time interval of T. Hence, unless T is indeed close to zero, the actual Doppler effect would appear difference from that predicted by applying dr/dt (or dP/dt). Generally, in principle, if $T \times dr/dt$ (or/and $T \times dP/dt$) is close to zero, the Doppler effect predicted from the dr/dt (or dP/dt) related formulas should provide sufficiently close approximation for the true Doppler effect.

Below we analyze the Doppler effects in some scenarios, when classic and relativistic kinematics, gravity, atmosphere, etc., are considered. The analysis mainly assumes EM waves, while the Doppler effect of acoustic waves is finally treated in Section 0.6.

Note that, in some motion scenarios, close zone and remote zone are distinguished. When receiver (or observer) falls in the remote zone of source, wave propagation is approximated to be in parallel, resulting in plane wave, and wave analysis does not involve explicitly the distance between source and receiver. By contrast, when receiver falls in the close zone of source, wave cannot be treated as plane wave but is spherical. In this case, the distance between source and receiver must be taken

[2] In (15), Tx and Rx are for transmitter (Tx) and receiver (Rx), respectively.

into account in wave analysis. Note furthermore that, close zone and remote zone can be divided according to the distance r between source and receiver relative to wavelength λ. For example, 3%-zoning means that in the close zone, $\lambda/r \geq 3\%$, and in the remote zone, $\lambda/r < 3\%$. As the results, when source and receiver are in each other's remote zones, their relative motion of one wavelength does not generate noticeable effect on the involved vectors, including moving velocity and the position vector of receiver referenced to source, or vice versa.

0.3 Doppler Effect in Uniform Motion

In this section, several methods for analyzing the Doppler effect are introduced by considering the simplest uniform motion between wave source and its receiver (observer). For clarity of explanation, a unit vector, $\hat{\boldsymbol{r}}$, is defined to point in the direction from source to receiver, the velocity of source or receiver is $\boldsymbol{v} = v\hat{\boldsymbol{v}}$, where $\hat{\boldsymbol{v}}$ is a unit vector in the direction of $\boldsymbol{v}$ and v is the magnitude, i.e., speed. Furthermore, the angle between $\hat{\boldsymbol{r}}$ and $\hat{\boldsymbol{v}}$ is expressed as θ, governed by the relation of

$$\cos\theta = \hat{\boldsymbol{r}} \cdot \hat{\boldsymbol{v}},\ 0 \leq \theta < \pi \tag{17}$$

where $\cdot$ is inner product operation.

Note that, when considering Doppler effect, a wave source may be the communication transmitter or a scatter (reflector) in communication channel. Similarly, a wave receiver may be the communication receiver or a scatter (reflector) in communication channel.

Also note that in the analysis of classic Doppler effect, a rest reference frame, in addition to transmitter and receiver, is implied, which can usually be the medium, such as air, water, in which wave propagates. The motion states of transmitter, receiver or objects in environments are defined relative to this rest frame.

0.3.1 Non-Relativistic Doppler Effect in Remote Zones

0.3.1.1 Stationary Source and Moving Receiver

First, assume that wave source is stationary and receiver is moving with velocity $\boldsymbol{v}$, as shown in Fig. 1(a). Consider that source emits two adjacent maxima (wave crests) at $t_1 = t_0$ and $t_2 = t_0 + T$. Correspondingly, the receiver receives two maxima at $t_1' = t_0'$ and $t_2' = t_0' + T'$. During T' of a period of received wave, the distance travelled by receiver in $\hat{\boldsymbol{r}}$ direction, which is wave's propagation direction, is given

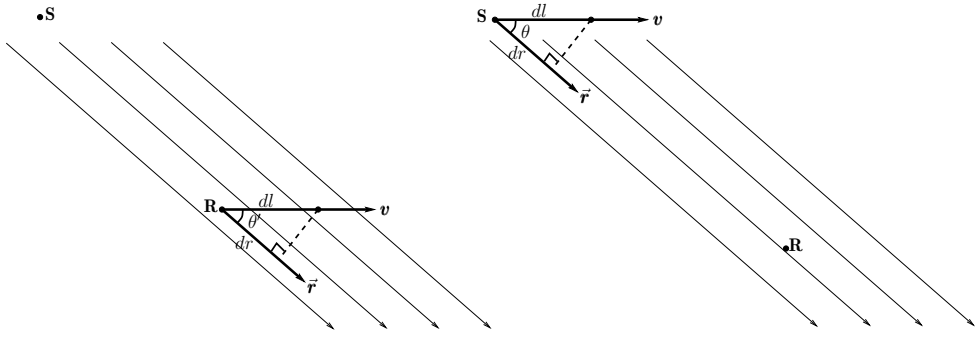

(a) Stationary source, moving receiver (b) Moving source, stationary receiver

Figure 1: A plane wave generated by a remote-zone static (or moving) source is received by a moving (or static) receiver.

by $dr = (\boldsymbol{v} \cdot \hat{\boldsymbol{r}})T' = v\cos\theta' T'$. Hence, the period of received wave satisfies

$$T' = t_2' - t_1' = T + \frac{dr}{c} = T + \frac{v\cos\theta' T'}{c} \tag{18}$$

making

$$\frac{T}{T'} = 1 - \frac{v\cos\theta'}{c} \tag{19}$$

and the received wave frequency and wavelength be

$$f' = f\left(1 - \frac{v\cos\theta'}{c}\right) \tag{20}$$

$$\lambda' = \lambda\left(1 - \frac{v\cos\theta'}{c}\right)^{-1} \tag{21}$$

respectively. (21) is obtained under the constraint of $c = f'\lambda' = f\lambda$. Accordingly, the Doppler shift is

$$f_D(v, \theta') = -\frac{fv\cos\theta'}{c} = -\frac{v\cos\theta'}{\lambda} \tag{22}$$

As shown in Fig. 1(a), when receiver moves away from source, $0 \le \theta < \pi/2$, the received frequency is lower than the source emitted frequency. Otherwise, if receiver moves towards source, $\pi/2 \le \theta < \pi$, the received frequency is increased by a Doppler shift.

0.3.1.2 Moving Source and Stationary Receiver

In the case that the wave source is moving and receiver is stationary, as shown in Fig. 1(b), let us again assume that source emits two adjacent maxima at $t_1 = t_0$ and $t_2 = t_0 + T$. Correspondingly, the receiver observes two maxima at $t_1' = t_0'$ and $t_2' = t_0' + T'$. As the source moves towards the receiver by a distance of $dr = v\cos\theta T$ during the period of T, T' satisfies

$$T' = T - \frac{dr}{c} = T\left(1 - \frac{v\cos\theta}{c}\right) \tag{23}$$

Accordingly, we have the formulas

$$\frac{T}{T'} = \left(1 - \frac{v\cos\theta}{c}\right)^{-1} \tag{24}$$

$$f' = f\left(1 - \frac{v\cos\theta}{c}\right)^{-1} \tag{25}$$

$$\lambda' = \lambda\left(1 - \frac{v\cos\theta}{c}\right) \tag{26}$$

The Doppler shift is

$$f_D(v,\theta) = f' - f = f\left(\frac{\frac{v\cos\theta}{c}}{1 - \frac{v\cos\theta}{c}}\right) \tag{27a}$$

$$\approx \frac{fv\cos\theta}{c} = \frac{v\cos\theta}{\lambda} \tag{27b}$$

where the approximation is hold, when $v << c$. Notice from Fig. 1(b) that $0 \leq \theta < \pi/2$ idicates source moving towards receiver, while $\pi/2 \leq \theta < \pi$ is the situation of source moving away from receiver.

When comparing (19) - (22) with (24) - (27), we can see that the Doppler effect in the case of moving source stationary receiver and that of stationary source moving receiver are not exactly the same on the received wave. In other words, the Doppler effects are asymmetric. While the Doppler shift is linearly related to the moving speed of receiver, it is non-linearly dependent on the moving speed of source. The Doppler effects due to moving source and receiver become the same, only when $v << c$. Otherwise, source moving towards receiver strengthens the Dopper effect due to $1 - \frac{v\cos\theta}{c} < 1$ in (27), and source moving away from receiver weakens the Doppler effect, as the result of $1 - \frac{v\cos\theta}{c} > 1$ in (27).

Example 1. *Assume that two imaginary children, S and R, are playing ball catching. Relative to ground, assume that S is stationary and stands at the origin, while R is*

running away from S at a speed of $v = 5$ m/s. The horizontal flying speed of ball is $c = 10$ m/s. Two balls are throwing with an interval of $T = 1$ second. At the time when the first ball is thrown at $t = 0$, R is $d = 30$ meters away from S. Find the interval T' between the two catches in the cases:

A) S is throwing the ball to R.

B) R is trowing the ball to S.

Solution. *A) In this case, the arrival time of the first ball follows $ct'_1 = d + vt'_1$, from which we obtain $t'_1 = 6$ second. The arrival time of the second ball follows $c(t'_2 - 1) = d + vt'_2$, from which we obtain $t'_2 = 8$ second. Hence, the interval between the two catches of R is $T' = t'_2 - t'_1 = 2$ seconds.*

B) In this case, the first ball arrives at $t'_1 = d/c = 3$ second. After $T = 1$ second, R moves away from S by $1v = 5$ meters and throws the second ball. Hence, the second ball needs to fly $d + 5 = 35$ meters, and arrives at S at $t'_2 = 35/10 + 1 = 4.5$ second. Therefore, the interval between the two catches of S is $T' = t'_2 - t'_1 = 1.5$ seconds.

Similarly, let us consider an example where balls are replaced by EM waves. The results are obtained directly from the formulas derived so far. Furthermore, instead of considering time intervals - which can be explained as periods - the resulted frequencies are aimed.

Example 2. *Consider a rocket escaping or approaching the Earth at a velocity of about 12 km/s communicates with a ground station on the 10 GHz x-band. Assume that the radio wave propagation is in line with the line connecting the rocket and ground station. Find the Doppler frequencies in the following cases.*

A) When rocket is escaping the Earth, the Doppler shift on the signal sent by rocket and received by ground station, and the Doppler shift on the signal sent by ground station and received by rocket.

B) When rocket is approaching the Earth, the Doppler shift on the signal sent by rocket and received by ground station, and the Doppler shift on the signal sent by ground station and received by rocket.

Solution. *A) When rocker is escaping the Earth, the Doppler shift on the signal sent by rocket and received by ground station is calculated from* (27a)*, giving $f_{D,RG} = -399984$ KHz. The Doppler shift on the signal sent by ground station and received by rocket is calculated by* (22)*, giving $f_{D,GR} = -400000$ Hz.*

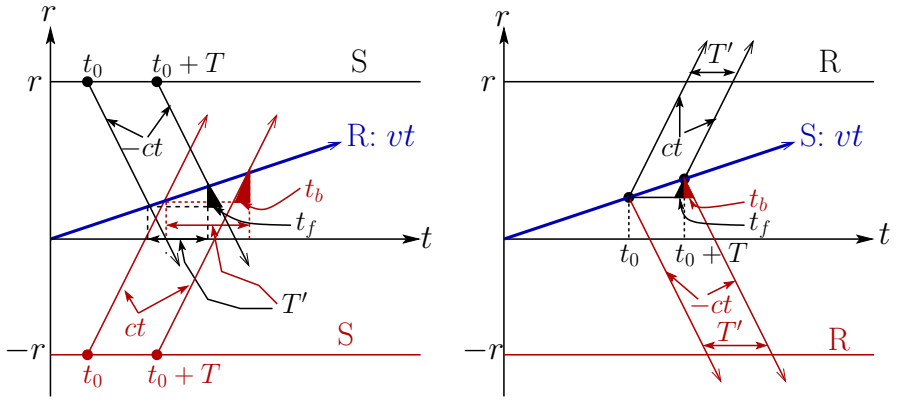

(a) Stationary Source, Moving Receiver (b) Moving Source, Stationary Receiver

Figure 2: Graphic explanation of the Doppler effect occurred in remote zones. S=Source, R=Receiver.

B) When a rocket approaching the Earth, the Doppler shift on the signal sent by rocket and received by ground station is calculated by (27a)*, which is* $f_{D,RG} = 400016$ *Hz, while the Doppler shift on the signal sent by ground station and received by rocket is obtained from* (22)*, yielding* $f_{D,GR} = 400000$ *Hz.*

As shown in Example 2, in both cases, the Doppler shift is dependent on whether source (receiver) are moving (stationary) or stationary (moving). They also show that the differences are small, even when the moving speed is as high as 12 km/s at the Earth escaping speed. The reason is that relative to c, the speed of light, this speed is still very small, the ratio is only about $v/c = 1.112 \times 10^{-8}$. Hence, in most practical cases, the formula $f_D = fv\cos\theta/c$ can be applied, regardless of moving source stationary receiver, or stationary source moving receiver, or other relative motion.

0.3.1.3 Geometric Analysis of Doppler Effect

Now an alternative geometric method [13–17] is introduced to derive the formulas obtained in the two cases as above-considered, i.e., the case of stationary source moving receiver and the case of moving source stationary receiver. For simplicity, we analyze only the longitudinal Doppler effect. This involves assuming that the source and receiver move purely along the line connecting them. Mathematically, this means that the angle between the velocity vector and the propagation vector is $0°$ or $180°$. For the general non-longitudinal case, one must use the velocity component projected onto the line of sight, i.e., replacing the scalar speed v with $\boldsymbol{v} \cdot \hat{\boldsymbol{r}}$.

The Doppler effect in the above-analyzed two cases can be analyzed with the aid of graphic drawings, as shown in Fig. 2, where Fig. 2(a) is for the case that source is stationary and receiver is moving, while Fig. 2(b) corresponds to the case that receiver is stationary and source is moving. In Fig. 2, r is distance: positive r indicates that source (or receiver) moves towards receiver (or source), while negative r means that source (or receiver) moves away from receiver (or source). Then, from Fig. 2(a) - upper part - and considering that receiver moves towards source, from the geometry, we have

$$T' = T - t_f = T - \frac{v(T' + t'_0) - vt'_0}{c} = T - \frac{vT'}{c} \tag{28}$$

yielding

$$\frac{T}{T'} = 1 + \frac{v}{c} \quad \text{or} \quad f' = f\left(1 + \frac{v}{c}\right) \tag{29}$$

which is (19) or (20) with $\cos\theta = -1$. When receiver moves away from source, from Fig. 2(a) - lower part, we have the relationship of

$$T' = T + t_b = T + \frac{v(t'_0 + T') - vt'_0}{c} = T + \frac{vT'}{c} \tag{30}$$

Therefore, we obtain

$$\frac{T}{T'} = 1 - \frac{v}{c} \quad \text{or} \quad f' = f\left(1 - \frac{v}{c}\right) \tag{31}$$

which is (19) or (20) with $\cos\theta = 1$.

When considering Fig. 2(b) - upper part, if source moves towards receiver, as shown in the drawing, T' and T satisfy the relation of

$$T' = T - t_f = T - \frac{v(t_0 + T) - vt_0}{c} = T - \frac{vT}{c} \tag{32}$$

Hence,

$$\frac{T}{T'} = \left(1 - \frac{v}{c}\right)^{-1} \quad \text{or} \quad f' = f\left(1 - \frac{v}{c}\right)^{-1} \tag{33}$$

Otherwise, when source moves away from receiver, as seen in Fig. 2(b) - lower part, T' and T are related by

$$T' = T + t_b = T + \frac{v(t_0 + T) - vt_0}{c} = T + \frac{vT}{c} \tag{34}$$

Accordingly,

$$\frac{T}{T'} = \left(1 + \frac{v}{c}\right)^{-1} \quad \text{or} \quad f' = f\left(1 + \frac{v}{c}\right)^{-1} \tag{35}$$

Explicitly, (33) and (35) are the same as (24) with $\cos\theta = 1$ and -1, respectively.

0.3.1.4 Moving Source and Moving Receiver

A more general case where both source and receiver are moving (relative to a fixed reference frame) can be analyzed as follows. Assume that source's moving velocity is v, the angle between which and $\hat{\boldsymbol{r}}$ is θ. Assume that receiver's moving velocity is v', the angle between which and $\hat{\boldsymbol{r}}$ is θ'. Assume that the wave transmitted by source has two adjacent crests occurring at $t_1 = t_0$ and $t_2 = t_0 + T$. Correspondingly, the crests in the received wave occur at $t_1' = t_0'$ and $t_2' = t_0' + T'$. During $T = t_2 - t_1$, source moves towards receiver by a distance $dr = v\cos\theta T$. During $T' = t_2' - t_1'$, receiver moves away from source by a distance $dr' = v'\cos\theta' T'$. Hence, T' and T have the relationship of

$$T' = T - \frac{v\cos\theta T}{c} + \frac{v'\cos\theta' T'}{c} \tag{36}$$

Re-arranging them gives

$$\frac{T}{T'} = \frac{1 - \dfrac{v'\cos\theta'}{c}}{1 - \dfrac{v\cos\theta}{c}} \tag{37}$$

Explicitly, when $v = 0$, (37) is reduced to (19) of the case of source stationary and reciver moving. When $v' = 0$, (37) is reduced to (24) of the case of source moving

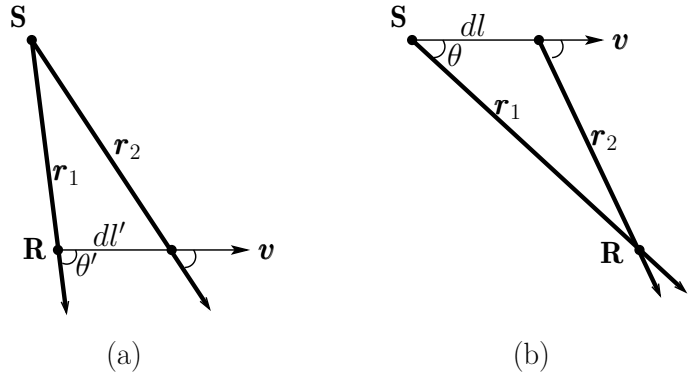

Figure 3: A source sends radio signals to a receiver in its close-zone: (a) stationary source and moving receiver, (b) moving source and stationary receiver.

while reciver stationary. From (37), the other related formulas are

$$f' = f\left(\frac{1-\frac{v'\cos\theta'}{c}}{1-\frac{v\cos\theta}{c}}\right) \tag{38}$$

$$\begin{aligned} f_D(v,v',\theta,\theta') =& f'-f \\ =& f\left(\frac{\frac{v\cos\theta}{c}-\frac{v'\cos\theta'}{c}}{1-\frac{v\cos\theta}{c}}\right) \\ \approx& f\left(\frac{v\cos\theta}{c}-\frac{v'\cos\theta'}{c}\right) \end{aligned} \tag{39}$$

0.3.2 Non-Relativistic Doppler Effect in Close Zones

When source and receiver fall in the close zone, spherical wave has to be considered. Fig. 3 illustrates the two cases of stationary souce and moving receiver (Fig. 3(a)), and moving source and stationary receiver (Fig. 3(b)). Let us first analyze the case of Fig. 3(a).

Assume that source emits two adjacent wave crests at $t_1 = t_0$ and $t_2 = t_0 + T$. Correspondingly, receiver measures the first wave crest at $t_1' = t_0'$, and the second wave crest at $t_2' = t_0' + T'$. As shown in Fig. 3(a), during $T' = t_2' - t_1'$, receiver moves in $\hat{\boldsymbol{v}}$-direction a distance of $dl' = vT'$. The position vectors of receiver with respect to source at t_1' and t_2' are denoted as $\boldsymbol{r}_1$ and $\boldsymbol{r}_2$, respectively. The angle between $\boldsymbol{v}$ and the position vector $\boldsymbol{r}_1$ is represented as θ'. Express $\boldsymbol{r}_i = r_i\hat{\boldsymbol{r}}_i$, $i = 1, 2$, where r_i

is the distance between source and receiver. Then, with the aid of the cosine rule,

$$\begin{aligned} dr = r_2 - r_1 =& \sqrt{r_1^2 + (dl')^2 - 2r_1 dl' \cos(\pi - \theta')} - r_1 \\ =& \sqrt{r_1^2 + (vT')^2 + 2r_1 vT' \cos(\theta')} - r_1 \end{aligned} \tag{40}$$

Therefore, T' and T have the relation of

$$\begin{aligned} T' =& T + \frac{dr}{c} \\ =& T + \frac{\sqrt{r_1^2 + (vT')^2 + 2r_1 vT' \cos(\theta')} - r_1}{c} \end{aligned} \tag{41}$$

which can be re-arranged to obtain an quadratic equation

$$a_0 T'^2 + a_1 T' + a_2 = 0 \tag{42}$$

with

$$\begin{aligned} a_0 =& c^2 - v^2 \\ a_1 =& -2(c\lambda - cr_1 + vr_1 \cos\theta') \\ a_2 =& \lambda^2 - 2\lambda r_1 \end{aligned}$$

where $\lambda = cT$. The closed-form solution to (42) is[3]

$$\begin{aligned} T' =& \frac{-a_1 + \sqrt{a_1^2 - 4a_0 a_2}}{2a_0} \\ =& \frac{c\lambda - cr_1 + vr_1 \cos\theta' + \sqrt{(c\lambda - cr_1 + vr_1 \cos\theta')^2 - (c^2 - v^2)(\lambda^2 - 2\lambda r_1)}}{c^2 - v^2} \end{aligned} \tag{43}$$

which is a function of r_1 - the distance between source and receiver at t_0', in addition to its dependance on $v \cos\theta'$.

[3]Note that the second solution to (42) has no practical meaning.

Here are three special cases corresponding to $\theta' = 0^o$, $\theta' = 90^o$ and $\theta' = 180^o$:

$$T'(0^o) = T\left(1 - \frac{v}{c}\right)^{-1} \tag{44a}$$

$$T'(90^o) = \frac{c\lambda - cr_1 + \sqrt{(c\lambda - cr_1)^2 - (c^2 - v^2)(\lambda^2 - 2\lambda r_1)}}{c^2 - v^2} = \frac{c^2T - cr_1 + \sqrt{(c^2T - cr_1)^2 - (c^2 - v^2)(c^2T^2 - 2cTr_1)}}{c^2 - v^2} \tag{44b}$$

$$T'(180^o) = T\left(1 + \frac{v}{c}\right)^{-1} \tag{44c}$$

Equation (44a) is the same as (19) with $\theta' = 0^o$, (44c) is the same as (19) with $\theta' = 180^o$. Hence, when receiver moves in the direction or opposite direction of the position vector from source to receiver, there is no distinction between close- and remote zones. In contrast, when $\theta' = 90^o$, the Doppler effect in remote-zone is zero, while that in close-zone is non-zero, as shown in (44b).

Notice that (41) can be written as

$$T' = T + \frac{(r_1 + vT')\sqrt{1 - \dfrac{2r_1vT'(1 - \cos\theta')}{(r_1 + vT')^2}} - r_1}{c} \tag{45}$$

If the first-order Taylor expansion is used to approximate the square-root term, an approximation to (45) is

$$T' \approx T + \frac{v^2T'^2 + r_1v\cos\theta'T'}{c(r_1 + vT')} \tag{46}$$

From (46), we obtain

$$\frac{f'}{f} = \frac{T}{T'} \approx 1 - \frac{v^2T' + r_1v\cos\theta'}{c(r_1 + vT')} = 1 - \frac{vdl'/r_1 + v\cos\theta'}{c(1 + dl'/r_1)} \tag{47}$$

Explicitly, if $r_1 >> vT' = dl'$, implying that source and receiver are in remote zone, (47) becomes (19).

Note that (47) can be computed by receiver, as it knows its velocity v and the distance dl' it travels in a duration of T', in addition to r_1 and θ'.

In the context of the scenario where source is moving and receiver is stationary, and they are in the close zone of each other, based on Fig. 3(b), applying the cosine

rule gives

$$\begin{aligned} r_2 =& \sqrt{r_1^2 + dl^2 - 2r_1 dl\cos\theta} \\ =& \sqrt{r_1^2 + v^2T^2 - 2r_1 vT\cos\theta} \end{aligned} \tag{48}$$

Hence,

$$T' = T + \frac{\sqrt{r_1^2 + v^2T^2 - 2r_1 vT\cos\theta} - r_1}{c} \tag{49}$$

which is dependent on r_1 of the distance between source and receiver at t_0.

For $\theta = 0^o,\ 90^o$ and 180^o,

$$T'(0^o) = T\left(1 - \frac{v}{c}\right) \tag{50a}$$

$$T'(90^o) = T + \frac{\sqrt{r_1^2 + v^2T^2} - r_1}{c} \tag{50b}$$

$$T'(180^o) = T\left(1 + \frac{v}{c}\right) \tag{50c}$$

Again, (50a) is the same as (23) with $\theta' = 0^\circ$, (50c) is the same as (23) with $\theta' = 180^\circ$. In these two cases, there is no distinction between close and remote zone. However, when $\theta = 90^\circ$, the Doppler effect in remote zone is zero, while that in close zone is non-zero, as shown in (44b).

Notice from (44b) and (50b) that T' converges to T when r_1 increases, meaning that, when the moving direction is perpendicular to the line connecting source and receiver, the Doppler effect becomes weaker, as the distance between source and receiver increases.

From (49), after neglecting $-r_1$, an approximation of

$$\frac{f'}{f} = \frac{T}{T'} \approx \left(1 + \frac{\sqrt{v^2 + (fr_1)^2 - 2vfr_1\cos\theta}}{c}\right)^{-1} \tag{51}$$

can be obtained. Reader can show that when assuming $c >> fr_1 >> v$, (51) reduces to (23).

Note that, to use (51) to sense the velocity of source, receiver requires to first know the moving direction of source relative to $\boldsymbol{r}_1$.

Let us now extend the above two special cases to a more general case where source moves at velocity $\boldsymbol{v}$ and receiver moves at velocity $\boldsymbol{v}'$. Assume at reference time $t_0 = 0$ that the position vectors of source and receiver are $\boldsymbol{r}_0$ and $\boldsymbol{r}'_0$, respectively. All position vectors are relative to the origin of the considered coordinate

system. Then, at time t,

$$\begin{aligned} \boldsymbol{r}(t) =& \boldsymbol{r}_0 + \boldsymbol{v}t \\ \boldsymbol{r}'(t) =& \boldsymbol{r}'_0 + \boldsymbol{v}'t \end{aligned} \tag{52}$$

Again, assume that source emits two adjacent wave crests at $t_1 = t_0$ and $t_2 = t_0 + T$. Accordingly, the position vectors are registered as $\boldsymbol{r}(t_0)$ and $\boldsymbol{r}(t_0 + T)$, respectively. Corresponding to the two crests emitted, assume that receiver observes the first wave crest at $t'_1 = t'_0$ and the second wave crest at $t'_2 = t'_0 + T'$, and the position vectors are $\boldsymbol{r}'(t'_0)$ and $\boldsymbol{r}'(t'_0 + T')$. Then, the Doppler effect can be retrieved from the relationship of

$$T' = T + \frac{\|\boldsymbol{r}'(t'_0 + T') - \boldsymbol{r}(t_0 + T)\| - \|\boldsymbol{r}'(t'_0) - \boldsymbol{r}(t_0)\|}{c} \tag{53}$$

where $\|\boldsymbol{r}'(t'_0) - \boldsymbol{r}(t_0)\|$ is the distance between source at t_0 and receiver at t'_0, while $\|\boldsymbol{r}'(t'_0 + T') - \boldsymbol{r}(t_0 + T)\|$ is the distance between source at $t_0 + T$ and receiver at $t'_0 + T'$, both of which can be derived once the velocities and the initial position vectors are known.

Remark 1. *From previous analysis and, in particular* (53)*, we can conceive that for communications, the Doppler related issues are relatively easy to deal with. Typically, in communications, the signal processing at transmitter and/or at receiver may need to address the challenges generated by the Doppler effect. However, in both cases, only the Doppler shift itself or its statistics is needed, regardless of the dynamics of transmitter, receiver and communication channels, although the Doppler effect is actually generated by these dynamics.*

By contrast, the Doppler effect in sensing applications is highly challenging. The objective of sensing is to derive the dynamics of transmitter, receiver and/or environments via the measurements of Doppler shifts at observers. While it is not difficult to find the Doppler effect based on (53) *by imposing appropriate assumptions, it may be extremely involved to find the mechanical quantities based on the measured Doppler effects at observers. For example, as seen in Fig. 3(b), while receiver may easily obtain the Doppler shift via measuring the change of its received frequency, it is very challenging to derive the velocity of source, as to achieve this, it also needs the knowledge of* r_1*,* r_2*,* dl*, as well as* θ*.*

0.3.3 Relativistic Doppler Effect

The *special theory of relativity* is based on two postulates proposed by Albert Einstein in 1950, which are stated as [18]:

1) The laws of physics are the same in all inertial reference frames;

2) The speed of light in free space has the same value c in all inertial reference frames.

Related to Doppler effect, the consequences of the special theory of relativity are time dilation and the effect on the analysis of Doppler shift. In this section, the Doppler effect is analyzed on the constraint of the above two postulates by Einstein. For further explanation of the special theory of relativity, the interested reader is referred to references, including [18–21].

Note that, starting from now on and when EM wave is considered, we will mainly state a receiver as an observer to follow the term widely used in description of the special/general theory of relativity. Furthermore, for simplicity of presentation, the following constant and variables are defined:

- c: speed of light in free space.
- c': speed of light in medium.
- $\boldsymbol{v}$ and $\boldsymbol{v}'$: velocity vectors of source and observer, $|\boldsymbol{v}|$ and $|\boldsymbol{v}'|$ represent speed of source or observer moving. Note that, $\boldsymbol{v}$ is always used if there is only one velocity involved.
- $\hat{\boldsymbol{r}}$ and $\hat{\boldsymbol{r}}'$: unit position vector pointing in the direction from observer to source, and unit position vector pointing in the direction from source to observer.
- $v = \boldsymbol{v} \cdot \hat{\boldsymbol{r}}$ and $v' = \boldsymbol{v}' \cdot \hat{\boldsymbol{r}}'$: velocity components on the line connecting source and observer. Note that, v is always used if there is only one velocity involved. Positive v is for moving away from each other and negative v is for moving towards each other.

Remark 2. *In the following formulas, only v or v' appears for accounting of the classic Doppler effect generated by relative motion. More general-form formulas can be obtained by replacing v with $\boldsymbol{v} \cdot \hat{\boldsymbol{r}}$ or $v' = \boldsymbol{v}' \cdot \hat{\boldsymbol{r}}'$. Note also that in the analysis of relativistic Doppler effect, it is the magnitude of $\boldsymbol{v}$, i.e., $|\boldsymbol{v}|$, that generates time dilation, not v, the speed along the line connecting source with observer. Additionally, unless specified, source and observer are assumed in each other's remote zone.*

The analysis of relativistic Doppler effect may be found in any textbook on modern physics, including in [19, 20], where the special theory of relativity is addressed. However, in most textbooks, only the longitudinal Doppler effect is analyzed, which assumes that the moving direction aligns with the line connecting source and observer, resulting in that the speed $|\boldsymbol{v}|$ generating time dilation and the speed $|v = \boldsymbol{v} \cdot \hat{\boldsymbol{r}}|$, which generates the (classic) Doppler effect[4], are equal, i.e, $|\boldsymbol{v}| = |\boldsymbol{v} \cdot \hat{\boldsymbol{r}}|$. Explicitly,

[4]To distinguish the Doppler effect generated in classic way and that by other effect due to special and general relativities, in following description, the phrase of '(classic) Doppler effect' is used to indicate the Doppler effect generated in classic way to avoid confusion.

this is not necessary true and, in fact, they are not the same in many practical scenarios. Furthermore, in most textbooks, the relativistic Doppler effect is analyzed in free space, without including propagation medium. Therefore, in this section, the longitudinal Doppler effect is first analyzed by following textbooks. Then, the analysis is generalized to consider: a) $|\boldsymbol{v}\cdot\hat{\boldsymbol{r}}|\neq|\boldsymbol{v}|$, and b) EM wave propagates in medium.

0.3.3.1 Longitudinal Relativistic Doppler Effect

Consider that in a free space, a system includes a source emitting EM-wave signals to an observer. The relative velocity between source and observer is v, the direction of which aligns with the line connecting them. This system involves two reference frames, the reference frame of source and the reference frame of observer. To analyze the Doppler effect, three sets of times, periods and frequencies are defined. The first set includes the proper time t, proper period T and proper frequency f at the source in the reference frame of source. The second set includes the proper time t', proper period T' and proper frequency f' at the observer in the reference frame of observer. The third set includes the time t'', period T'' and the frequency f'' either in the reference frame of source or in the reference frame of observer, depending on which of them is considered. This should become clear in the forthcoming analysis.

First, let us analyze the Doppler effect in the observer's reference frame. In this case, time t'', period T'' and frequency f'' are associated with source but in the reference frame of observer. Also, source's moving velocity is v relative to observer. Assume that in the reference frame of observer, source emits two adjacent wave crests at $t_1''=t_0''$ and $t_2''=t_0''+T''$. Then, following the analysis in Section 0.3.1, first, T' and T'' follow the relation of

$$T'=T''+\frac{vT''}{c}=T''\left(1+\frac{v}{c}\right) \tag{54}$$

which tributes to the (classic) Doppler effect. Second, since in the reference frame of observer, source is moving at a velocity v, its clock ticks slower than the clock in the reference frame of observer, yielding

$$T''=\frac{1}{\sqrt{1-v^2/c^2}}T \tag{55}$$

where $1/\sqrt{1-v^2/c^2}$ is the time dilation factor or Lorentz factor [20]. Substituting

this into (54) gives

$$\frac{f'}{f} = \frac{T}{T'} = \frac{\sqrt{1 - v^2/c^2}}{1 + v/c} = \sqrt{\frac{1 - v/c}{1 + v/c}} \tag{56}$$

or

$$f' = f \times \frac{\sqrt{1 - v^2/c^2}}{1 + v/c} \tag{57a}$$

$$= f \times \sqrt{\frac{1 - v/c}{1 + v/c}} \tag{57b}$$

Now let us turn to derive the Doppler effect in the reference frame of source. Under this assumption, time t'', period T'' and frequency f'' are associated with observer in the reference frame of source. Relative to source, observer's moving velocity is v. Accordingly, T and T'' are related by the formula

$$T'' = T + \frac{vT''}{c} \tag{58}$$

giving

$$T = T'' \left(1 - \frac{v}{c}\right) \tag{59}$$

Since in the source's reference frame, observer is moving at a velocity v. According the Lorentz transformation [20],

$$T'' = \gamma T' = \frac{1}{\sqrt{1 - v^2/c^2}} T' \tag{60}$$

Substituting it into (59) and after some arrangement, the Doppler effect can be obtained as

$$f' = f \times \frac{1 - v/c}{\sqrt{1 - v^2/c^2}} \tag{61a}$$

$$= f \times \sqrt{\frac{1 - v/c}{1 + v/c}} \tag{61b}$$

Equations (57b) and (61b) show that the Doppler effect formula derived in view of source and that in view of observer are the same, fully agreeing with the postulates

by Einstein. In fact, in the free space where two objects experience relative motion, any object can only observe that the other one is moving. Hence, to observer, it is always the case that source is moving, and the signals received from source experience both time dilation and (classic) Doppler effect. In other words, to analyze the relativistic Doppler effect in free space, it is sufficient to consider the scenario of source moving observer stationary.

Remark 3. *In the analysis of the classic Doppler effect in Section 0.3.1, two different formulas are obtained respectively for the cases of source rest observer moving and source moving observer rest, which are* (29)*/*(31)*, and* (33)*/*(35) *for moving towards or away from each other. Since* $c >> v$ *in most applications, one may attempt to get an approximate formula for application in both cases. One way to reach this objective is first multiplying* (29) *with* (33) *in the case of moving towards each other, or multiplying* (31) *with* (35) *in the case of moving away from each other, and then taking the square-root on both sides of the resulted equations. After integrating the* $+$ *and* $-$ *signs explaining moving states into* v*, these operations result in the formula*

$$f' = f \times \sqrt{\frac{1 - v/c}{1 + v/c}} \tag{62}$$

However, it is surprise to see that this formula is exactly the one in (57b)*, or* (61b)*, derived under the constraints of the special theory of relativity [19, 20], with both time dilation and classic Doppler effect included. This is in fact not a coincidence, but the consequence of the special theory of relativity. The time dilation effect inherent in special relativity precisely bridges the gap between the two asymmetric classical scenarios, forcing a symmetric outcome that is accurately captured by their geometric mean. This can also be illustrated by multiplying* (57a) *with* (61a) *and taking the square-root of the product, giving*

$$f' = f \times \sqrt{\frac{\sqrt{1 - v^2/c^2}}{1 + v/c} \times \frac{1 - v/c}{\sqrt{1 - v^2/c^2}}} \tag{63a}$$

$$= f \times \sqrt{\frac{1 - v/c}{1 + v/c}} \tag{63b}$$

It is shown in (63a) *that the time dilation factors yielded by the two reference frames are ideally cancelled, leaving only the asymmetric (classic) Doppler effects viewing respectively from the two reference frames.*

Example 3. *Considering the situations and assumptions in Example 2, find the relativistic Doppler shifts, respectively, when rocket is moving towards or moving away from the Earth.*

Solution. *When the rocket is moving towards the Earth, the Doppler shift* $f_D = f' - f$ *can be found from* (57b) *with* $v = -12$ *km/s, giving* $f_D = 400008$ *Hz.*

When the rocket is moving away from the Earth, the Doppler shift can be found from (57b) *with* $v = 12$ *km/s, which is* $f_D = -399992$ *Hz.*

Comparing the results in Example 3 with the corresponding results in Example 2 tells that the time dilation in Example 3 has only very light effect on the Doppler shift, even when the rocket flies at the Earth escaping speed.

0.3.3.2 Relativistic Doppler Effect in Uniform Medium

We now generalize the previous analysis, expanding the context from the longitudinal free space scenario to more general cases. This generalization involves two aspects.

First, considering that most EM waves propagate in media in practical applications - such as wireless communications, optical communications, and radar sensing, to name a few - the analysis is extended to include wave propagation media. Accordingly, the wave propagation speed is expressed as c' to distinguish it from c, the speed of light in a vacuum.

Second, in the longitudinal scenario, the velocity that generates time dilation is the same as the velocity that generates the (classic) Doppler effect. However, in general cases, these two velocities can be different. Hence, the previous analysis is also generalized to encompass this situation. The speed responsible for time dilation is denoted as $|\boldsymbol{v}|$, the magnitude of the velocity vector $\boldsymbol{v}$, while the speed responsible for the (classic) Doppler effect is expressed as v (or v'), which is positive when source and observer move away from each other and negative when they move towards each other.

Moving Source and Rest Observer:

Consider a system that involves three reference frames, the reference frame of source, the reference frame of observer and the reference frame of medium. The motion states of source and observer are relative to the medium. Assume that a source moving at a velocity $\boldsymbol{v}$ sends EM signals via a propagation medium to a rest observer. The wave propagation speed in medium is denoted as c'. The velocity along the line connecting source with observer is expressed as v. Again, to analyze the Doppler effect, three sets of times, periods and frequencies are defined. The first set is associated with source, expressed as t, T and f, the second set is associated with observer, denoted as t', T' and f', and finally, the third set is associated with the medium, expressed as t'', T'' and f''.

Assume that source in its reference frame emits two adjacent wave crests at time $t_1 = t_0$ and $t_2 = t_0 + T$. Due to the time dilation, the clock resting in the frame

of medium ticks faster than the clock resting in the reference frame of source. According to [18, 19], in the reference frame of media, source emits two adjacent wave crests at time $t_1'' = t_0''$ and $t_2'' = t_0'' + T''$, where T'' is related to T by the Lorentz transformation [20]

$$T'' = \frac{1}{\sqrt{1 - |\boldsymbol{v}|^2/c^2}} T \tag{64}$$

The distance source travelled during T'' is $dr = vT''$. Accordingly, the observer resting in the frame of medium measures two adjacent crests at time $t_1' = t_0'$ and $t_2' = t_0' + T'$ in its reference frame, which is the same as the medium's frame. Hence, T' and T'' have the relation of

$$T' = T'' + \frac{vT''}{c'} = T'' \left(1 + \frac{v}{c'}\right) \tag{65}$$

Substituting (64) into (65) gives

$$T' = T \frac{1 + v/c'}{\sqrt{1 - |\boldsymbol{v}|^2/c^2}} \tag{66}$$

from which

$$f' = f \times \left(\frac{\sqrt{1 - |\boldsymbol{v}|^2/c^2}}{1 + v/c'} \right) \tag{67}$$

Eq.(67) is the generalized formula for the relativistic Doppler effect, which has rarely seen in textbooks, such as, [18–20]. In addition to including propagation media, this generalized formula allows the velocity component generating (classic) Doppler effect and the velocity accounting for time dilation to be different.

Example 4. *Consider that a station fixed on the Earth is receiving EM signals from a spaceship directly above the station and flying over with a velocity $\boldsymbol{v}$. Explain its resulted Doppler effect.*

Solution. *As in the considered case $\boldsymbol{v}$ is perpendicular to the line connecting spaceship and station, $v = 0$, there is no (classic) Doppler effect. However, the time dilation coefficient $\gamma = 1/\sqrt{1 - |\boldsymbol{v}|^2/c^2}$ in* (67) *results in $f' < f$, making the received signals by the station experience red-shift.*

In (67), if $c' = c$ and $v = \pm|\boldsymbol{v}|$, it reduced to (57b), the relativistic Doppler effect in the longitudinal scenario.

Rest Source and Moving Observer:

When source rests and observer moves in the reference frame of medium, time dilation occurs from observer's frame to medium's frame. Hence, we let t'', T'' and f'' represent the observed time, period and frequency of the received signals by observer in the reference frame of medium. Assume that source emits two adjacent wave crests at time $t_1 = t_0$ and $t_2 = t_0 + T$. Correspondingly, in the reference frame of medium, observer receives these two adjacent wave crests at time $t''_1 = t''_0$ and $t''_2 = t''_0 + T''$. Considering that observer moves a distance of $dr = vT''$ during T'' in the reference frame of medium, the relationship of

$$T'' = T + \frac{vT''}{c'} \tag{68}$$

holds. Arranging it gives

$$T = T'' \left(1 - \frac{v}{c'}\right) \tag{69}$$

Since observer is moving relative to the frame of medium, the clock in medium's frame ticks faster than the clock in observer's frame. Hence, the Lorentz transformation gives

$$T'' = \frac{T'}{\sqrt{1 - |\boldsymbol{v}|^2/c^2}} \tag{70}$$

Substituting it into (68) and applying $T' = 1/f'$ and $T = 1/f$, we obtain

$$f' = f \times \left(\frac{1 - v/c'}{\sqrt{1 - |\boldsymbol{v}|^2/c^2}}\right) \tag{71}$$

Comparing (67) with (71) explains that, when EM waves propagate in media, the Doppler effect resulted from moving source stationary observer and that resulted from stationary source moving observer are different and, hence, asymmetric. Furthermore, even in free space, if $v \neq |\boldsymbol{v}|$, the above two Doppler effects are asymmetric. As demonstrated by the results shown in Example 4 and the following Example 5.

Example 5. *Following Example 4, consider that a spaceship directly above a station fixed on the Earth flies over the station with a velocity $\boldsymbol{v}$, and is receiving signals from the station. Explain its resulted Doppler effect.*

Solution. *Again, $v = 0$ and hence there is no (classic) Doppler effect. However, from* (71)*, the time dilation makes $f' > f$, making the received signals by spaceship experience blue-shift.*

Again, if $c' = c$ and $v = |\boldsymbol{v}|$, (71) and (67) become the same formula of (57b),

and hence, the relativistic Doppler effects are symmetric.

Moving Source and Moving Observer:

Assume that, along the line connecting source and observer, source moves at velocity v and observer moves at velocity v'. Accordingly, their velocities are $\boldsymbol{v}$ and $\boldsymbol{v}'$. All velocities are relative to the reference frame of medium. Assume that in source's reference frame, source emitted two adjacent wave crests at $t_1 = t_0$ and $t_2 = t_0 + T$. These time instants become $t_1'' = t_0''$ and $t_2'' = t_0'' + T''$ in medium's reference frame. Hence, we have

$$T'' = \frac{T}{\sqrt{1 - |\boldsymbol{v}|^2/c^2}} \tag{72}$$

In medium's reference frame, source moves a distance $dr = vT''$ during a period T''.

In medium's reference frame, observer receives the two crests at $t_1^* = t_0^*$ and $t_2^* = t_0^* + T^*$, and during T^*, observer moves a distance $dr' = v'T^*$. Hence, T^* is related to T'' by

$$T^* = T'' + \frac{dr + dr'}{c'} = T'' + \frac{vT'' + v'T^*}{c'} \tag{73}$$

Rearranging it gives

$$T^* \left(1 - \frac{v'}{c'}\right) = T'' \left(1 + \frac{v}{c'}\right) \tag{74}$$

As observer moves at v' ($\boldsymbol{v}'$) relative to medium, T^* is related to T' by

$$T^* = \frac{T'}{\sqrt{1 - |\boldsymbol{v'}|^2/c^2}} \tag{75}$$

Finally, substituting (72) and (75) into (74), the Doppler effect follows an expression of

$$f' = f \times \left(\frac{1 - v'/c'}{1 + v/c'}\right) \times \left(\frac{\sqrt{1 - |\boldsymbol{v}|^2/c^2}}{\sqrt{1 - |\boldsymbol{v'}|^2/c^2}}\right) \tag{76}$$

Notice that (76) is a general formula of Doppler effect in uniform motion, which includes all the formulas derived so far for the Doppler effect in this section, except only those in close zone. First, it is straightforward to reduce (76) to the formulas for the classic Doppler effect considered in Section 0.3.1. Second, by setting $v' = 0$ or $v = 0$, the formula is reduced to that obtained above in this section for the case of

source moving observer rest or the case of source rest observer moving. Third, if we set $v = |\boldsymbol{v}|$, $v' = |\boldsymbol{v}'|$, $c = c'$ and assume free space, whether is the formula returned to the form of (61b) - the longitudinal relativistic Doppler effect that is only relied on the relative speed between source and observer. The answer is confirmative, as detailed now.

When $v = |\boldsymbol{v}|$, $v' = |\boldsymbol{v}'|$ and $c = c'$, it can be readily analyzed to obtain

$$f' = f \times \sqrt{\frac{1 - v/c - v'/c + vv'/c^2}{1 + v/c + v'/c + vv'/c^2}} \tag{77}$$

In the square-root, dividing both the numerator and denominator by $1 + vv'/c^2$ yields

$$f' = f \times \sqrt{\frac{1 - \dfrac{1}{c} \cdot \dfrac{v + v'}{1 + vv'/c^2}}{1 + \dfrac{1}{c} \cdot \dfrac{v + v'}{1 + vv'/c^2}}} \tag{78}$$

Define

$$u = \frac{v + v'}{1 + vv'/c^2} \tag{79}$$

which is the relative speed between source and observer, obtained by the addition of v and v' under the special relativity. Then, (78) becomes

$$f' = f \times \sqrt{\frac{1 - u/c}{1 + u/c}} \tag{80}$$

which is (61b) for the longitudinal relativistic Doppler effect, when the relative speed between source and observer is u.

0.4 Doppler Effect in General Motion

In this section, non-relativistic Doppler-effect in general motion is analyzed in Section 0.4.1 and relativistic Doppler-effect in general motion is addressed in Section 0.4.2.

0.4.1 Non-relativistic Doppler Effect in General Motion

In this section, the non-relativistic Doppler effect, or (classic) Doppler effect, in general motion is analyzed. First, the Doppler effect is analyzed when source or observer,

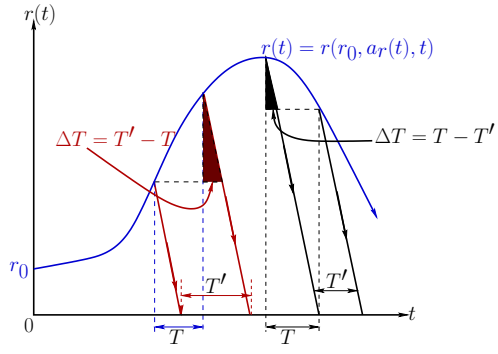

Figure 4: Graphic representation of the Doppler effect in general motion.

or both are in general motion. Then, the Doppler effects in several special scenarios are analyzed.

0.4.1.1 General Motiving Source and Stationary Observer

Assume that source has the distance equation expressed as $r(t)$ with respect to an observer. For example, it may be represented as

$$r(t) = r(r_0, a_r(t), t) \tag{81}$$

which, in addition to time, is a function of the initial distance r_0 and the acceleration $a_r(t)$, which may also be a time-dependent function. For example, $r(t)$ may have a function as shown in Fig. 4, which assumes that an observer seats at the origin.

Based on (12b), we can immediately have a formula for the Doppler shift as

$$f_D(t) \approx -\frac{1}{\lambda}\frac{dr(t)}{dt} = -\frac{1}{\lambda}\left[\frac{\partial r(t)}{\partial t} + \frac{\partial r(t)}{\partial a_r(t)} \times \frac{d(a(t))}{dt}\right] \tag{82}$$

However, as mentioned with (12b), the formula obtained from (82) is only an approximation. Below we derive the accurate formula for the Doppler effect based on the graphic representation [15, 16], as shown, for example, in Fig. 4.

As shown in Fig. 4, it is assumed that source has a distance equation with respect to observer expressed as $r(t)$. First, consider the case when source moves away from observer, as shown by the left-side scenario in Fig. 4. When assuming that source sends two adjacent maxima (crests) at time instants of $t_1 = t$ and $t_2 = t + T$, from

the graph, we can readily know that the period of received signal by observer is [16]

$$T'(t) = T + \frac{1}{c}\left[r(t+T) - r(t)\right] \tag{83}$$

where $T'(t)$ is surely time-dependent if there is acceleration.

In the case that source moves towards observer, as shown by the right-side scenario in Fig. 4, it can be shown that the period of received signal by observer has the same expression of (83).

From (83), the Doppler frequency-shift can be derived to be

$$\begin{aligned} f'(t) =& \frac{f}{1 + \frac{1}{cT}\left[r(t+T) - r(t)\right]} && \text{(84a)} \\ \approx& f\left(1 - \frac{1}{cT}\left[r(t+T) - r(t)\right]\right) \\ f_D(t) =& -\frac{f'(t)}{c} \times \frac{1}{T}\left[r(t+T) - r(t)\right] && \text{(84b)} \\ \approx& -\frac{f}{c} \times \frac{1}{T}\left[r(t+T) - r(t)\right] && \text{(84c)} \end{aligned}$$

where $f'(t) = 1/T'(t)$, $f = 1/T$ and $f_D(t) = f'(t) - f$. The approximations require that $\left(\left[r(t+T) - r(t)\right]/cT\right)^2$ is ignorable. Explicitly, $\bar{v}(t) = \left[r(t+T) - r(t)\right]/T$ is the average speed over one period T of source relative to observer. Accordingly, (84a) and (84b) can be represented as

$$\begin{aligned} f'(t) =& \frac{f}{1 + \frac{\bar{v}(t)}{c}} && \text{(85a)} \\ f_D(t) =& -\frac{f\bar{v}(t)}{c + \bar{v}(t)} && \text{(85b)} \end{aligned}$$

Comparing (84) with (82) shows that, to use (82), $f'(t) \approx f$ and $T \to 0$ are expected. Alternatively, using $f'(t) = 1/T'(t)$ in (84b) and then substituting $T'(t)$ by that from (83), the Doppler frequency can be expressed as

$$f_D(t) = -\frac{1}{\lambda} \times \frac{\frac{1}{T}\left[r(t+T) - r(t)\right]}{1 + \frac{1}{\lambda}\left[r(t+T) - r(t)\right]} \tag{86}$$

which shows that, to use (82), $T \to 0$, and $\frac{1}{\lambda}\left[r(t+T) - r(t)\right] \approx 0$, meaning that the distance of source moving within one period should be much smaller than wavelength. This in turn means that source's moving velocity should be small, yielding

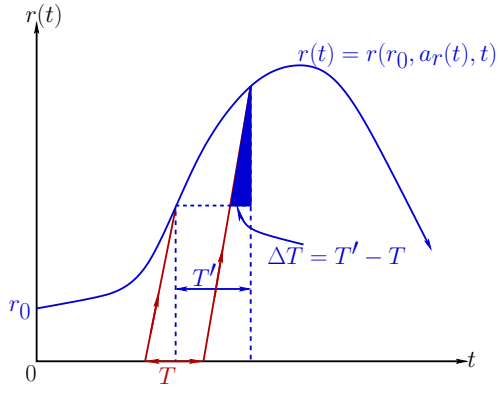

Figure 5: Graphic representation of the Doppler effect in general motion.

$f'(t) \approx f$.

0.4.1.2 Stationary Source and General Motiving Observer

As an example, Fig. 5 shows the graphic representation of the scenario where a stationary source is located at origin, while an observer moves following a motion equation $r(t)$ with respect to source. Following the previous description for (83), there is a relationship of

$$T'(t') = T + \frac{1}{c}\left[r(t' + T'(t')) - r(t')\right] \tag{87}$$

where $T'(t')$ is a function of t', which is the time instant when observer receives the first maxima. From (87), we can obtain

$$f'(t') = \frac{f}{1 + \frac{1}{cT}\left[r(t' + T'(t)) - r(t')\right]} \tag{88a}$$

$$f_D(t') = -\frac{f'(t')}{c} \times \frac{1}{T}\left[r(t' + T'(t)) - r(t')\right] \tag{88b}$$

Comparing (88a) and (88b) respectively with (84a) and (84b) reveals that, when source is moving and observer is rest, the average speed $\bar{v}(t) = [r(t+T) - r(t)]/T$ is source's average speed in $[t, t+T]$. In contrast, in the scenario where source is stationary while observer is moving, in (88a) and (88b), the involved average speed $\bar{v}(t') = [r(t' + T'(t)) - r(t')]/T$ is the distance variant over a period of observed signal but averaged by the period of source's emitted signal. If we make $\bar{v}'(t') = [r(t' + T'(t)) - r(t')]/T'(t)$ the average speed of observer in $[t', t' + T'(t)]$, (88a)

and (88b) are represented (easier to derive from (87)) as

$$f'(t') = f\left(1 - \frac{\bar{v}'(t')}{c}\right) \tag{89a}$$

$$f_D(t') = -\frac{f\bar{v}'(t')}{c} \tag{89b}$$

It is worth noting that when there is acceleration, $\bar{v}(t)$ and $\bar{v}'(t')$ are different, although both are calculated from the change of the distance between source and observer made over one period.

0.4.1.3 General Moving Source and Observer

Following the two scenarios considered above, the Doppler effect in the scenario where both source and observer are in general motion can be straightforwardly derived. The analysis is under the assumption that there is a third reference frame, which seats at a point on the line connecting source and observer. With this in mind, assume source moves according to $r(t)$ and observer moves according to $r'(t')$, which represent the distances of, respectively, source and observer relative to this reference frame. Then, following the previous definitions, we have

$$T'(t') = T + \frac{1}{c}\left([r(t+T) - r(t)] + \left[r'(t' + T'(t')) - r(t')\right]\right) \tag{90}$$

where, in the second term at the right-hand side, the first bracket is the distance added by the moving source in T, and the second bracket is the distance added by the moving observer in $T'(t)$. Using $f'(t') = 1/T'(t')$ and $f = 1/T$ in (90) obtains

$$f'(t') = f\left[1 + \frac{1}{c}\frac{r(t+T) - r(t)}{T} + \frac{1}{c}\frac{f}{f'(t')}\frac{r'(t' + T'(t')) - r(t')}{T'(t')}\right]^{-1} \tag{91}$$

Let $\bar{v}(t) = r(t+T) - r(t)/T$ and $\bar{v}'(t') = r'(t' + T'(t')) - r(t')/T'(t')$ represent the average speed of source in $[t, t+T]$ and the average speed of observer in $[t', t' + T'(t')]$, respectively. Then, (91) becomes

$$f'(t') = f\left[1 + \frac{\bar{v}(t)}{c} + \frac{\bar{v}'(t')}{c}\frac{f}{f'(t')}\right]^{-1} \tag{92}$$

Simplifying it yields[5]

$$f'(t') = f \times \frac{1 - \dfrac{\bar{v}'(t')}{c}}{1 + \dfrac{\bar{v}(t)}{c}} \tag{93}$$

showing that, without considering f, it is the product of (85a) and (89a).

Furthermore, if $(\bar{v}'(t')/c)(\bar{v}(t)/c)$ and $(\bar{v}(t)/c)^2$ are negligible, an approximation equation is

$$f'(t') = f\left(1 - \frac{\bar{v}'(t')}{c} - \frac{\bar{v}(t)}{c}\right) \tag{94}$$

giving the Doppler frequency of

$$f_D(t') = -\frac{f\bar{v}'(t')}{c} - \frac{f\bar{v}(t)}{c} \tag{95}$$

Remark 4. *As considered in Remark 3, we may consider to use one formula of the Doppler effect for all the scenarios. For this sake, we can let $v(t) = v'(t')$, which represents the relative speed between source and observer, and then, take the square-root of the product of* (85a) *and* (89a)*, giving*

$$f'(t) = f\sqrt{\frac{1 - \frac{\bar{v}(t)}{c}}{1 + \frac{\bar{v}(t)}{c}}} \tag{96}$$

Note again that, if in free space, this formula incorporates the time dilation resulted from the relative motion between source and observer, but only in terms of their average speed. Further details on the relativistic Doppler effect in general motion will be provided in Section 0.4.2.

Below the Doppler effect in two application scenarios is considered, where EM waves are emitted from acceleration objects.

0.4.1.4 Linearly Uniform Acceleration

Assume on a straight line represented by x-axis, as shown in Fig. 6, an observe seats at the origin, while an EM-wave source moves in the x-direction. Assume that, at $t = 0$, source is at $-r_0$ and moves at the speed of v_0. The acceleration is a constant

[5] Eq. (93) can also be directly derived from (90) after applying the average speeds as defined.

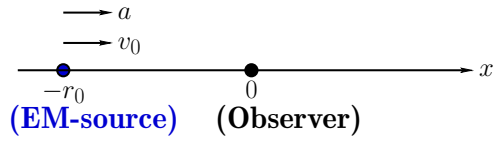

Figure 6: Uniformly accelerating EM-source moves in x-axis direction.

a. Then, the distance from source to observer is give by the equation

$$r(t) = \left| x(t) = -r_0 + v_0 t + \frac{at^2}{2} \right|, \; t \geq 0 \tag{97}$$

Accordingly, following (83), when source is approaching observer, meaning that both $x(t) < 0$ and $x(t+T) < 0$, the Doppler effect is

$$\begin{aligned} T'(t) =& T + \frac{1}{c}\left[r(t+T) - r(t)\right] \\ =& T + \frac{1}{c}\left[-x(t+T) + x(t)\right] \\ =& \frac{T}{c}\left[c - v_0 - at - aT/2\right] \end{aligned} \tag{98}$$

When source is leaving observer, meaning that both $x(t) > 0$ and $x(t+T) > 0$, the Doppler effect is then

$$T'(t) = \frac{T}{c}\left[c + v_0 + at + aT/2\right] \tag{99}$$

From (98) and (99), the Doppler frequency can be found to be

$$f'(t) = f\left(1 \pm \frac{\bar{v}(t)}{c}\right)^{-1} \tag{100}$$

where $\bar{v}(t) = v_0 + at + aT/2$ is the average speed in the time $[t, t+T]$, while '$+$' and '$-$' are for leaving and approaching observer, respectively.

In addition to the above cases, there is a situation that source passes observer between the transmissions of two adjacent crests, which correspond to $x(t) < 0$ but $x(t+T) > 0$. In this situation, the period of received signal by observer can still be

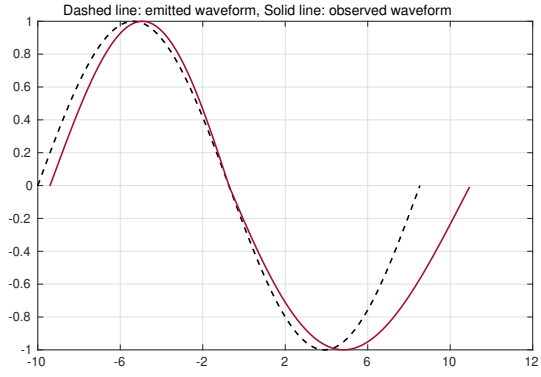

Figure 7: Ilustration of Doppler distortion, where the frond part is contracted and the rear part is dilated.

found using (83), giving

$$\begin{aligned} T'(t) =& T + \frac{1}{c}\left[r(t+T) - r(t)\right] \\ =& T + \frac{1}{c}\left[x(t+T) + x(t)\right] \\ =& \frac{1}{c}\left[cT - 2r_0 + 2v_0 t + v_0 T + at^2 + aTt + aT^2/2\right] \end{aligned} \tag{101}$$

Due to the involvement of $-2r_0$, the Doppler effect can be positive or negative, depending on t when the first crest is emitted.

While the period in this situation can be found by (101), we should note that the waveform of a period at the instant of source passing observer is different from that in the first two cases considered above. In the first and second cases, the Doppler effect is either positive or negative over a whole period, predicated by (98) or (99). By contrast, in the third case, over one period, the front part waveform experiences positive Doppler shift, while the rear part receives negative Doppler shift.

For example, assume that a source emitting single-tone sine-waveform passes the observer exactly in the middle of a waveform, i.e., at the phase of $(2n+1)\pi$. Then, the observed waveform containing the passing instant may look like the one shown in Fig. 7. The front half of original waveform is squeezed, while the rear half is stretched. If acceleration is positive, the amount of stretching is more than that of squeezing.

Due to the involvement of T^2, it is cumbersome to directly obtain the closed-from equations for the Doppler frequency from (98) and (99). For that, let us express the distance travelled with an initial speed 0 in a period T be expressed as $H = aT^2/2$,

which is a constant. From it we obtain $T = \sqrt{2H/a}$. Replacing T by this in the brackets of (98) and (99), replacing $T'(t) = 1/f'(t)$ and the other T by $T = 1/f$, and combining (98) and (99) into one give

$$\begin{aligned} f'(t) =& \frac{f}{\left(1 \pm \frac{v_0+at+\sqrt{\frac{aH}{2}}}{c}\right)} = \frac{f\left(1 \mp \frac{v_0+at+\sqrt{\frac{aH}{2}}}{c}\right)}{\left(1 \pm \frac{v_0+at+\sqrt{\frac{aH}{2}}}{c}\right)^2} \\ \approx& f\left(1 \mp \frac{v_0 + at + \sqrt{\frac{aH}{2}}}{c}\right) \end{aligned} \tag{102}$$

where the last approximation is due to the assumption of $c >> \left|v_0 + at + \sqrt{\frac{aH}{2}}\right|$. From this last approximation, the Doppler frequency is

$$f_D(t) \approx \pm \frac{f\left(v_0 + at + \sqrt{\frac{aH}{2}}\right)}{c} \tag{103}$$

Specifically, when source starts moving at $t = 0$ with an initial speed $v_0 = 0$, the Doppler frequency at $t = 0$ is

$$f_D \approx \pm \frac{f\sqrt{\frac{aH}{2}}}{c} \tag{104}$$

which shows explicitly the contribution of acceleration to Doppler shift.

Note that an enquiry of (98), (99) and (103) discovers that there is a problem to apply these formulas, as for a constant acceleration a, speed at - and hence the Doppler frequency - goes towards infinity with the increase of t. Therefore, these formulas can only be used for a resulted speed that is small enough to be considered ignorable when relative to c of the speed of light. Otherwise, the relativistic Doppler effect discussed in Section 0.4.2 should be considered.

0.4.1.5 Circularly Uniform Motion

It is well known that the circularly uniform motion exists an centripetal acceleration, whose magnitude is constant while direction is always toward the center of the circle. To analyze the Doppler effect of this system, as shown in Fig. 8, we assume that node **S**(**O**) - which may be a satellite, spaceship, a sensor on a flying wheel, etc., and may be source or observer - moves circularly on the xy-plane with a constant speed v.

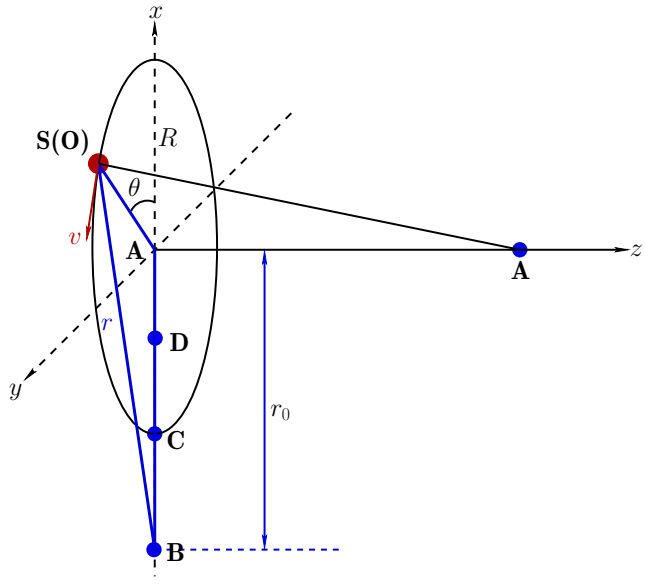

Figure 8: Illustration of circularly uniform acceleration, where **A**, **B**, **C** and **D** are source/observer locations, and **S** (**O**) is for moving source (observer).

The radius of the circle is represented by R. Then, assuming that **S**(**O**) is positioned at the positive direction of x-axis at $t = 0$, the phase θ is

$$\theta(t) = \frac{vt}{R} = \omega t,\ t \geq 0 \tag{105}$$

where $\omega = v/R$ is the angular speed. The period and frequency of **S**(**O**) moving are $T_0 = 2\pi/\omega$ and $f_0 = \omega/2\pi$, respectively.

Now let us analyze the Doppler effect, when another node seats on the z-axis or x-axis, such as at location **A**, **B**, **C** or **D**. This node may be a ground station in satellite systems, a sensor in industrial applications, etc.

First, consider the situation that **S**(**O**) is the signal source and, correspondingly, the nodes at **A**, **B**, **C** or **D** are observers. Hence, **S**(**O**) is reduced to **S** in description. The analysis of Doppler effect is as follows.

When an observer is on the z-axis, such as, at the location of **A**, the distance from any point on the circle to **A** is equal. Hence, without considering the effect from acceleration itself in terms of general relativity, the Doppler effect is zero. This can also be verified by the fact that the velocity $\boldsymbol{v} = v\hat{\boldsymbol{v}}$ is always perpendicular with the line connecting source and an observer, provided that it is on the z-axis, including the circle's center.

When an observer is on the x-axis, we only need to consider the case that observer is on the negative side of x-axis, such as at location **B**, **C** or **D**. Furthermore, owing to symmetry, this scenario is general, provided that observer is in the xy-plane[6]. Assume that the distance between an observer and the origin of circle is r_0, as shown in Fig. 8. Accordingly, the distance between source and observer is

$$\begin{aligned} r(t) =& \sqrt{R^2 \sin^2 \omega t + (R\cos\omega t + r_0)^2} \\ =& R\sqrt{\left(1 - \frac{r_0}{R}\right)^2 + \frac{4r_0}{R}\cos^2\left(\frac{\omega t}{2}\right)},\ t \geq 0 \qquad (106) \\ =& r_0\sqrt{\left(1 - \frac{R}{r_0}\right)^2 + \frac{4R}{r_0}\cos^2\left(\frac{\omega t}{2}\right)},\ t \geq 0 \qquad (107) \end{aligned}$$

Taking the derivative of, say (106), with respect to t gives the speed of source relative to observer expressed as

$$\begin{aligned} v_{s-o}(t) =& \frac{dr(t)}{dt} \\ =& -\frac{r_0 v \sin(\omega t)}{R\sqrt{\left(1 - \frac{r_0}{R}\right)^2 + \frac{4r_0}{R}\cos^2\left(\frac{\omega t}{2}\right)}} \end{aligned} \qquad (108)$$

Hence, we have an approximate formula for the Doppler frequency expressed as

$$f_D(t) = \frac{r_0 v \sin(\omega t)}{\lambda R\sqrt{\left(1 - \frac{r_0}{R}\right)^2 + \frac{4r_0}{R}\cos^2\left(\frac{\omega t}{2}\right)}} \qquad (109)$$

Before deriving the more accurate formulas for the Doppler effect, several special cases can be obtained from (109). First, when $r_0 \to 0$, meaning that observer is near the center of circle, (106) gives constant distance of $r(t) = R$ and (109) gives $f_D = 0$. Second, if $r_0 \to \infty$, (109) can be simplified to

$$f_D(t) = \frac{v\sin(\omega t)}{\lambda} \qquad (110)$$

Straightforwardly, $f_D(t) = 0$, when $wt = n\pi$ with n being an integer, and $|f_D(t)| = v/\lambda = fv/c$ is maximum, when $\omega t = n\pi \pm \pi/2$. Furthermore, when $r_0 = R$, i.e.,

[6]This model can mirror many application scenarios, for example, a sensor on a satellite (ground station) observes the signals sent from a ground station (satellite), or a stationary observer receives the signals sent by a sensor installed on a wheel in industrial applications.

when observer is at **C**,

$$f_D(t) = \frac{v\sin(\omega t)}{2\lambda\left|\cos\frac{\omega t}{2}\right|} = \pm\frac{v\sin\left(\frac{\omega t}{2}\right)}{\lambda} \tag{111}$$

where $+/-$ is determined by whether source is approaching or leaving observer. Explicitly, the maximum Doppler effect is generated when $\omega t = (2n+1)\pi$.

Now, let us derive the more accurate formula for the Doppler effect. Assume that source emits two adjacent maxima at $t_1 = t$ and $t_2 = t + T$. Then, observer receives the two maxima at $t_1' = t + r(t)/c$ and $t_2' = t + T + r(t+T)/c$. The period of received signal by observer is given by

$$T'(t) = t_2' - t_1' = T + \frac{r(t+T) - r(t)}{c} \tag{112}$$

After substituting (107) into (112), we obtain

$$\begin{aligned} T'(t) = T + \frac{r_0}{c}\Bigg[&\sqrt{\left(1-\frac{R}{r_0}\right)^2 + \frac{4R}{r_0}\cos^2\left(\frac{\omega(t+T)}{2}\right)} \\ &-\sqrt{\left(1-\frac{R}{r_0}\right)^2 + \frac{4R}{r_0}\cos^2\left(\frac{\omega t}{2}\right)}\Bigg],\ t \geq 0 \end{aligned} \tag{113}$$

This is a general formula that can be used for predicting the Doppler effect, when an observer lying on the same plane of the source's moving circle receives signals from the source, after necessary rotation to make x-axis align with the observer. For example, if **S** is a satellite, a ground station may be located at **D**. **S** at **C** is the situation that the satellite is directly overhead of the ground station.

Specifically, if observer is at **C** as seen in Fig. 8 , we have $r_0 = R$. Applying this into (113) and after some simplification, we obtain

$$T' = T + \frac{2R}{c}\left[\left|\cos\left(\frac{\omega(t+T)}{2}\right)\right| - \left|\cos\left(\frac{\omega t}{2}\right)\right|\right],\ t \geq 0 \tag{114}$$

Referring to Fig. 8, if $(\omega t)\ _{\mod 2\pi} \geq 0$ and $(\omega(t+T))\ _{\mod 2\pi} \leq \pi$, where ' $\mod$ ' is modulo-operation, (114) becomes

$$\begin{aligned} T' =& T + \frac{2R}{c}\left[\cos\left(\frac{\omega(t+T)}{2}\right) - \cos\left(\frac{\omega t}{2}\right)\right] \\ =& T - \frac{4R}{c}\sin\left(\frac{\omega T}{4}\right)\sin\left(\frac{\omega(2t+T)}{4}\right),\ t \geq 0 \end{aligned} \tag{115}$$

If $(\omega t)\ _{\ \mathrm{mod}\ 2\pi} \geq \pi$ and $(\omega(t+T))\ _{\ \mathrm{mod}\ 2\pi} \leq 2\pi$, (114) becomes

$$\begin{aligned} T' =& T + \frac{2R}{c}\left[-\cos\left(\frac{\omega(t+T)}{2}\right) + \cos\left(\frac{\omega t}{2}\right)\right] \\ =& T + \frac{4R}{c}\sin\left(\frac{\omega T}{4}\right)\sin\left(\frac{\omega(2t+T)}{4}\right),\ t \geq 0 \end{aligned} \tag{116}$$

Furthermore, if $\omega T \approx 0$, (115) and (116) can be approximated as

$$T' \approx T\left[1 \mp \frac{\omega R}{c}\sin\left(\frac{\omega t}{2}\right)\right],\ t \geq 0 \tag{117}$$

when they are represented in one compact form. Accordingly, the Doppler frequency is

$$\begin{aligned} f_D(t) \approx& \frac{\pm\frac{v}{\lambda}\sin\left(\frac{\omega t}{2}\right)}{1 \mp \frac{v}{c}\sin\left(\frac{\omega t}{2}\right)} \\ \approx& \pm\frac{v}{\lambda}\sin\left(\frac{\omega t}{2}\right) \end{aligned} \tag{118}$$

where $v/c \to 0$ is applied for obtained the second equation from the first one. Notice that (118) is the same as (111).

Now, let us consider the case that **S**(**O**) is the observer, hence using **O** to avoid confusion, while source is at **A**, **B**, **C** or **D**. Again, it is easy to analyze that the Doppler effect is zero, provided that source is on the z-axis including **A** and the centre of the circle. For the other cases that source is at **B**, **C** or **D**, assume that source emits two adjacent crests at $t_1 = t$ and $t_2 = t + T$. Assume that **O** is on the positive x-axis at $t = 0$. Then, **O** receives the first crest at $t'_1 = t + r(t'_1)/c$ and the second crest at $t'_2 = t + T + r(t'_1 + T'(t'_1))/c$. Denoting $t' = t'_1$, we can obtain a relation between $T'(t')$ and T expressed as

$$\begin{aligned} T'(t') = T + \frac{r_0}{c}\Bigg[&\sqrt{\left(1 - \frac{R}{r_0}\right)^2 + \frac{4R}{r_0}\cos^2\left(\frac{\omega(t' + T'(t'))}{2}\right)} \\ &- \sqrt{\left(1 - \frac{R}{r_0}\right)^2 + \frac{4R}{r_0}\cos^2\left(\frac{\omega t'}{2}\right)}\Bigg] \end{aligned} \tag{119}$$

with $t' = t + r(t')/c$, $t \geq 0$.

As seen in (119), t' and $T'(t')$ are included in the cosine term at the right-hand side, making it hard to simplify the equation to obtain a straightforward relation between $T'(t')$ and T. In this case, the Doppler frequency may only be obtained by

numerical search for a $T'(t')$ with $t' = t + r(t')/c$, to make.

$$\left| T'(t') - T - \frac{r_0}{c}\left[\sqrt{\left(1-\frac{R}{r_0}\right)^2 + \frac{4R}{r_0}\cos^2\left(\frac{\omega(t'+T'(t'))}{2}\right)} - \sqrt{\left(1-\frac{R}{r_0}\right)^2 + \frac{4R}{r_0}\cos^2\left(\frac{\omega t'}{2}\right)}\right]\right| \to 0 \qquad (120)$$

In the evaluation of the Doppler effect in this case, two approximation methods can be considered.

First, assume the case of large R, which is the case, for example, of satellite communications. In this kind of applications, approximations of $r(t') \approx r(t)$ and $r(t' + T'(t')) \approx r(t + T)$ can be very accurate. Accordingly, the same relation as (113) can be obtained, except that $T'(t)$ needs to be replaced by $T'(t')$. Since $t' \approx t + r(t)/c$, comparing to the case where source moving observer stationary, the same Doppler frequency in the case of source stationary observer moving comes slightly later, by a time of about $r(t)/c$. Note that, due to the same relation of (113) [7], all the specific cases considered following (113) are also satisfied. This explains that when R is large, the same formulas can be simultaneously used in both the case of source moving and observer stationary, and the case of source stationary and observer moving.

Second, assume a small R and also that the distance between source and observer is relatively small, which is usually the case in indoor and industrial applications. If R is small, the motion spanning one wavelength may be significant. However, as the result of a small distance between source and observer, the wave propagation time from source to observer can be ignored, yielding $t' \approx t$. Hence, (119) can be approximated by a formula of

$$T'(t) = T + \frac{r_0}{c}\left[\sqrt{\left(1-\frac{R}{r_0}\right)^2 + \frac{4R}{r_0}\cos^2\left(\frac{\omega(t+T'(t))}{2}\right)} - \sqrt{\left(1-\frac{R}{r_0}\right)^2 + \frac{4R}{r_0}\cos^2\left(\frac{\omega t}{2}\right)}\right],\ t \geq 0 \qquad (121)$$

Nonetheless, due to the term of $\cos^2\left(\frac{\omega(t+T'(t))}{2}\right)$, it is not straightforward to obtain a simple relation between $T'(t)$ and T. Hence, searching methods may be needed for finding $T'(t)$ for given T.

[7] Eq. (113) can be easily computed, as $T'(t)$ is a simple function of T.

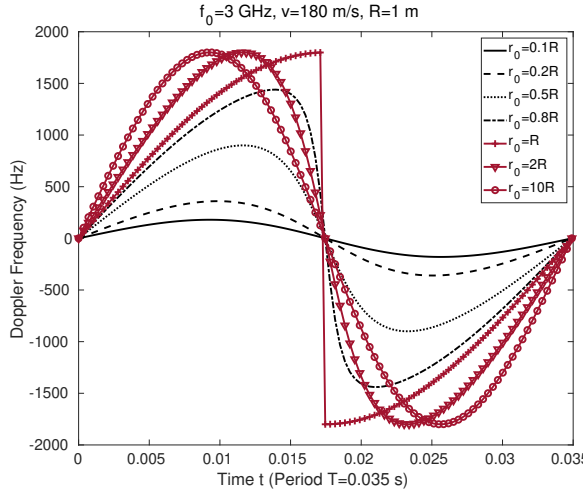

Figure 9: Doppler effect of a circularly moving source on its transmitted radio signals received by a stationary observer.

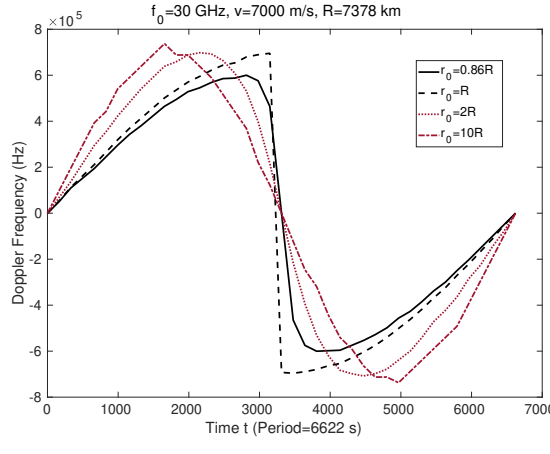

Figure 10: Doppler effect of a circularly moving source on its transmitted radio signals received by a stationary observer.

Example 6. *Fig. 9 shows the Doppler frequency generated by a radio emitter installed on, such as, a wheel of one meter of radius, rotating at a speed of about 29 turns per second. The observer is on the same plane of the wheel and has the different distances from the wheel center as shown in the figure. It shows that, when* $r_0 < R$*, the Doppler frequency increases as* r_0 *increases, with the phase of generating the*

maximum Doppler frequency shifting towards $\omega t = 2n + \pi$ as r_0 increases towards R. At $r_0 = R$, the change of Doppler frequency is not continuous at $\omega t = 2n + \pi$. In contrast, when $r_0 > R$, the maximum Doppler frequency is not much affected by r_0, which can be implied by (109) *- where the $\cos(\omega t)$ term is insignificant - and* (110)*. Furthermore, the phase giving the maximum Doppler frequency converges to $\omega t = 2n\pi \pm \pi/2$, which is also implied by* (110)*.*

Example 7. *Fig. 10 shows the Doppler frequency generated by a satellite travelling at a speed of about 7000 m/s relative to the Earth's surface, when the radio signals emitted by the satellite are detected by an observer at $r_0 = 0.86R$, on the Earth's surface and at the opposite pole of satellite's orbit $r_0 = R$, and at two other altitudes of $r_0 = 2R$ and $10R$, respectively. Explicitly, the Doppler effect appears similarly as that shown in Fig. 9, with the actual Doppler frequency depended on the radio frequency, in addition to the other parameters as above-mentioned.*

0.4.2 Relativistic Doppler Effect in General Motion

To deal with the relativistic Dopper effect, the analysis in Section 0.3.3 explained that *the relativistic Doppler effect is determined by two proper time intervals relating to two different pairs of events occurring in two different reference frames, i.e., the reference frame of source and the reference frame of observer* [22]. Hence, given a proper time interval, expressed as T, in the source's reference frame, the proper time interval, referred to as T', in an observer's reference frame is not only contributed by the proper time interval itself in the source's reference frame, but also by the effect from the relative motion - uniform or accelerated motion - between source and observer. Section 0.3.3 considered the relativistic Doppler effect in uniform motion, which yields inertial reference frames. In this section, the relativistic Doppler effect in the general motion scenarios where acceleration may exist is analyzed. Hence, non-inertial frames instead of inertial frames must be considered. Below, the relativistic Doppler effect in general motion is first considered. Then, the relativistic Doppler effects in several special application scenarios experiencing accelerated motions are analyzed. Main references followed for the analysis are [22–25].

Note that in the analysis below, we again assume that the relative velocity between source and observer is positive when they move away from each other, while negative when they move towards each other. We assume that source and observer do not pass each other during the time of considering the Doppler effect. Otherwise, the velocity within a period has both positive and negative Doppler effect, making a part of waveform contracted and the other part stretched, as that shown in Fig. 7.

In the analysis of the Doppler effect in systems with general motion, one issue should be emphasised is - as pointed out in [22] - the time dilatation formula is correct only when applied with an inertial frame of reference, but not correct when applied

with a non-inertial frame. In other words, the time dilatation formula should not be mistakenly applied with the frames in acceleration.

Additionally, the general analysis is focused, while formulas in special cases are provided. Hence, the analysis is based on the definitions of $\boldsymbol{v}(t)$, $\boldsymbol{a}(t)$, v, $r(t)$, c, c', etc., having similar meanings as those defined in Section 0.3.3.

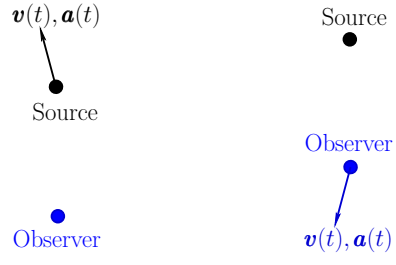

(a) Moving source, inertial observer. (b) Inertial source, moving observer.

Figure 11: Scenarios of (a) random moving source and inertial observer, and (b) inertial source and random moving observer.

0.4.2.1 General Moving Source and Inertial Observer

For the scenario of a moving source sending EM signals to a stationary observer in a medium, as shown in Fig. 11(a), there are three reference frames involved, the non-inertial reference frame of source, the inertial reference frame of medium and the inertial reference frame of observer, which is rest in medium and hence the same inertial reference frame of medium. To analyse the Doppler effect, as in Section 0.3.3, three types of times, periods and frequencies are defined, the proper time t, proper period T and the proper frequency f of source in the reference frame of source, the time t'', period $T''(t'')$ and the frequency $f''(t'')$ of the source in the reference frame of medium, and the proper time t', proper period $T'(t)$ and the proper frequency $f'(t)$ of observer in the reference frame of observer. The distance between source and observer in the reference frame of medium is expressed as $r(t'')$ and all velocities are measured with respect to the reference frame of medium. Since observer rests in medium's reference frame, we have $t'' = t'$, i.e., the clock holding by observer runs synchronously as that in medium.

As explained in Section 0.2, Dopper effect can be explained by the ratio of two periods or two frequencies of the emitted signal at source and, correspondingly, received signal by observer. When relativisitc Doppler effect is considered, an refine-

ment is the ratio of two proper periods or two proper frequencies, expressed as

$$\frac{T}{T'(t')} = \frac{f'(t')}{f} \tag{122}$$

From these ratios, the Doppler frequency can be expressed as

$$f'_D(t') = f\left(\frac{f'(t')}{f} - 1\right) = \frac{1}{T}\left(\frac{T}{T'(t')} - 1\right) \tag{123}$$

Since the general moving non-inertial source and inertial observer are considered, the time dilation should be derived with respect to the inertial reference frame of observer (or medium). Assume that two adjacent maxima are emitted by source at $t_1 = t$ and $t_2 = t + T$ in its reference frame. Accordingly, when observed in the reference frame of medium, these two maxima are emitted at $t''_1 = t''$ and $t''_2 = t'' + T''(t'')$[8] at the distances of $r(t'')$ and $r(t'' + T''(t''))$. Hence, following Section 0.4.1 (See Fig. 4), $T'(t')$ and $T''(t'')$ in the reference frame of medium follow the relationship of

$$T'(t') = T''(t'') + \frac{r(t'' + T''(t'')) - r(t'')}{c'} \tag{124}$$

To find the Doppler effect of $T/T'(t')$, a relation between T and $T''(t)$ is needed. In principle, this can be obtained from the differential equation built on the time dilation relationship of

$$dt'' = \frac{dt}{\sqrt{1 - \beta^2(t'')}} \;\leftrightarrow\; dt = \sqrt{1 - \beta^2(t'')}dt'' \tag{125}$$

where $\beta(t'') = |\boldsymbol{v}(t'')|/c$ with $|\boldsymbol{v}(t'')|$ being the speed of source measured in the reference frame of medium. As above assumed, $t''_1 = t''$ corresponds to $t_1 = t$, and $t''_2 = t'' + T''(t)$ corresponds to $t_2 = t + T$. Hence, upon integrating (125) over these ranges, we can obtain a relationship between $T''(t)$ and T as

$$T = \int_{t''}^{t''+T''(t'')} \sqrt{1 - \beta^2(\tau)}d\tau \tag{126}$$

Based on (126), once a $\boldsymbol{v}(t)$ is given, we can obtain a function $T = f(T''(t''), t'')$, from which $T''(t'')$ can be obtained. Then, substituting it into (124), we can obtain the formula for the Doppler effect of $T/T'(t)$.

[8]Note that, while T is independent of t, $T''(t'')$ is dependent on t'', since the transformation from the non-inertial reference frame of source to the inertial reference frame of observer is dependent on the velocity of source, which is a function of t''.

However, solving (126) may be highly involved due to $\boldsymbol{v}(t)$ and the square-root operation. In most radio and optical-based wireless communication scenarios, $\beta(t'') = |\boldsymbol{v}(t'')|/c$ resulted from source's motion is nearly the same across one period $T''(t'')$. Hence, in general, the approximation of

$$T''(t'') \approx \frac{T}{\sqrt{1-\bar{\beta}^2(t'')}} \tag{127}$$

can be used, where $\bar{\beta}(t'') = \overline{|\boldsymbol{v}(t'')|}/c$ with $\overline{|\boldsymbol{v}(t'')|}$ the average speed of source over one period of $T''(t'')$. Substituting (127) into (124) gives

$$T'(t') = \frac{T}{\sqrt{1-\bar{\beta}^2(t'')}} + \frac{r(t''+T''(t'')) - r(t'')}{c'} \tag{128}$$

Furthermore, if express $r(t''+T''(t'')) - r(t'') = \bar{v}(t'')T''(t'') = \bar{v}(t'')T/\sqrt{1-\bar{\beta}^2(t'')}$, and apply it into (128), a formula for the Doppler effect can be found to be

$$\frac{f'(t)}{f} = \frac{T}{T'(t')} = \sqrt{1-\bar{\beta}^2(t'')}\left(1+\frac{\bar{v}(t'')}{c'}\right)^{-1} \tag{129a}$$

$$\approx \sqrt{1-\bar{\beta}^2(t'')}\left(1-\frac{\bar{v}(t'')}{c'}\right) \tag{129b}$$

$$= \sqrt{1-\bar{\beta}^2(t')}\left(1-\frac{\bar{v}(t')}{c'}\right) \tag{129c}$$

where the approximation is due to ignoring an insignificant term of $\bar{v}^2(t)/c^2$, and (129c) is due to $t' = t''$. In (129b), $\bar{v}(t'')$ is the average speed of source moving on the line connecting source and observer, $\overline{|\boldsymbol{v}(t'')|}$ in $\bar{\beta}(t'')$ is the magnitude of $\boldsymbol{v}(t'')$.

Example 8. *A Low Earth Orbit (LEO) satellite travels at a speed of about $v = 7.8$ km/s ($28,000$ km/h(our)), orbiting at an altitude of about $h = 200$ km above Earth's surface. The communication signals sent by this LEO satellite is operated on the frequency of $f = 28$ GHz in the Ka-band. Assume that $c' = c$. a) Find the non-relativistic and relativistic Doppler frequencies, when a receiver is located directly below the LEO satellite or at the center of the spherical Earth. b) Find the maximum non-relativistic and relativistic Doppler frequencies, when a receiver is fixed at a location on the satellite's orbit.*

Solution. *a) When the receiver is directly below the LEO satellite or at the center of the Earth, the velocity of satellite is approximately perpendicular with the line connecting the satellite and receiver. Hence, the non-relativistic Doppler frequency is zero.*

The relativistic Doppler frequency can be found from (129b) *by letting* $\bar{v}(t'') = 0$ *due to the above, and* $|\boldsymbol{v}(t'')| = 7.8$ *km/s, giving*

$$f'_D = f(\sqrt{1 - \bar{\beta}^2(t)} - 1) = -9.48\ Hz$$

Hence, the frequency is slightly red-shifted.

b) When the receiver is fixed at a location on the orbit of LEO satellite, the maximum Doppler shift is reached when the satellite approaches the receiver with a speed of $\bar{v}(t'') = 7.8$ *km/s. The non-relativistic Doppler frequency is given by*

$$f'_D = f\left(1 + \frac{\bar{v}(t'')}{c}\right)^{-1} - f = 728522.9\ Hz$$

From (129b)*, the relativistic Doppler frequency is given by*

$$f'_D = f\sqrt{1 - \bar{\beta}^2(t)}\left(1 + \frac{\bar{v}(t'')}{c}\right)^{-1} - f \approx 728513.5\ Hz$$

The difference between the relativistic and non-relativistic Doppler shifts is about 9.4 *Hz, approximately the value given in the case of a).*

0.4.2.2 Inertial Source and General Moving Observer

When the scenario of inertial source resting in medium and general moving observer in Fig. 11(b) is considered, the frames of source and medium are inertial, but the frame of observer is non-inertial, if observer's moving velocity is not constant. Hence, the time dilation should be derived with respect to the reference frame of medium.

Assume that the variables defind in the previous Section 0.4.2.1 are reused. Assume that two adjacent maxima are emitted by source at $t_1 = t$ and $t_2 = t + T$ in its reference frame. Accordingly, in medium's reference frame, these two maxima are received by observer at $t''_1 = t''$ and $t''_2 = t'' + T''(t'')$[9] at the distances $r(t'')$ and $r(t'' + T''(t))$ between observer and source. Since source rests in the reference frame of medium, we have $t = t''$, i.e., the clock holding by source runs synchronously as that in medium. Hence, following Section 0.4.1, we have

$$T''(t'') = T + \frac{r(t'' + T''(t'')) - r(t'')}{c'} \tag{130}$$

To find the Doppler effect of $T/T'(t)$, a relation between $T''(t'')$ and $T'(t')$ is

[9]Note that, while T is independent of t, $T''(t'')$ is dependent on t'', as the result that observer is moving relative to source in medium's reference frame.

needed. This may be obtained with the aid of the differential equation

$$dt'' = \frac{dt'}{\sqrt{1-\beta^2(t'')}} \;\leftrightarrow\; dt' = \sqrt{1-\beta^2(t'')}dt'' \tag{131}$$

where $\beta(t'') = |\boldsymbol{v}(t'')|/c$ with $|\boldsymbol{v}(t'')|$ being the speed of observer measured in medium's reference frame. However, solving (131) may be highly involved.

In the applications where $\beta(t'') = |\boldsymbol{v}(t'')|/c$ resulted from observer's motion is nearly the same across one period of $T''(t'')$, the approximation of

$$T''(t'') \approx \frac{T'(t')}{\sqrt{1-\bar{\beta}^2(t'')}} \tag{132}$$

can be used, where $\bar{\beta}(t'') = \overline{|\boldsymbol{v}(t'')|}/c$ and $\overline{|\boldsymbol{v}(t'')|}$ is the average magnitude of $|\boldsymbol{v}(t'')|$ over one period of $T''(t'')$. Substituting (132) into (130) gives

$$\frac{T'(t')}{\sqrt{1-\bar{\beta}^2(t'')}} = T + \frac{r(t''+T''(t'')) - r(t'')}{c'} \tag{133}$$

Furthermore, if express $r(t''+T''(t''))-r(t'') = \bar{v}(t'')T''(t'') = \bar{v}(t'')T'(t')/\sqrt{1-\bar{\beta}^2(t'')}$, and apply it to (133), a formula for the Doppler effect can be found to be

$$\begin{aligned}\frac{f'(t')}{f} = \frac{T}{T'(t')} =& \frac{1}{\sqrt{1-\bar{\beta}^2(t'')}} \times \left(1 - \frac{\bar{v}(t'')}{c'}\right) \\ =& \frac{1}{\sqrt{1-\bar{\beta}^2(t)}} \times \left(1 - \frac{\bar{v}(t)}{c'}\right)\end{aligned} \tag{134}$$

where the equality in the second line is due to $t = t''$.

Example 9. *Assume that a LEO satellite system has the geometric and signaling parameters as that in Example 8. Now the receiver is on the satellite. a) Find the non-relativistic and relativistic Doppler frequencies, when a transmitter is located directly below the LEO satellite or at the center of the Earth. b) Find the maximum non-relativistic and relativistic Doppler frequencies, when a transmitter is fixed at a location on the satellite's orbit.*

Solution. *a) When transmitter is directly below the LEO satellite, the velocity of LEO satellite is perpendicular with the line connecting the satellite and transmitter. Hence, the non-relativistic Doppler frequency is zero.*

The relativistic Doppler frequency can be found from (134) *by letting* $\bar{v}(t) = 0$

due to the above mentioned, and $|\boldsymbol{v}(t)| = 7.8$ *km/s, giving*

$$f_D = f\left[\left(\sqrt{1-\bar{\beta}^2(t)}\right)^{-1} - 1\right] = 9.48\ Hz \tag{135}$$

Hence, the frequency is slightly blue-shifted.

b) The maximum Doppler-shift is reached when satellite starts passing the transmitter. Hence the speed for both (classic) Doppler effect and time dilation is -7.8 *km/s. Hence, the non-relativistic Doppler frequency is*

$$f'_D = f\left(1 - \frac{\bar{v}(t)}{c}\right) - f = 728504\ Hz$$

From (134)*, the relativistic Doppler frequency is calculated to be*

$$f'_D \approx 728513.5\ Hz$$

The difference between the relativistic and non-relativistic Doppler shifts is about 9.5 *Hz, the approximated value given in the case of a).*

0.4.2.3 General Moving Source and Observer

To analyze the relativistic Doppler effect in this more general scenario where both source and observer are moving relative to medium [22, 26], in addition to the definitions used above, we associate the set of variables of $\{t'', T''_S(t''_S), f''_S(t''_S)\}$ with source and the set of variables of $\{t^*, T^*(t^*), f^*(t^*)\}$ with observer, both are relative to medium. Furthermore, we assume that, in medium's reference frame, there is an Ex-observer always resting on the line connecting source and observer, so that the distance between source and observer is equal to the distance $r(t'')$ between source and Ex-observer plus the distance $r(t^*)$ between Ex-observer and observer. Then, assuming that source emits two adjacent maxima at $t_1 = t$ and $t_2 = t + T$, in the medium's frame, these two events occur at $t''_1 = t''$ and $t''_2 = t'' + T''(t'')$ with the distances of $r(t'')$ and $r(t'' + T''(t''))$ from the Ex-observer, respectively. These two maxima are received by observer at $t^*_1 = t^*$ and $t^*_2 = t^* + T^*(t^*)$ with the distances of $r(t^*)$ and $r(t^* + T^*(t^*))$ from the Ex-observer. Hence, in the reference frame of medium, the relationship of

$$T^*(t) = T''(t'') + \frac{r(t'' + T''(t'')) - r(t'')}{c'} + \frac{r(t^* + T^*(t^*)) - r(t^*)}{c'} \tag{136}$$

'approximately' holds. Here, the use of 'approximately' is because during the events related to (136), the Ex-observer may not always be on the line connecting source and observer, making the change of distance between source and observer is only

approximately the sum of the second and third terms in (136).

Let us express $\bar{v}''(t'') = [r(t''+T''(t''))-r(t'')]/T''(t'')$ and $\bar{v}^*(t^*) = [r(t^*+T^*(t^*))-r(t^*)]/T^*(t^*)$, respectively, the average velocities of source and observer move on the line connecting source and observer. These velocities are relative to the medium, with positive and negative mean moving away and towards the Ex-observer, respectively. Then, (136) can be written as

$$T^*(t)\left(1-\frac{\bar{v}^*(t^*)}{c'}\right) = T''(t'')\left(1+\frac{\bar{v}''(t'')}{c'}\right) \tag{137}$$

Now considering the time dilation due to the motions of source and observer relative to medium, there are relations of

$$T^*(t^*) = \frac{T'(t')}{\sqrt{1-\bar{\beta}^2(t^*)}} \tag{138a}$$

$$T''(t'') = \frac{T}{\sqrt{1-\bar{\beta}^2(t'')}} \tag{138b}$$

where $\bar{\beta}(t^*) = \overline{|\boldsymbol{v}^*(t^*)|}/c$ and $\bar{\beta}(t'') = \overline{|\boldsymbol{v}''(t'')|}/c$. Upon substituting (138a) and (138b) into (137) and some simplification, the Doppler effect can be expressed as

$$\frac{f'(t')}{f} = \left(\frac{1-\bar{v}^*(t^*)/c'}{1+\bar{v}''(t'')/c'}\right)\times\left(\frac{\sqrt{1-\bar{\beta}^2(t'')}}{\sqrt{1-\bar{\beta}^2(t^*)}}\right) \tag{139}$$

Explicitly, (129b) and (134) are the special cases of (139). Furthermore, if $\overline{|\boldsymbol{v}^*(t^*)|} = \bar{v}^*(t^*)$ and $\overline{|\boldsymbol{v}''(t'')|} = \bar{v}''(t'')$, meaning that both source and observer are moving on a line, and if also $c' = c$, (139) is reduced to

$$\frac{f'(t')}{f} = \sqrt{\frac{1-\bar{v}''(t'')/c}{1+\bar{v}''(t'')/c}}\times\sqrt{\frac{1-\bar{v}^*(t^*)/c}{1+\bar{v}^*(t^*)/c}} \tag{140a}$$

$$= \sqrt{\frac{1-\bar{v}''(t'')/c-\bar{v}^*(t^*)/c+\bar{v}''(t'')\bar{v}^*(t^*)/c^2}{1+\bar{v}''(t'')/c+\bar{v}^*(t^*)/c+\bar{v}''(t'')\bar{v}^*(t^*)/c^2}} \tag{140b}$$

$$= \sqrt{\frac{1-\bar{u}(t,t')/c}{1+\bar{u}(t,t')/c}} \tag{140c}$$

where, by definition,

$$\bar{u}(t,t') = \frac{\bar{v}''(t'')+\bar{v}^*(t^*)}{1+\bar{v}''(t'')\bar{v}^*(t^*)/c^2} \tag{141}$$

which is the relative moving velocity between source and observer, measured at t in terms of source or at t' in terms of observer in free space. Note that in free space, there exists no medium reference, i.e., there are no t'' and t^*. Hence, on the lefthand side of (141), $\bar{u}(t,t')$ is directly represented with respect to the reference frames of source and observer.

Specifically, if both source and observer move along the same line at a uniform velocity v, then $\bar{v}'' = v$ and $\bar{v}^* = -v$ (or vice versa). In this case, (140) yields $f'(t')/f = 1$, indicating that no relativistic Doppler effect occurs regardless of the value of v. We will return the formulas in (139) and (141) in Section 0.5.1, when considering the scenario where source and observer are in the same uniform accelerated frame.

Above in Sections 0.4.2.1 - 0.4.2.3, the relativistic Doppler effect in general motion has been analyzed. It is shown that the Doppler effect is contributed by two components, one component accounts for the (classic) Doppler effect, and the other one is due to the time dilation resulted from relative motion. Furthermore, it is shown that the components for (classic) Doppler effect have the similar expressions obtained in Section 0.3.3 for uniform motion, with the uniform velocities in uniform motion replaced by the time-variant average velocities in general motion. Based on these observations, the relativistic Doppler effects in linear acceleration and circularly uniform motion are briefly analyzed below in Section 0.4.2.4 and 0.4.2.5, by following the analysis in Section 0.4.1.4 and 0.4.1.5.

0.4.2.4 Linearly Uniform Acceleration

Assume a linear acceleration system between source and observer, which has an acceleration a and initial velocity v_0. Positive a and v_0 represent departing, while negative a and v_0 mean approaching, but the total effect is relied on their resulted $v_0 + at$. Then, according to the special relativity [27], the resultant velocity is given by

$$v(t) = \frac{v_0 + at}{\sqrt{1 + \frac{(v_0+at)^2}{c^2}}} \tag{142}$$

Hence, the time-variant average velocity over one period is

$$\bar{v}(t) = \frac{1}{T}\int_t^{t+T} \frac{v_0 + a\tau}{\sqrt{1 + \frac{(v_0 + a\tau)^2}{c^2}}} d\tau \tag{143}$$

Completing the integration gives

$$\bar{v}(t) = \frac{c^2}{aT}\left[\sqrt{1+\frac{(v_0+a(t+T))^2}{c^2}} - \sqrt{1+\frac{(v_0+at)^2}{c^2}}\right] \tag{144}$$

Assume that a is small enough for using the formula $H = aT^2/2$ - the distance travelled in $[0, T]$ for an initial velocity $v_0 = 0$. Then, we have $T = \sqrt{2H/a}$. Substituting it into (144) gives a T-independent formula of

$$\bar{v}(t) = \frac{c^2}{\sqrt{2aH}}\left[\sqrt{1+\frac{(v_0+a(t+\sqrt{2H/a}))^2}{c^2}} - \sqrt{1+\frac{(v_0+at)^2}{c^2}}\right] \tag{145}$$

It can be shown that

$$\lim_{t\to\infty} \bar{v}(t) = c \tag{146}$$

Hence, no matter what a is, the resultant speed will never goes beyond c of the speed of light.

Hence, when source is moving and observer is stationary, following (129a), we have

$$\frac{f'(t)}{f} = \sqrt{1-\bar{\beta}^2(t)}\left(1+\frac{\bar{v}(t)}{c'}\right)^{-1} \tag{147}$$

where $\bar{\beta}(t) = \bar{v}(t)/c$. Similarly, when source is stationary and observer is moving, following (134), we have

$$\frac{f'(t')}{f} = \frac{1}{\sqrt{1-\bar{\beta}^2(t')}} \times \left(1-\frac{\bar{v}(t')}{c'}\right) \tag{148}$$

where $\bar{v}(t')$ is the same as (145) with H replaced by $H' = a(T'(t'))^2/2$, denoting the distance of observer travelling in $[0, T'(t)]$ for an initial velocity of $v_0 = 0$, while $\bar{\beta}(t') = \bar{v}(t)/c$.

An inspection of equations (147) and (148) reveals that the relativistic Doppler frequency will never approach infinity as t increases. This outcome sharply contrasts with the non-relativistic Doppler frequency discussed in Section 0.4.1.4, where the frequency increases linearly with t and can, therefore, potentially exceed the source frequency f and eventually go to infinity.

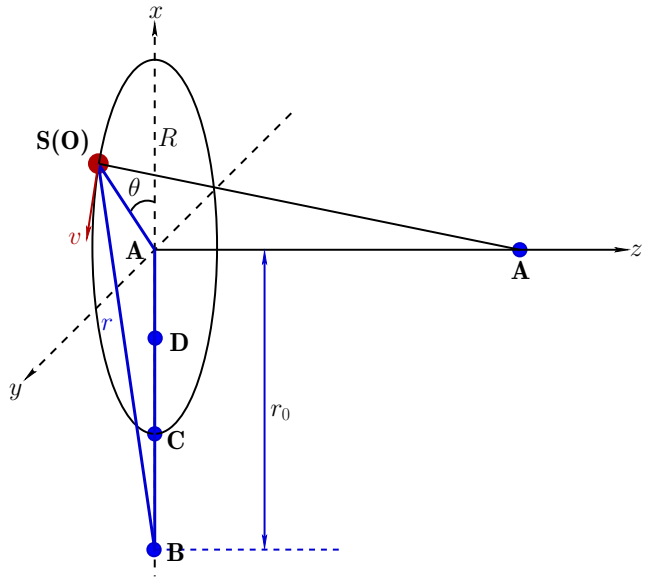

Figure 12: Illustration of circularly uniform acceleration, where **A**, **B**, **C** and **D** are source/observer locations, and **S** (**O**) is for moving source (observer).

0.4.2.5 Circularly Uniform Motion

For circularly uniform motion, the same system as that in Section 0.4.1.5 is considered. All the assumptions and settings considered there are also applied here, except the relativistic Doppler effect is analyzed now. For convenience of reading, Fig. 8 is repeated here as Fig. 12.

Following the scenarios considered in Fig. 8, if an observer (or source) is installed on the z-axis, the average velocity projected on the line connecting source and observer is zero. Hence, the (classic) Doppler frequency shift is zero. However, source (or observer) has a speed of $v = R\omega$, which generate time dilation, resulting in frequency shift. Specifically, if source is moving on the circle and observer is fixed on z-axis, there is

$$\begin{aligned} \frac{f'}{f} =& \sqrt{1 - v^2/c^2} \\ =& \sqrt{1 - R^2\omega^2/c^2} \end{aligned} \tag{149}$$

Hence, $f' < f$, generating red-shift. In contrast, if source is fixed on z-axis while

observer is rotating around the circle, the relation is

$$\frac{f'}{f} = \frac{1}{\sqrt{1 - R^2\omega^2/c^2}} \tag{150}$$

Therefore, there is blue-shift, as $f' > f$.

In the case that observer is on the x-axis, in Section 8, it has given the general formula of (113) for the Doppler effect, when an observer is located, such as, at **B**, **C** or **D**, which has a distance r_0 from the center of the circle. When relativistic Doppler effect is considered, this formula is only correct when all variables are defined in the reference frame of medium. Accordingly, the formula needs to be presented as

$$T'(t') = T'' + \frac{r_0}{c'}\left[\sqrt{\left(1 - \frac{R}{r_0}\right)^2 + \frac{4R}{r_0}\cos^2\left(\frac{\omega(t'' + T'')}{2}\right)}\right.$$
$$\left. - \sqrt{\left(1 - \frac{R}{r_0}\right)^2 + \frac{4R}{r_0}\cos^2\left(\frac{\omega t''}{2}\right)}\right], \; t'' \geq 0 \tag{151}$$

where t'' and T'' are the variables associated with the moving source in the reference frame of medium. With the aid of the Lorentz transformation,

$$t'' = \frac{t}{\sqrt{1 - R^2\omega^2/c^2}}, \; T'' = \frac{T}{\sqrt{1 - R^2\omega^2/c^2}} \tag{152}$$

Substituting them into (151), a relationship between $T'(t)$ and T, i.e., the relativistic Doppler effect can be obtained.

Note that (151) is not mathematically accurate, as some minor effects are ignored. For example, the change of distance in one period, i.e., the amount given by the bracket of (151), should be small relative to the speed of light. Otherwise, special relativity in terms of the change needs to be involved. Additionally, in the Lorentz transformation of time, the effect of source motion is also ignored.

Since the Lorentz factor is a constant, it can be expected that the relativistic Doppler frequency behaves similarly as the (classic) Doppler frequency, for example, as shown in Example 7. There might be slight corrections on time and frequency, depending on the velocity of circular motion.

Similarly, when source is on the x-axis while an observer is rotating on the circle,

in the reference frame of medium, there is a relation of

$$T''(t'') = T + \frac{r_0}{c'}\left[\sqrt{\left(1-\frac{R}{r_0}\right)^2 + \frac{4R}{r_0}\cos^2\left(\frac{\omega(t''+T''(t''))}{2}\right)} - \sqrt{\left(1-\frac{R}{r_0}\right)^2 + \frac{4R}{r_0}\cos^2\left(\frac{\omega t''}{2}\right)}\right],\ t'' \geq 0 \tag{153}$$

Accordingly, the Lorentz transformations are

$$t'' = \frac{t'}{\sqrt{1-R^2\omega^2/c^2}},\ T''(t'') = \frac{T'(t')}{\sqrt{1-R^2\omega^2/c^2}} \tag{154}$$

Substituting them into (153), the relation for estimating the relativistic Doppler effect can be obtained.

So far, the analysis in the previous sections has covered the Doppler effect in various scenarios, ranging from uniform motion to general motion, and from the (classic) Doppler effect to the relativistic Doppler effect. As a final remark, whenever a wave propagation medium was assumed in the analysis, only a static and uniform medium was considered in the analysis. In other words, medium was assumed to be a static reference frame, while the states of source and observer were defined relative to the medium. In practice, both non-uniform medium and moving medium affect the characteristics of wave propagation within them. A static, non-uniform medium does not introduce a Doppler effect; it only distorts the propagation speed and wavelength. However, a moving medium may impact the Doppler effect. An example is provided below to illustrate this impact.

Assume that a wave source is flying away at a speed v_s relative to a fixed receiver, and is sending EM signals of frequency f. We further assume that the wave propagation medium between source and receiver has a refractive index of n, and that this medium moves in the direction from receiver to source at a speed v_m. The wave propagation speed in the medium is $c' = c/n$. Accordingly, in the principles of special relativity, the wave propagation speed from the source to the receiver (as observed by the receiver) is [20]

$$c^* = \frac{c' - v_m}{1 - c'v_m/c^2} = \frac{c/n - v_m}{1 - v_m/(nc)} \tag{155}$$

Then, following the previous analysis in Section 0.3.3.2, the Doppler frequency is

expressed as

$$f' = f \times \left(\frac{\sqrt{1 - v_s^2/c^2}}{1 + v_s/c^*} \right) \tag{156}$$

Explicitly, the moving medium affects the observed Doppler frequency specifically through the value of c^*, which represents the wave propagation speed relative to the receiver's frame.

0.5 Doppler Effect in Accelerated Motion and Gravitational Fields

In Section 0.4.2, the relativistic Doppler effect in general motion has been analyzed, which can be specialized to the following scenarios containing non-inertial acceleration frame(s):

- source is in acceleration and observer is in an inertial frame,
- source is in an inertial frame and observer is in acceleration, and
- both source and observer are in acceleration.

In this section, we first specifically analyze the Doppler effect in uniform acceleration and, then, extend it to the Doppler effect (or red/blue shift) by gravity, which is the focus of this section. Accordingly, we assume that EM waves propagate in free space and that the direction of wave propagation is collinear with the motion of source and observer, meaning that wave propagates either along or opposite to the direction of acceleration.

0.5.1 Relativistic Doppler Effect in Uniform Acceleration

In Feynman's lecture notes [28] and other modern physics textbooks [20], the Doppler effect by acceleration has been derived directly from the formula of the relativistic Doppler frequency, as seen in (61b). Specifically, when free space and the above-mentioned assumptions are considered, and when the relative speed between source and observer is expressed as Δv, (61b) can be re-written as

$$f' = f \times \sqrt{\frac{1 - \Delta v/c}{1 + \Delta v/c}} \tag{157}$$

where positive and negative values of Δv indicate that source and observer are moving away from and toward one another, respectively. However, in some cases, such as,

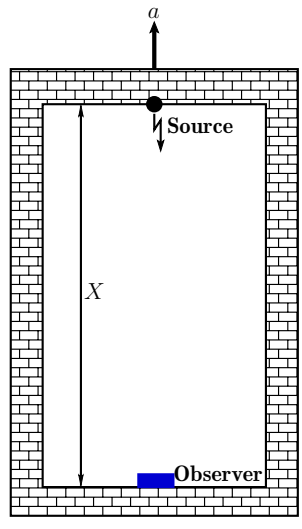

Figure 13: An accelerating frame in which source emits EM signals to an observer of distance X away.

in acceleration frame, the sign of $\Delta v/c$ should be determined based on 'tendency'. If source and observer tend to move away from each other, $\Delta v/c$ is positive. Otherwise, when source and observer tend to move towards each other, $\Delta v/c$ is negative.

Following [20, 28], let us consider Fig. 13, where source and observer separated by a distance X are in the same chamber (frame) that is accelerated with an acceleration of a. Assume that source emits an EM wave of frequency f at t. Accordingly, the velocity of source at t is expressed as v. Assume that $v << c$. Then, the time required for the wave to propagate to observer is $\Delta t = X/c$. Hence, when observer receives the wave, it has a velocity $v' = v + a\Delta t = v + aX/c$. These make $\Delta v = -aX/c$, where the negative sign is because source and observer are tend to move toward each other based on the settings shown in the figure. Moreover, the sign of $\Delta v/c$ can be determined as follows. When wave propagates in the same direction of acceleration a, the sign is positive. Otherwise, when wave propagates in the opposite direction of acceleration a, the sign is negative. Substituting $\Delta v = -aX/c$ into (157) yields

$$f' = f \times \sqrt{\frac{1 + aX/c^2}{1 - aX/c^2}} \tag{158a}$$

$$\approx f\left(1 + \frac{aX}{c^2}\right) \tag{158b}$$

where the approximation is obtained by ignoring a term of a^2X^2/c^4. From (158b),

the Doppler shift satisfies

$$\frac{f_D(=f'-f)}{f} \approx \frac{aX}{c^2} \tag{159}$$

Hence, when the wave propagates in the opposite direction to the acceleration, the Doppler frequency is positive, resulting in a blueshift. Conversely, when the wave propagates in the same direction as the acceleration (making a negative in (159)), the Doppler frequency is negative, resulting in a redshift. In other words, if in the chamber of Fig. 13, when light is emitted in the direction from observer to source, the light will experience redshift.

The formula of (158b) or (159) is derived as a first-order approximation from the relativistic Doppler effect of (157), under the assumption of $v << c$, and the assumptions that the EM signal's period is small, the acceleration a is small, or their joint effect is ignorable. Under these assumptions but except $v << c$, in [29], the relativistic Doppler effect for source/observer in any uniform acceleration was accurately analyzed, showing that the formula of (158b) or (159) is in fact accurate. In other words, no assumption of $v << c$ is needed and the approximation in (158b) or (159) is in fact equality. This is achieved because all the other effects are ideally cancelled by themselves, leaving the Doppler effect exactly the same as that shown in (158b) or (159).

This can also be derived from (140), which is the result from a rigorous analysis of relativistic Doppler effects. For the current accelerating system shown in Fig. 13, let us assume a parallel reference frame moving at the same speed as the source's moving speed at time t, which can be set to $t = 0$ for convenience. Hence, viewing from this parallel reference frame, the speed of source and observer at $t = 0$ is $v = v' = 0$. Since an infinitesimal signal period is considered. We can assume that source emits an EM impulse at $t = 0$. Then, we have $\bar{v} = 0$ and $\bar{v}' = v'(t')$, where $v'(t')$ is the velocity of observer at t' when it receives the impulse. Assume that within t', the distance that observer moves is ΔX. Then, we have the following relations [29, 30]

$$\Delta X = \frac{c^2}{a}\left[\sqrt{1+\left(\frac{at'}{c}\right)^2}-1\right] \tag{160a}$$

$$t' = \frac{X-\Delta X}{c} \tag{160b}$$

$$\bar{v}' = -\frac{at'}{\sqrt{1+\left(\frac{at'}{c}\right)^2}} \tag{160c}$$

where, again, the negative sign associated with $\bar{v}'$ is because observer moves towards source. From (160a) and (160b), t' can be obtained as [29]

$$t' = \frac{X}{c}\left(\frac{1+\frac{aX}{2c^2}}{1+\frac{aX}{c^2}}\right) \tag{161}$$

Substituting it into (160c) gives

$$\bar{v}' = -\frac{\frac{aX}{c}\left(1+\frac{aX}{2c^2}\right)}{\frac{1}{2}\left(\frac{aX}{c^2}\right)^2+\frac{aX}{c^2}+1} \tag{162}$$

Finally, substituting $\bar{v}''(t'') = 0$ and $\bar{v}^*(t^*) = \bar{v}'$ into (140a) or (140c), it can be simplified to obtain

$$\frac{f'}{f} = 1+\frac{aX}{c^2} \tag{163}$$

where f' is independent of t' as the result that both source and observer move in the same acceleration frame. Hence, the formula of (158b) or (159) derived as a first-order approximation from the relativistic Doppler effect of (157) is accurate, on the condition that the period of EM wave is infinitesimal. Below we analyze the Doppler effect without imposing this condition.

The system considered is graphically represented in Fig. 14, where the first and second triangles explain the transmision states of the first and second crests of an EM-wave. In the graph, it is assumed that at $t = 0$, in the parallel frame, source is at X and observer is at $x = 0$. From Fig. 14, the following geometric relations can be

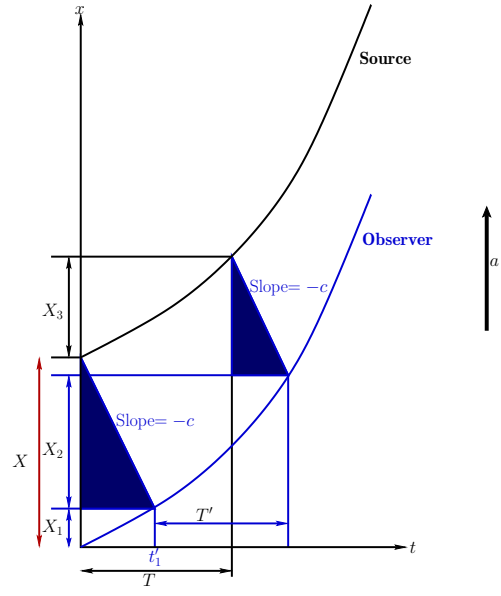

Figure 14: Graphic representation of EM-wave propgation from source to observer within an acceleration frame.

identified:

$$X_1 = \frac{c^2}{a}\left[\sqrt{1+\left(\frac{at_1'}{c}\right)^2}-1\right] \tag{164a}$$

$$X_1 + X_2 = \frac{c^2}{a}\left[\sqrt{1+\left(\frac{a(t_1'+T')}{c}\right)^2}-1\right] \tag{164b}$$

$$X_3 = \frac{c^2}{a}\left[\sqrt{1+\left(\frac{aT}{c}\right)^2}-1\right] \tag{164c}$$

$$t_1' = \frac{X - X_1}{c} \tag{164d}$$

$$T' + t_1' - T = \frac{X + X_3 - X_1 - X_2}{c} \tag{164e}$$

Applying (164d) to (164e) yields

$$T' - T = \frac{X_3 - X_2}{c} \tag{165}$$

From (164a) and (164d), t_1' can be derived to be

$$t_1' = \frac{X}{c}\left(\frac{1+\frac{aX}{2c^2}}{1+\frac{aX}{c^2}}\right) \tag{166}$$

which is a fixed value. Hence, based on (164a) - (164c) and (165), it can be shown that T' and T follow the relation of

$$T'-T = \frac{c}{a}\left[\sqrt{1+\left(\frac{aT}{c}\right)^2}-\sqrt{1+\left(\frac{a(t_1'+T')}{c}\right)^2}+\sqrt{1+\left(\frac{at_1'}{c}\right)^2}-1\right] \tag{167}$$

From (167), although it is cumbersome to obtain an explicit formula for $T/T' = f'/f$, for a given T, an explicit formula for $f' = 1/T'$ can be obtained, which can be expressed as

$$f' = \frac{2k(A+kt_1')}{A^2-k^2(t_1')^2-1} \tag{168}$$

associated with the definitions of

$$k = \frac{a}{c} \tag{169a}$$

$$A = kT+\left[\sqrt{1+\left(\frac{aT}{c}\right)^2}+\sqrt{1+\left(\frac{at_1'}{c}\right)^2}-1\right] \tag{169b}$$

Example 10. *Consider that in an accelerating system with an acceleration* $a = 1000\ m/s^2,\ 10^9\ m/s^2$ *and* $9.18\times10^9\ m/s^2$*, respectively, a source sends radio signals of* $f = 1$ *GHz to an observer having a distance* $X = 1000$ *m behind the source. Find the frequencies of the signals received by the observer, when the formulas* (163) *and* (168) *are respectively applied.*

Solution. *First, when* (163) *is used, the frequencies are*

$$\begin{aligned} f' =& 1,000,000,000.011\ \textit{Hz}\ (\textit{for}\ a = 1000\ m/s^2)\\ =& 1,011,126,500.56\ \textit{Hz}\ (\textit{for}\ a = 10^9\ m/s^2)\\ =& 1,102,131,014.23\ \textit{Hz}\ (\textit{for}\ a = 9.18\times10^9\ m/s^2) \end{aligned}$$

Second, when (168) *is used, the frequencies are*

$$\begin{aligned} f' =& 1,000,000,000.011\ Hz\ (for\ a = 1000\ m/s^2) \\ =& 1,011,126,500.55\ Hz\ (for\ a = 10^9\ m/s^2) \\ =& 1,102,131,013.23\ Hz\ (for\ a = 9.18 \times 10^9\ m/s^2) \end{aligned}$$

The differences between the frequencies calculated from the two formulas are respectively about 10^{-8} *Hz* (*for* $a = 1000\ m/s^2$), 0.01 *Hz* (*for* $a = 10^9\ m/s^2$), *and* 1 *Hz* (*for* $a = 9.18 \times 10^9\ m/s^2$).

The above examples demonstrate that: a) the Doppler effect by acceleration is typically very small and can be ignored for most events; b) the approximated formula (163) is safe to use even when the acceleration is as high as $10^{10}\ m/s^2$. Note that the accelerations on such order can only be found in extreme environments like the vicinity of neutron stars or within high-energy particle accelerators. Nevertheless, nowadays, it is possible for electrons to be accelerated with an acceleration up to $10^{22}\ m/s^2$ by the Laser-Plasma Wakefield Accelerators (LPFA). In the situation of this kind, more accurate evaluation than that by (163) be necessary.

0.5.2 Clock Postulate and Kündig's Experiment Induced Researches

In the above subsection, although the acceleration on Doppler effect is addressed, the Doppler effect is in fact by the acceleration resulted velocity, not by the acceleration itself, as seen from (157) to (158b), for example. This means that the *clock postulate (hypothesis)* [18, 31–33] has been implicitly applied in the analyses. The clock postulate can be stated as that the rate of an ideal clock depends only on its instantaneous velocity, not on its acceleration or other higher-order derivatives of motion [31]. Considering specifically the Doppler effect, the clock postulate can be explained as follows.

Assume a rest source and a general accelerating observer, which has an acceleration $a(t)$ relative to the source. Furthermore, assume that the velocity of observer at t is $v(t)$. In this system, the following reference frames and corresponding time intervals can be defined:

$$\mathcal{K}_s\ (dt, dt_v) \rightarrow \mathcal{K}_v\ (dt_a) \rightarrow \mathcal{K}_a\ (dt') \tag{170}$$

where $\mathcal{K}_s$ and $\mathcal{K}_a$ are the reference frames of source and the accelerating observer, respectively, while $\mathcal{K}_v$ is an inertial frame moving at velocity $v(t)$ in parallel with the observer's reference frame, which is referred to as a *momentarily comoving inertial frame (MCIF)*. Accordingly, dt is time interval at source and dt_v is time interval at observer, both of which are in $\mathcal{K}_s$, while dt_a and dt' are the time intervals in $\mathcal{K}_v$ and

$\mathcal{K}_a$, respectively. With these definitions, the Doppler effect can be represented as

$$\begin{aligned}\frac{f'(t)}{f} =& \frac{dt}{dt'} \\ =& \frac{dt}{dt_v} \times \frac{dt_v}{dt_a} \times \frac{dt_a}{dt'}\end{aligned} \tag{171}$$

The clock postulate explains that, in the above equation,

$$\frac{dt_v}{dt_a} \times \frac{dt_a}{dt'} = \frac{dt_v}{dt'} \tag{172}$$

is satisfied, meaning that observer's accelerating frame $\mathcal{K}_a$ does not need to be considered. In other words, the transformation from $\mathcal{K}_v$ to $\mathcal{K}_a$ is identity, the Doppler effect is only affected by the instantaneous velocity resulted by the acceleration, and the acceleration itself does not generate Doppler effect. Therefore, (171) becomes

$$\begin{aligned}\frac{f'(t)}{f} =& \frac{dt}{dt_v} \times \frac{dt_v}{dt'} \\ =& \left(\frac{f'(t)}{f}\right)_{\text{classic}} \times \frac{1}{\sqrt{1 - v^2(t)/c^2}}\end{aligned} \tag{173}$$

where the first term is the classic Doppler effect in frame $\mathcal{K}_s$, and the second term is due to the Lorentz transformation between $\mathcal{K}_s$ and $\mathcal{K}_v$. But what if the clock postulate is not true? Here comes Kündig's experiment and some researches induced by the results obtained from the experiment.

The experiment by W. Kündig in 1963 measured the transverse Doppler effect in an accelerated system by means of the Mössbauer effect [34]. In the experiment, the transverse Doppler effect was measured via a rotating disk, with the source located at the disk center and the observer (absorber) on the rim of the disk, at a distance $R = 9.3$ cm away from the center. Note that the classic Doppler effect in the experiment is $(f'(t)/f)_{\text{classic}} = 1$. The experimental objective was to test the relativistic dilation of time based on the formula

$$\frac{E_s - E_o}{E_s} = \frac{\Delta E}{E_s} = \sqrt{1 - \frac{v^2}{c^2}} - 1 \approx -\frac{v^2}{2c^2} \tag{174}$$

where E_s and E_o represent the particle (Co^{57}) energy emitted at source and measured at observer, respectively, and $v = R\omega$ with ω the angular velocity.

The experiments with $\omega/2\pi$ between 300 and $35,000$ revolutions per minutes

(RPM) were carried out, obtained the results satisfying [34, 35]

$$\frac{\Delta E}{E_s} = -(1.0065 \pm 0.011)\frac{v^2}{2c^2} \tag{175}$$

which agreed closely with (174). Due to this, Mössbauer's rotor experiments were not repeated for about half a century, until 2008 when Kholmetskii et al. [35] found an error in the data processing of the results obtained from Kündig's experiment. They re-analyzed the results, yielding the relationship of

$$\frac{\Delta E}{E_s} = -(1.192 \pm 0.011)\frac{v^2}{2c^2} \tag{176}$$

which is about 20% higher than Kündig's result or the theoretical result of $v^2/2c^2$.

The finding by Kholmetskii et al. has inspired a lot of the followed researches, as shown in [25] and the references therein. Specifically, relating to the Doppler effect, in light of the Maximal Acceleration theory by Caianiello [36][10], in [37], Friedman suggested to introduce a time dilation by acceleration to the Doppler effect. Reviewing (171), this means that the transformation from frame $\mathcal{K}_v$ to frame $\mathcal{K}_a$ is not identity, but introduces a time dilation of $dt_a/dt' = 1/\sqrt{1 - a^2/a_{\max}}$, in addition to the time dilation $dt_v/dt_a = 1/\sqrt{1 - v^2(t)/c^2}$ yielded by the transformation from frame $\mathcal{K}_s$ to frame $\mathcal{K}_v$. Consequently, the Doppler effect follows a formula of

$$\frac{f'(t)}{f} = \frac{1}{\sqrt{1 - v^2(t)/c^2}} \times \frac{1}{\sqrt{1 - a^2/a_{\max}}} \times \left(\frac{f'(t)}{f}\right)_{\text{classic}} \tag{177}$$

One of the objectives of [37] was to find the maximum acceleration using the results obtained from Kündig's experiment, which was given as $a_{\max} = (1.006 \pm 0.063) \times 10^{19}\ m/s^2$. However, as mentioned in [25], the analysis in [38] shows that the lowest limit of maximum acceleration, if exists, should be near $10^{21}\ m/s^2$.

Some of other researches carried out experiments trying to find a constant k in

$$\frac{\Delta E}{E_s} = -k\frac{v^2}{c^2} \tag{178}$$

These include [39–42], and their results demonstrated a value of $k = 2/3$.

[10] In [36], Caianiello analyzed the fundamental upper limit of a particle's acceleration based on the Heisenberg uncertainty principles in quantum mechanics, showing that $a_{\max} = 2mc^3/\hbar$, where m is particle's rest mass and $\hbar$ is the normalized Planck's constant.

0.5.3 Relativistic Doppler Effect by Gravity

In a uniform gravitational field with field strength g, its Doppler effect can be directly obtained by Einstein's *principle of equivalence*, which states [20]: "There is no local experiment that can be done to distinguish between the effects of a uniform gravitational field in a non-accelerating inertial frame and the effects of a uniformly accelerating (non-inertial) reference frame." Here by local it means that the experiment is carried out within a sufficiently small space in which the gravitational field is uniform. Relating to Doppler effect, the principle of equivalence means that the Doppler effect generated by a uniform gravitational field of strength g is the same as the Doppler effect generated by an accelerating reference frame with the acceleration g.

Hence, following our analysis in Section 0.5.3, all the formulas can be directly applied for estimating the Doppler effect by the gravitational field, by letting $a = g$ and $X = \Delta h$, where Δh denotes the difference in height between source and observer. Specifically, for simplicity, corresponding to (158b)

$$f' \approx f\left(1 + \frac{g\Delta h}{c^2}\right) \tag{179a}$$

$$= f\left(1 + \frac{\Delta\Phi}{c^2}\right) \tag{179b}$$

where $\Delta\Phi$ is the difference between the gravitational potential at source and that at observer, expressed as

$$\Delta\Phi = \Phi_s - \Phi_o \tag{180}$$

The gravitational potential by a body of mass M is defined as [19, 43]

$$\Phi_a = -\frac{GM}{r_a} \tag{181}$$

with "a" for "s" or "o", and $G = 6.674 \times 10^{-11}\ m^3 \cdot kg^{-1} \cdot s^{-2}$ is the gravitational constant. The formula of (181) explains that the gravitational potential at $r_a = \infty$ is zero. However, we note that the location of r_a should be an external point of mass M, meaning that both source and observer are outside mass M. Otherwise, if mass M is spherical, the gravitational potential at any point inside the mass is the same [19].

Substituting (180) and (181) into (179b)

$$f' = f\left(1 + \frac{\Phi_s - \Phi_o}{c^2}\right) \tag{182a}$$

$$= f\left(1 + \frac{GM}{c^2}\left[\frac{1}{r_o} - \frac{1}{r_s}\right]\right) \tag{182b}$$

Hence, when source is above observer, i.e., when the altitude of source is higher than that of observer, (182b) gives $f' > f$, yielding blueshift. By contrast, when source is below observer, (182b) gives $f' < f$, yielding redshift.

Let $f' = 1/dt_o$ and $f = 1/dt_s$. The time dilation between source and observer in a gravitational field of strength g can be approximately expressed as

$$dt_o = dt_s\left(1 + \frac{GM}{c^2}\left[\frac{1}{r_o} - \frac{1}{r_s}\right]\right)^{-1} \tag{183}$$

Above, while the analysis starts with a constant acceleration g, the ended formulas in (182) and (183) are general, where no condition on constant g is required. One of its applications is in satellite communication systems. When a ground station with a smaller r_s, and larger g, sends radio signals to a satellite with a larger r_o, and smaller g, gravitational field will generate redshift on the radio signals. On the opposite way, gravitational field will generate blueshift on the radio signals. Also, a clock on satellite ticks faster than a clock on Earth's surface.

Moreover, in (182a), the two gravitational potentials are not required to be generated by a same body of mass, but can be separately by two bodies, meaning that $\Phi_s = -GM_s/r_s$ and $\Phi_o = -GM_o/r_0$, giving

$$f' = f\left(1 + \frac{G}{c^2}\left[\frac{M_o}{r_o} - \frac{M_s}{r_s}\right]\right) \tag{184}$$

For example, when a photon leaving a star's surface with the potential of about -1.9×10^{11} Joules (J)/kg is observed on the Earth, where the gravitational potential is about -6.2×10^7 J/kg, the relative redshift is about $\Delta f/f = (1.9 \times 10^{11} - 6.2 \times 10^7)/c^2 = 2.11 \times 10^{-6}$, when assuming that the star and the Earth do not impact each other, and there are also no other impacts.

Example 11. *A ground navigation device, at $r_o = 6370$ km, receives the positioning signals on $f = 1.5$ GHz band from a GPS satellite that has an altitude of $26,600$ km. a) Calculate the frequency shift generated by the gravitational differences. b) Calculate the total time shift of the clock on the GPS satellite with respect to the time on Earth over one day.*

Solution. *a) Substituting the respective values into* (182b) *gives*

$$\begin{aligned} f_D =& f' - f = f\left(\frac{GM}{c^2}\left[\frac{1}{r_o} - \frac{1}{r_s}\right]\right) \\ =& 1.5 \times 10^9 \left(\frac{6.674 \times 10^{-11} \times 5.972 \times 10^{24}}{9 \times 10^{16}}\left[\frac{1}{6.37 \times 10^6} - \frac{1}{2.66 \times 10^7}\right]\right) \\ =& 0.7931\ Hz \end{aligned}$$

b) Following the above calculations, the total time shift over one (Earth) day is

$$dt_s = 24 \times 3600 \times 0.7931/1.5 \times 10^9 = 45.68\ \textit{microseconds}\ (\mu s)$$

This example demonstrates that although the Doppler shift is insignificant, the accumulation of time shifts due to gravity is significant.

Above the Doppler effect and time dilation yielded by gravitational field are purely obtained from the principle of equivalence and the extension, no general relativity theory is needed. However, the principle of equivalence is only applicable for uniform gravitational fields, but not for non-uniform, typically, spherical, gravitational fields. Therefore, there is no theoretical basis for (182b) - (184). To fill this gap, let us consider the spherically symmetric gravitational field. In this field, Einstein's field equation (EFE) has a unique solution given by the *Schwarzschild metric* [32, 43], which, after re-introducing the constant c, can be expressed as[11]

$$ds^2 = -c^2\left(1 - \frac{2GM}{rc^2}\right)dt^2 + \left(1 - \frac{2GM}{rc^2}\right)^{-1} dr^2 + r^2\left(d\theta^2 + \sin^2\theta d\phi^2\right) \tag{185}$$

where $r,\ \theta$ and ϕ are the usual spherical polar coordinates, and ds represents the infinitesimal distance. From the Schwarzschild metric we understand that a stationary observer ($dr = d\theta = d\phi = 0$) located at a radial distance r from the body of mass M measures a time interval of

$$dt_r^2 = -\frac{ds^2}{c^2} = \left(1 - \frac{2GM}{rc^2}\right)dt^2 \tag{186}$$

i.e.,

$$dt_r = dt\sqrt{1 - \frac{2GM}{rc^2}} = dt\sqrt{1 + \frac{2\Phi(r)}{c^2}} \tag{187}$$

where dt is the time interval that a stationary observer measures at a distance of

[11] Note that in [32, 43], the Schwarzschild metric is represented with $c = 1$.

$r \to \infty$, and $\Phi(r) = -GM/r$ is the gravitational potential at radius r. Note that the potential $\Phi(r) = -GM/r$ is obtained from assuming that Earth is spherical. If non-spherical Earth is required for high accuracy measurement in, such as, Section 0.7.1, $\Phi(r)$ should include the oblateness term, having the formula of [44]

$$\Phi(r) = -\frac{GM}{r}\left[1 - J_2\left(\frac{a_1}{r}\right)^2 L_2(\cos\phi)\right] \tag{188}$$

where $J_2 = 1.0826300 \times 10^{-3}$ is Earth's quadrupole moment coefficient, $a_1 = 6.3781370 \times 10^6$ is Earth's equatorial radius in meter, ϕ is the polar angle measured downward from the axis of rotational symmetry, and L_2 is the Legendre polynomial of degree 2.

According to [44], dt_r in (187) can also be formulated relative to dt_0 of a clock on the geoid (or surface of the Earth) as

$$dt_r = dt_0\sqrt{1 + \frac{2(\Phi(r) - \Phi_0)}{c^2}} \tag{189}$$

where Φ_0 is the gravity potential at the geoid.

Now assume two observers, located at the radial distances of r_1 and $r_2(> r_1)$, respectively. Then, we have

$$\begin{aligned}\frac{f_{r_1}}{f_{r_2}} = \frac{dt_{r_2}}{dt_{r_1}} =& \frac{dt_{r_2}}{dt_0} \times \left(\frac{dt_{r_1}}{dt_0}\right)^{-1} \\ =& \sqrt{\frac{1 + 2(\Phi(r_2) - \Phi_0)/c^2}{1 + 2(\Phi(r_1) - \Phi_0)/c^2}}\end{aligned} \tag{190}$$

which gives both the time relationship and the frequency relationship between the two observers.

The formulas in (190) are exact results. When both $r_1c^2 >> 2GM$ and $r_2c^2 >> 2GM$, the following approximations hold:

$$\begin{aligned}\frac{f_{r_1}}{f_{r_2}} =& \frac{dt_{r_2}}{dt_{r_1}} \\ \approx& \sqrt{(1 + 2(\Phi(r_2) - \Phi_0)/c^2)(1 - 2(\Phi(r_1) - \Phi_0)/c^2)} \\ \approx& \sqrt{1 + 2\Phi(r_2)/c^2 - 2\Phi(r_1)/c^2} \\ \approx& 1 + \frac{\Phi(r_2)}{c^2} - \frac{\Phi(r_1)}{c^2}\end{aligned} \tag{191}$$

which is (182), obtained via the extension of the result given by the principle of equivalence.

Remark 5. *From* (186) *or* (187) *we find that when* $r = R_s = 2GM/c^2$, $dt_r = 0$. *This* R_s *is the Schwarzschild radius, defines the event horizon of a black hole [32, 43].*

0.6 Doppler Effect by Atmosphere

The Earth's atmosphere significantly affects satellite communications and navigation systems [45]. It diminishes radio signals through processes of scattering and absorption. The non-uniform distribution of air in the atmosphere also obstructs direct LoS signal transmission, introducing timing delays. Furthermore, dynamic atmospheric phenomena, such as rapid fluctuations of electrons in the ionosphere, and variations in temperature, pressure, and humidity within the troposphere, introduce serious randomness to the signals propagating through it. Crucially, this randomness is often difficult to accurately model and predict.

The dynamics in Earth's atmosphere also introduces Doppler effect. In principle, static media do not generate Doppler effect on the signals propagating through them, while dynamic media do. Before analyzing the Doppler effect by the dynamics of Earth's atmosphere, let us consider two simple scenarios to explain the principles.

First, assume that an EM-signal is emitted by a stationary source in vacuum. Then, this signal is propagated through a first layer of medium with a refractive index n_1, and a second layer of medium with a refractive index n_2, to an observer that is rest in the second medium. Assume that the distances that the signal travelled in the first and second media are r_1 and r_2, respectively. Now assume that source emits two adjacent wave crests at $t_1 = 0$ and $t_2 = T$. Ignoring the common distance travelled in the vacuum, observer receives the first crest at $t_1' = \frac{r_1}{c/n_1} + \frac{r_2}{c/n_2}$, and the second at $t_2' = T + \frac{r_1}{c/n_1} + \frac{r_2}{c/n_2}$. Hence, the period of received signal is $T' = t_2' - t_1' = T$. There is no Doppler effect.

Second, following the above example, now assume that the first medium is not on top of the second medium. Instead, the first wave crest is propagated through the first medium directly to observer, and the second wave crest is propagated through the second medium directly to observer. In both cases, the geometric distances that signal travels in media are the same, expressed as r. Accordingly, the first crest is received by observer at $t_1' = \frac{r}{c/n_1}$, and the second crest at $t_2' = T + \frac{r}{c/n_2}$. Consequently, the period of received signal is $T' = t_2' - t_1' = T + \frac{r}{c/n_2} - \frac{r}{c/n_1}$, yielding the Doppler effect expressed as

$$f' = f\left(1 + \frac{r[n_2 - n_1]}{\lambda}\right)^{-1} \tag{192}$$

Hence, there is Doppler effect if $n_2 \neq n_1$, $n_2 > n_1$ yields redshift, while $n_2 < n_1$ yields blueshift.

The Doppler effect, and also the other effects to be addressed in Chapter **??**, by Earth's atmosphere on radio propagations are primarily driven by the troposphere and ionosphere. The troposphere extends from the Earth's surface to an altitude of several tens of kilometers. It is the non-ionized portion of the atmosphere and contains the bulk of its air and water vapor. Above it lies the ionosphere, which extends upward for several hundred kilometers. Because of their distinct physical properties, these layers affect radio propagation differently. Consequently, the following sections analyze their respective Doppler effects separately, beginning with the ionosphere and followed by the troposphere.

For simplicity, the following Doppler effect analysis is based on (16), repeated as

$$f_D = -\frac{f}{c}\frac{dP(n,t)}{dt} \tag{193a}$$

$$= -\frac{f}{c}\frac{d}{dt}\int_{\mathcal{P}(t)} n(p,t)dp \tag{193b}$$

where, to clarify, $P(n,t)$ is the phase path from wave source (satellite or ground station) to observer (ground station or satellite, correspondinly), $\mathcal{P}(t)$ is the geometric path from source to observer, which is not necessary a straight line, and $n(p,t)$ is the refractive index at a point p on $\mathcal{P}(t)$.

Assume that source and observer are at $p_s(t)$ and $p_o(t)$, respectively, which are the starting and ending points of $\mathcal{P}(t)$ at t. Then, with the aid of the Leibniz integral rule, (193b) can be written as

$$\begin{aligned} f_D =& -\frac{f}{c}\left[\int_{\mathcal{P}(t)} \frac{\partial n(p,t)}{\partial t}dp + n(p_o(t),t)\frac{p_o(t)}{dt} - n(p_s(t),t)\frac{p_s(t)}{dt}\right] \\ =& f_{DA} + f_{DM} \end{aligned} \tag{194}$$

where, by definition,

$$f_{DA} = -\frac{f}{c}\int_{\mathcal{P}(t)} \frac{\partial n(p,t)}{\partial t}dp \tag{195a}$$

$$f_{DM} = -\frac{f}{c}\left[n(p_o(t),t)\frac{p_o(t)}{dt} - n(p_s(t),t)\frac{p_s(t)}{dt}\right] \tag{195b}$$

Explicitly, f_{DM} is the Doppler effect because of the relative motion between source and observer, which has been analyzed in the previous sections. In contrast, f_{DA} is the Doppler effect by the medium along the propagation path. Hence, f_{DA} captures the frequency shifts caused by time-varying atmospheric conditions (e.g., passing weather fronts, pressure changes, or ionospheric fluctuations), even if both source

and observer are stationary. Hence, to focus on the atmospheric Doppler effect, contributions from other phenomena, such as motion and gravity, are excluded from the analysis, unless their inclusion is essential. In other words, the following analyses focus mainly on f_{DA}.

In the expression for f_{DA} in (195a), the time derivative of the refractive index, $\partial n/\partial t$, is a scalar field. Consequently, its line integral with respect to the arc length dp is independent of the direction of integration. This is expressed as

$$f_{DA} = -\frac{f}{c}\int_{\mathcal{P}(t)} \frac{\partial n(p,t)}{\partial t} dp = -\frac{f}{c}\int_{-\mathcal{P}(t)} \frac{\partial n(p,t)}{\partial t} dp \tag{196}$$

In the context of satellite communications, this mathematical identity implies that the atmospheric Doppler contribution for the ground-to-satellite link (uplink) is identical to that of the satellite-to-ground link (downlink) for a given path at time t.

Furthermore, because line integration satisfies the additive property, the total path $\mathcal{P}(t)$ can be partitioned into component segments. Specifically, by dividing the path into $\mathcal{P}_T(t)$, traversing the troposphere, and $\mathcal{P}_I(t)$, passing through the ionosphere, we obtain

$$f_{DA} = \underbrace{-\frac{f}{c}\int_{\mathcal{P}_T(t)} \frac{\partial n(p,t)}{\partial t} dp}_{f_{DA,T}} \underbrace{-\frac{f}{c}\int_{\mathcal{P}_I(t)} \frac{\partial n(p,t)}{\partial t} dp}_{f_{DA,I}} \tag{197}$$

This demonstrates that the Doppler effects induced by the troposphere and ionosphere can be analyzed as independent, additive terms.

Below we first analyze the Doppler effect by the ionosphere, i.e., $f_{DA,I}$ in (197).

0.6.1 Doppler Effect by Ionosphere

As shown in the expression (197), the analysis of the ionospheric Doppler effect depends on two issues: a) the mathematical modeling of the propagation path $\mathcal{P}(t)$, and b) the mathematical modeling of the local refractive index n associated with $\mathcal{P}(t)$. The refractive index n is primarily determined by the local electron density and distribution, which, in cold plasma, can be calculated from the Appleton-Hartree equation [46–48]

$$n^2 = 1 - \frac{X}{1 - jZ - \dfrac{Y^2\sin^2\theta}{2(1-X-jZ)} \pm \sqrt{\dfrac{Y^4\sin^4\theta}{4(1-X-jZ)^2} + Y^2\cos^2\theta}} \tag{198}$$

where

- $j = \sqrt{-1}$;
- $X = f_N^2/f^2$: the ratio of the square of the plasma frequency f_N to the wave frequency f;
- $Y = f_H/f$: the ratio of the electron gyro-frequency f_H to the wave frequency;
- $Z = f_v/f$: the ratio of the electron collision frequency f_v to the wave frequency;
- θ: the angle between the wave vector and the magnetic field vector;
- $Y\cos\theta$ and $Y\sin\theta$: Longitudinal and transverse components of Y relative to the wave propagation direction;
- $\pm$ signs: '+' is for the refractive index of ordinary wave, while '-' is for the refractive index of extraordinary wave.

Furthermore, $f_N = (2\pi)^{-1}\sqrt{N_e q^2/\varepsilon_0 m_e}$, where N_e is the electron density, ε_0 is the free space dielectric permittivity, q is the electron charge and m_e is the mass of electron. $f_H = (2\pi)^{-1} qB_0/m_e$, with B_0 the strength of geomagnetic field.

Explicitly, it is not easy to analytically derive an expression for n that can be applied to (197) for further Doppler effect analysis. The refractive index in various ionospheric scenarios has been analyzed in [46]. In our case of focusing on the principles and considering satellite communications, which typically use frequencies > 1 GHz, the refractive index can be approximately expressed as [49, 50]

$$n \approx \sqrt{1 - X} = \sqrt{1 - \frac{\kappa N_e}{f^2}} \tag{199}$$

where $\kappa = q^2/4\pi^2\varepsilon_0 m_e = 80.61\ m^3/s^2$. When $\kappa << f^2$, n can be further approximated as

$$n \approx 1 - \frac{\kappa N_e}{2f^2} \tag{200}$$

which is a function of the electron density distribution. Substituting this into $f_{DA,I}$ in (197) gives

$$f_{DA,I} = \frac{\kappa}{2fc}\int_{\mathcal{P}_I(t)} \frac{\partial N_e(p,t)}{\partial t} dp \tag{201}$$

Example 12. *Assume that signals are transmitted from ground station to satellite. Assume that Earth's ionosphere is modeled as a simple flat ionosphere layer [49] in*

which the electron density increases linearly with altitude above a minimum height h_0 and changes with time, expressed as

$$N_e(z,t) = \alpha[z - h_0],\ z \geq h_0 \tag{202}$$

where both α and h_0 may be functions of time, depending on the models.

In relation with this simple ionosphere model, a ray model for propagation path is proposed, which is a straight line from ground to h_0, and then traces a parabola above h_0, represented as [46, 49]

$$x = h_0 \cot\theta_E + \frac{2f^2}{\alpha\kappa}\cos\theta_E \left(\sin\theta_E - \left[\sin^2\theta_E - \frac{\alpha\kappa(z-h_0)}{f^2}\right]^{1/2}\right),\ z \geq h_0 \tag{203}$$

where x is the horizontal distance, measured from the wave launching point, and θ_E is the ray's launch elevation angle, which is the angle between the local horizontal plane and the ray's direction towards a considered satellite.

In (202)*, when assuming that α is a constant while h_0 is time-varying, according to [49], the Doppler frequency can be found to be*

$$f_{DA,I} = -\frac{fV_z}{c}\left(\sin\theta_E + \cos^2\theta_E \times \log\left[\sqrt{\frac{1+\sin\theta_E}{1-\sin\theta_E}}\right]\right) \tag{204}$$

where $V_z = dh_0/dt$ is the time-varying rate of h_0.

Note that, in [49], the case of time-varying α and constant h_0 in (202) *has also been considered, giving*

$$f_{DA,I} = -\frac{f}{c}\sin\theta_E\left(\frac{D}{3\cos^2\theta_E} - \frac{8f^2\sin\theta_E\cos\theta_E}{3\alpha\kappa}\right)\frac{d\theta_E}{dt} \tag{205}$$

where D is a constant given by

$$D = 2\left(h_0\cot\theta_E + \frac{2f^2}{\alpha\kappa}\cos\theta_E\sin\theta_E\right) \tag{206}$$

Other models of electron density includes the exponential model, which can in general be expressed as [51]

$$N_e(h,t) = N_0\exp(-\alpha[h - h_0]),\ h \geq h_0 \tag{207}$$

where h is altitude and the other parameters can be set according to scenarios, as seen, for example, in [51].

Another fundamental model for the electron density in the ionosphere is the

Chapman model [46, 52–54]. Specifically, the widely used model for the vertical profile of electron density in the E and F layers is represented by the α-Chapman function as

$$N_e(h) = N_{\max} \exp\left(0.5[1 - z - \exp(-z)]\right) \tag{208}$$

where $N_{\max}$ is the peak electron density and $z = (h - h_{\max})/H$. Here $h_{\max}$ is the altitude of peak density, typically 250-400 km for the F2 layer, and $H = \kappa_B T_K/mg$ is the ionospheric scale height, where κ_B is the Boltzmann constant, T_K is the absolute plasma temperature, m is the mean ion mass and g is the acceleration by gravity.

Example 12 demonstrates that, even for such a simple ionospheric scenario, deriving the analytical solution for the Doppler shift is highly involved. Hence, for convenience of ionospheric calculations, the total electron content (TEC) is introduced, which is defined as the integral of the free electron density along the direct path between the satellite (A) and the receiver (B), expressed as

$$\text{TEC} = \int_A^B N_e(s) ds \tag{209}$$

Accordingly, for a high-frequency satellite link, when applying (209) into (201), the Doppler shift introduced specifically by the ionosphere can be written as

$$f_{DA,I} = \frac{\kappa}{2fc} \frac{d(\text{TEC})}{dt} \tag{210}$$

Note that, at the NASA CDDIS Global Ionosphere Maps and NOAA's GloTEC Data Center[12], real-time and historical vertical TEC (VTEC) values for specific grid coordinates on Earth are regularly published in IONEX format. Once VTEC data are known, they can be converted to slant TEC (STEC) data for path-specific ionospheric calculations using a geometric mapping function [55].

0.6.2 Doppler Effect by Troposphere

To analyze the Doppler effect by the troposphere, let us return (193b), which includes the effect from both medium and relative motion. To focus on the effect by medium

[12] https://www.swpc.noaa.gov/products/us-total-electron-content, https://www.earthdata.nasa.gov/data/space-geodesy-techniques/gnss/data-products-holdings

in troposphere, its Doppler effect can be written as

$$\begin{aligned} f_{DA,T} =& -\frac{f}{c}\frac{d}{dt}\left[\int_{\mathcal{P}_T(t)} n(p,t)dp - \int_{\mathcal{G}_T} dp\right] \\ =& -\frac{f}{c}\frac{d}{dt}(\Delta p(n,t)) \end{aligned} \tag{211}$$

with Δp defined as

$$\Delta p(n,t) = \int_{\mathcal{P}_T(t)} n(p,t)dp - \int_{\mathcal{G}_T} dp \tag{212}$$

Consider the case that signals are transmitted from a ground station to a satellite. Then, in (212), the first integral in the bracket is taken along the bended signal path through the troposphere, while the second integral is along the tropospheric potion of the slant path[13]. It is shown that [56], when n along path $\mathcal{P}_T(t)$ and that along path $\mathcal{G}_T$ are sufficiently similar, $\int_{\mathcal{P}_T(t)} n(p,t)dp \approx \int_{\mathcal{G}_T} n(p,t)dp$, giving

$$\begin{aligned} \Delta p(n,t) \approx& \int_{\mathcal{G}_T} n(p,t)dp - \int_{\mathcal{G}_T} dp \\ =& \int_{\mathcal{G}_T} [n(p,t)-1)]dp \end{aligned} \tag{213}$$

As noted in [56], the error generated by the replacement of $\mathcal{P}_T(t)$ using $\mathcal{G}_T$ is a second-order effect, which may reach about 10% of Δp at the horizon, but is typically negligible provided that the elevation angle is above 3^o or 4^o.

Since the refractive index n of air in troposphere is very small, the refractivity defined as $N \equiv 10^6(n-1)$ is usually instead used in studies. Applying this into (213) yields

$$\Delta p(n,t) = 10^{-6}\int_{\mathcal{G}_T} N(p,t)dp \tag{214}$$

In contrast to the ionosphere, where refractive index is depended on frequency and ions, as shown in (198) and (200), typically, the refractivity in the troposphere is a function of temperature, pressure and humidity. Considering these factors, for example, an expression that is good to 0.5% in N for frequencies upto 30 GHz has

[13]The slant path between a ground station and a satellite is the LoS path from the ground station to the satellite.

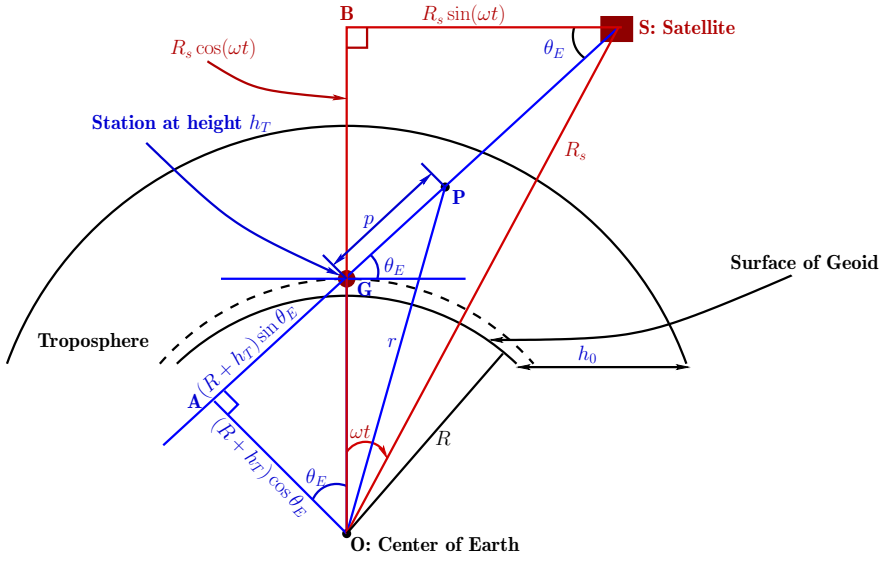

Figure 15: Illustration of geometries for tropospheric analysis.

been obtained from a set of meteorological ballon data, which is expressed as [57]

$$N = \frac{77.6}{T_K}\left(P + \frac{4810e}{T_K}\right) \tag{215}$$

where P is the total pressure and e is the partial presure of water vapor, both in millibars, and T_K is absolute temperature.

Furthermore, during the passing interval of a satellite, the refractivity N of air in the troposphere is approximately a function of height above the Earth, but is independent of both the horizontal locations and time. Therefore, (214) can be further approximated as

$$\Delta p(n,t) \approx 10^{-6} \int_{R+h_T}^{R+h_0} N(r)\left(\frac{dp}{dr}\right) dr \tag{216}$$

where r is the radial distance from the Earth's center, R is the radius of the Earth (or of the geoid at the ground station), h_T is the height of the ground station, and h_0 is the height above which the tropospheric refraction becomes negligible, as shown in Fig. 15.

Substituting (216) into (211) gives the Doppler effect by the troposphere ex-

pressed as

$$f_{DA,T} \approx -\frac{10^{-6} f}{c} \frac{d}{dt} \int_{R+h_T}^{R+h_0} N(r) \left(\frac{dp}{dr}\right) dr \tag{217}$$

From Fig. 15 we can know that, in (217), p is a function of r and the elevation angle θ_E. For a given r, the elevation angle θ_E is time-varying during the passing of a satellite. Considering these relationships, (217) can be then represented as

$$\begin{aligned} f_{DA,T} =& -\frac{10^{-6} f}{c} \int_{R+h_T}^{R+h_0} N(r) \frac{\partial}{\partial \theta_E} \left(\frac{dp}{dr}\right) \frac{d\theta_E(t)}{dt} dr \\ =& -\frac{10^{-6} f}{c} \left[\int_{R+h_T}^{R+h_0} N(r) \frac{\partial}{\partial \theta_E} \left(\frac{dp}{dr}\right) dr\right] \frac{d\theta_E(t)}{dt} \\ =& \frac{10^{-6} f}{c} \times f(\theta_E) \times \frac{d\theta_E(t)}{dt} \end{aligned} \tag{218}$$

where $f(\theta_E)$ is defined as

$$f(\theta_E) = -\int_{R+h_T}^{R+h_0} N(r) \frac{\partial}{\partial \theta_E} \left(\frac{dp}{dr}\right) dr \tag{219}$$

Based on the geometries shown in Fig. 15 (using $\triangle$OAP and $\triangle$OAG), it can be found that

$$p(r, \theta_E) = \sqrt{r^2 - (R + h_T)^2 \cos^2 \theta_E} - (R + h_T) \sin \theta_E \tag{220}$$

Then, the derivative of p first with respect to r and then with respect to θ_E can be calculated to be

$$\frac{\partial}{\partial \theta_E} \left(\frac{dp}{dr}\right) = -\frac{r(R + h_T)^2 \sin(2\theta_E)}{2[r^2 - (R + h_T)^2 \cos^2 \theta_E]^{3/2}} \tag{221}$$

Substituting it into (219) and completing the integration for a given $N(r)$, $f(\theta_E)$ can be obtained.

Next, to derive $d\theta_E(t)/dt$ in (218), for simplicity, the Earth is assumed to be a sphere with radius R, the orbit of satellite is assumed to be circular with a radiun of R_s, and the angular speed of satellite is expressed as ω. Then, from the geometries shown in Fig. 15 (using $\triangle$SBO and $\triangle$SBG), we have

$$\tan \theta_E(t) = \frac{R_s \cos(\omega t) - (R + h_T)}{R_s \sin(\omega t)} \tag{222}$$

when it is assumed that $t = 0$ occurs at the point when the satellite is right over the

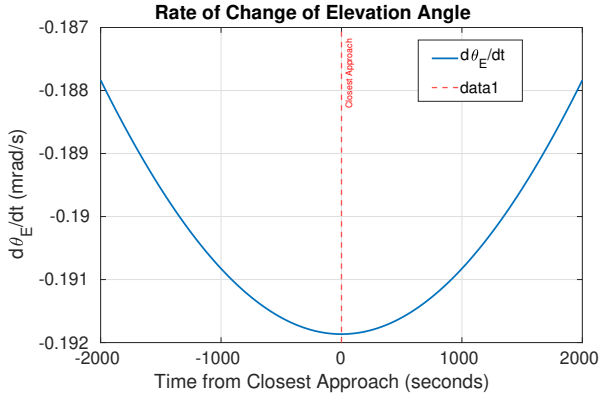

Figure 16: Illustration of $d\theta_E/dt$ for a GPS satellite with the parameters of $R = 6378.137$ km, $R_s = 26560$ km and the orbital period of $T_s = 43082$ s (12 h).

ground station. Then, it can be shown that

$$\begin{aligned}\frac{d\theta_E}{dt} =& \omega \left[\frac{R_s(R+h_T)\cos(\omega t) - R_s^2}{R_s^2 + (R+h_T)^2 - 2R_s(R+h_T)\cos(\omega t)} \right] \\ \approx& \omega \left[\frac{R_s R\cos(\omega t) - R_s^2}{R_s^2 + R^2 - 2R_s R\cos(\omega t)} \right] \end{aligned} \tag{223}$$

where the approximation is due to $h_T << R$.

Consider a GPS satellite, which has the orbital period of about $T_s = 12$ hours, Fig. 16 shows the rate of change of elevation angle during the passing time of a satellite, where $t = 0$ in the middle aligns with the point when the satellite is overhead of the ground station. As the absolute value of $d\theta_E/dt$ reaches its maximum at $t = 0$, the angular sensitivity of the signal path through the atmosphere is greatest when the satellite is directly overhead. Consequently, the dynamics of the elevation-dependent Doppler corrections are most pronounced at this point of closest approach.

Remark 6. *In [56], the reference of* $t = 0$ *was defined at the point when satellite is closest to the center of Earth. Accordingly, the expression for* $d\theta_E/dt$ *was derived, which is different from* (223).

In literature, there are various formulas proposed for modeling $N(r)$ [51, 56–58]. Below two examples from [56, 58] as well as their resulted $f(\theta_E)$ are provided.

Example 13. *In [56], an quadratically approximated model of* $N(r)$ *to the three-*

part model [51] was proposed, which is expressed as

$$N(r) = a\left[r - (R + h_0)\right]^2 \tag{224}$$

where a can be obtained from boundary conditions. For example, given N_T at $r = R + h_T$ (location of ground station), a can be found to be $a = N_T/(h_0 - h_T)$. Upon substituting this and (221) *into* (219) *and completing the integration, it can be shown that*

$$\begin{aligned} f(\theta_E) =& N_T r_T \left[\cos\theta_E + \frac{r_T \sin(2\theta_E)}{h_{tro}^2}\left[\sqrt{r_T^2 \sin^2\theta_E + 2r_T h_{tro} + h_{tro}^2}\right.\right. \\ & \left.\left. - r_T \sin\theta_E + r_{tro} \ln\left(\frac{r_T(1+\sin\theta_E)}{r_{tro} + \sqrt{r_T^2 \sin^2\theta_E + 2r_T h_{tro} + h_{tro}^2}}\right)\right]\right] \end{aligned} \tag{225}$$

where, by definition, $r_T = R + h_T$, $h_{tro} = R - h_T$ and $r_{tro} = R + h_0$.

The results provided in [56] demonstrated that, with the aid of this quartic tropospheric refractivity model, approximately 90% of the tropospheric effect on the Doppler effect could be removed, and hence allowing to achieve the satellite-relied navigation of higher accuracy.

Example 14. *In [58], a quartic tropospheric refractivity model was developed for evaluation of Doppler effect in troposphere. In this model, the refractivity profile in* (215) *is divided into two components, expressed as*

$$N(r) = N_d(r) + N_w(r) \tag{226}$$

where N_d is the 'dry' component for dry air, and N_w is the 'wet' component for water vapour. The models for these components are expressed as

$$N_x(r) = \begin{cases} \frac{N_{T_x}}{(h_{0x} - h_T)^4}(h_{0x} - r)^4, & r \le h_{0x} \\ 0, & r > h_{0x} \end{cases} \tag{227}$$

where 'x' stands for 'd' or 'w'. In (227)*, N_{T_x} is the refractivity at ground station, and h_{0d} and h_{0w} are the heights above which the corresponding tropospheric refraction becomes negligible*[14]*. All heights are measured with respect to the geoid. Then,*

[14]Note that, as shown in [58], the height h_{0d} may reach about 40 km, while h_{0w} only reaches 12 km of maximum.

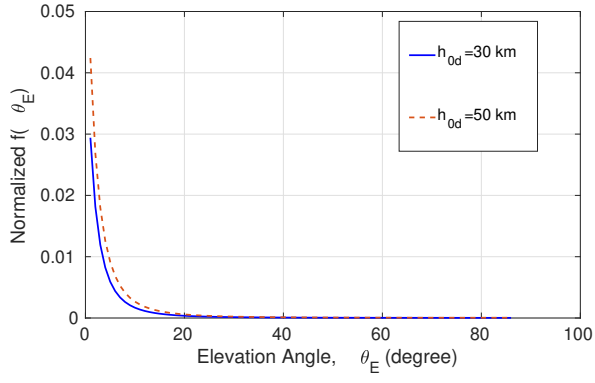

Figure 17: Illustration of $f(\theta_E)$ for $h_{0d} = 30$ and 50 kilometers, when other parameters are $R = 6378.137$ km, $h_T = 0$, $N_{T_d} = 315$, $N_{T_w} = 50$ and $h_{0w} = 12$ km.

according to [58], it can be derived that

$$f(\theta_E) = r_T \times \sum_{x\in\{d,w\}} N_{T_x} F_{4x}(\theta_E) \tag{228}$$

where for $x \in \{d, w\}$, $F_{4x}(\theta_E)$ *is expressed as*

$$\begin{aligned} F_{4x}(\theta_E) = &\cos\theta_E \left(1 + \frac{4l_1}{h_{tro_x}^4}\left[\frac{l_{3x}^3 - l_1^2}{3} + l_{3x}\left(l_2^2 + \frac{3r_{tro_x}^2}{2}\right)\right.\right. \\ &- l_1\left(l_2^2 - \frac{3r_T r_{tro_x}}{2} + 3r_{tro_x}^2\right) \\ &\left.\left. + \left(\frac{3r_{tro_x} l_2^2}{2} + r_{tro_x}^2\right)\ln\left(\frac{r_T + l_1}{r_{tro_x} + l_{3x}}\right)\right]\right) \end{aligned} \tag{229}$$

In (229), $r_T = R + h_T$, $h_{tro_x} = h_{0x} - h_T$, $r_{tro_x} = r_T + h_{tro_x}$, $l_1 = r_T \sin\theta_E$, $l_2 = r_T \cos\theta_E$, *and* $l_{3x} = \sqrt{r_{tro_x}^2 - l_2^2}$.

The results provided in [58] show that the Doppler effects by both 'dry' and 'wet' can be closely modelled by the proposed models for $N_d(r)$ *and* $N_w(r)$. *Their effectiveness is evidenced by their close matching to any local average profile of refractivity, in terms of the reduction of Doppler residuals and navigation errors.*

Fig. 17 illustrates the profile of $f(\theta_E)$ *with* θ_E, *showing that the impact reduces as the elevation angle increases. Note that the model also becomes less accurate as the elevation angle is small, such as, below* 10 *degree. Note additionally that* $f(\theta_E)$, *i.e.,* (225), *in Example 13 appears a similar shape as the curves in Fig. 17, as shown in [56].*

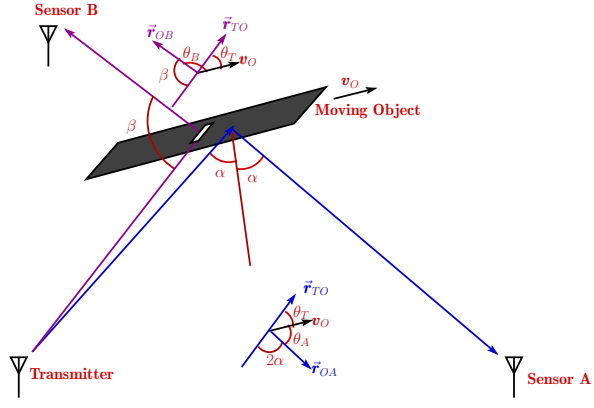

Figure 18: Illustration for analyzing the Doppler shift by a moving object being sensed.

0.7 Doppler Effect in Applications

Having analyzed the Doppler effect by individual phenomena in previous sections, in this section, we examine two representative applications where multiple Doppler-generating factors may occur simultaneously.

0.7.1 Land Target Sensing

Fig. 18 shows a land wireless sensing scenario where a transmitter sends signals of frequency f to probe objects in the vicinity. Transmitter, sensors and object are all assumed on the same, such as xy, plane. Although the analyses are similar, two sensing scenarios are considered. In Scenario A, signals sent by transmitter are reflected to Sensor A, where the Doppler shift is estimated. In this case, the angle of incidence is equal to the angle of reflection, both expressed as α in Fig. 18. By contrast, in Scenario B, signals sent by transmitter is diffracted by the moving object to Sensor B, where the Doppler shift is estimated.

Both transmitter and sensors are assumed to be fixed, while the object being sensed is moving with a velocity vector $\boldsymbol{v}_o$, and $\hat{\boldsymbol{r}}_{XY}$ is a unit vector in the direction from position X to position Y. Let $\arg(\boldsymbol{z})$ be the angle of $\boldsymbol{z}$ defined referred to x-axis. The angles in the figure are defined as follows: $\theta_A = \arg(\boldsymbol{v}_o) - \arg(\hat{\boldsymbol{r}}_{OA})$, $\theta_T = \arg(\hat{\boldsymbol{r}}_{TO}) - \arg(\boldsymbol{v}_o)$, $\theta_B = \arg(\hat{\boldsymbol{r}}_{OB}) - \arg(\boldsymbol{v}_o)$, and $\beta = 180 - (\arg(\hat{\boldsymbol{r}}_{OB}) - \arg(\hat{\boldsymbol{r}}_{TO}))$. As in previous sections, the relative velocity of moving away is positive and that moving towards each other is negative. To embrace generality, relativistic Doppler effect is analyzed, with motion is relative to the Earth's reference frame. Also assumed is signal transmission in vacuum.

Let us first analyze Scenario A. According to Fig. 18, the velocity projected on

the line connecting transmitter and object is

$$v_{TO} = |\boldsymbol{v}_o| \cos\theta_T \tag{230}$$

and the velocity projected on the line connecting object and sensor A is

$$v_{OA} = -|\boldsymbol{v}_o| \cos\theta_A \tag{231}$$

Assume that the proper times at transmitter, object and Sensor A are expressed as T, T_o and T', respectively. Signal transmission from transmitter to object follows the case of rest source moving observer, which has been analyzed in Section 0.3.3. Then, by combining (69) and (70), T and T_o has the relation of

$$T = T_o \frac{1 - v_{TO}/c}{\sqrt{1 - |\boldsymbol{v}_o|^2/c^2}} \tag{232}$$

By contrast, signal transmission from object to Sensor A is in the case of moving source rest observer, which has also been analyzed in Section 0.3.3. Correspondingly, based on (66), the relationship between T_o and T' can be represented as

$$T_o = T' \times \frac{\sqrt{1 - |\boldsymbol{v}_o|^2/c^2}}{1 + v_{OA}/c} \tag{233}$$

Substituting T_o of (233) into (232) gives

$$T = T' \frac{1 - v_{TO}/c}{1 + v_{OA}/c} \tag{234}$$

Eq.(234) shows that the relativistic terms in (232) and (233) cancel each other, making the formulas in both relativistic and non-relativistic cases the same. This result is expected, as both transmitter and Sensor A are in the same reference frame, and the motion of object is also relative to this reference frame.

From (234) the Doppler shift $f_D = f' - f = 1/T' - 1/T$ can be derived to have the formula of

$$\begin{aligned} f_D &= -\frac{f(v_{TO}/c + v_{OA}/c)}{1 + v_{OA}/c} \\ &\approx -\frac{f(v_{TO} + v_{OA})}{c} \end{aligned} \tag{235}$$

Substituting (230) and (231) into (235) yields

$$f_D(\theta_T, \theta_A) = -\frac{f|\boldsymbol{v}_o|(\cos\theta_T - \cos\theta_A)}{c} \tag{236}$$

Furthermore, according to the geometry in Fig. 18, we have $\theta_A = 180 - 2\alpha - \theta_T$. Applying this into (236) results in

$$f_D(\alpha, \theta_T) = -\frac{f|\boldsymbol{v}_o|[\cos\theta_T + \cos(2\alpha + \theta_T)]}{c} \tag{237}$$

When $\alpha \neq 0$, the Doppler shift of (237) is that in the bi-static sensing scenario [59, 60], where signal transmitter and sensor are at different locations, hence unable to share a common clock. By contrast, in the mono-static sensing scenario where transmitter and sensor are co-located [61], allowing to share the same clock, $\alpha = 0$. Accordingly, (237) becomes

$$f_D(\alpha, \theta_T) = -\frac{2f|\boldsymbol{v}_o|\cos\theta_T}{c} \tag{238}$$

In the context of Scenario B, following the similar steps as above, a Doppler shift formula similar to (236) is

$$f_D(\theta_T, \theta_B) = -\frac{f|\boldsymbol{v}_o|(\cos\theta_T - \cos\theta_B)}{c} \tag{239}$$

According to the geometry in Fig. 18, the relationship of $\theta_B = 180 - \beta + \theta_T$ holds. Hence,

$$f_D(\beta, \theta_T) = -\frac{f|\boldsymbol{v}_o|[\cos\theta_T + \cos(\beta - \theta_T)]}{c} \tag{240}$$

In practice, when the locations of transmitter, Sensor A and Sensor B are known, and when α and β are already estimated, the velocity $\boldsymbol{v}_o$ of the object may be calculated after Sensors A and B estimated the respective Doppler shifts. This can be achieved via solving the simultaneous equations of (237) and (240) for $|\boldsymbol{v}_o|$ and θ_T.

0.7.2 Satellite Navigation

In satellite communication and navigation systems, the motion states and positions are all given with respect to the Earth-Centered Inertial (ECI) frame. Referring to Fig. 19, the coordinates in the ECI frame are defined as follows [62, 63]:

- Origin: Located at the Earth's center of mass (geocenter).
- $z^{(c)}$-axis: Aligned with the Earth's rotation axis, pointing towards the North Pole.
- $x^{(c)}$-axis: Points towards the vernal equinox, defined as the intersection of the Earth's equatorial plane and the ecliptic plane (the plane of the Earth's orbit around the sun).

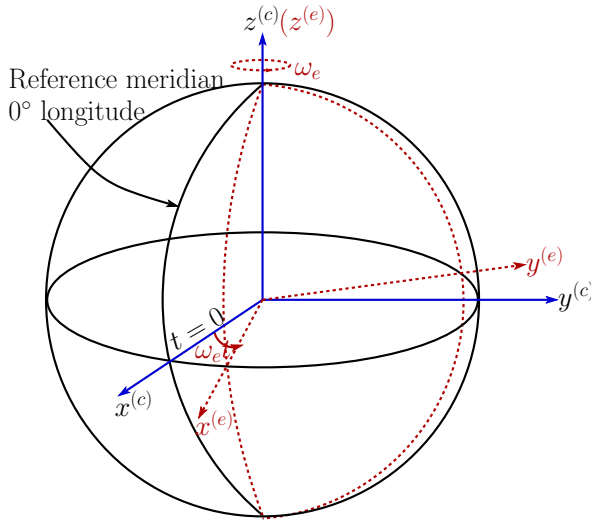

Figure 19: Illustration of ECI and ECEF frames.

- $y^{(c)}$-axis: Completes a right-handed orthogonal system, lying in the equatorial plane and directed $90°$ east of the $x^{(c)}$-axis.

By contrast, in satellite-based navigation or sensing, the motion states and positions of objects, such as land vehicles, airplanes, unmanned aerial vehicles (UAVs), etc., on or near Earth's surface, are referred to the Earth-Centered, Earth-Fixed (ECEF) frame, i.e., Earth's surface or ground. Referring to Fig. 19, the coordinates in the ECEF frame are defined as follows [62, 63]:

- Origin: Coincident with the Earth's center of mass, which is the same as the origin in ECI frame.
- $z^{(e)}$-axis: Points toward the North Pole, specifically aligned with the Conventional Terrestrial Pole (CTP).
- $x^{(e)}$-axis: Formed by the intersection of the equatorial plane and the reference meridian (Greenwich meridian).
- $y^{(e)}$-axis: Completes a right-handed orthogonal system, lying in the equatorial plane and directed $90°$ east of the $x^{(e)}$-axis.

Hence, to use the signals sent by satellites to carry out sensing/navigation, the motion states and position vectors need to be transformed from the ECEF frame to the ECI frame. Express the angular velocity of Earth's rotation relative to the ECI frame as $\boldsymbol{\omega}_{ce}^{(e)} = [0, 0, \omega_e]^T$, which is the angular velocity of the ECEF frame rotating

with respect to the ECI frame. Then, referring to Fig. 19, it can be shown that the transformation matrix from the ECI frame to the ECEF frame is [62]

$$\boldsymbol{R}_{ec} = \begin{bmatrix} \cos(\omega_e t) & \sin(\omega_e t) & 0 \\ -\sin(\omega_e t) & \cos(\omega_e t) & 0 \\ 0 & 0 & 1 \end{bmatrix} \tag{241}$$

where $t = 0$ is defined as the instant when the $x^{(e)}$-axis of the ECEF frame aligns with the $x^{(c)}$-axis of the ECI frame. $\boldsymbol{R}_{ec}$ is an orthonormal matrix for carrying out the transformation from ECI frame to ECEF frame.

Accordingly, the transformation matrix from the ECEF frame to the ECI frame is

$$\boldsymbol{R}_{ce} = \boldsymbol{R}_{ec}^{-1} = \boldsymbol{R}_{ec}^{T} \tag{242}$$

$\boldsymbol{R}_{ce}$ carries out the transformation from ECEF frame to ECI frame.

With the above preparation, we can now go ahead to analyze the Doppler effect experienced by a signal sent by a satellite and received by a moving sensing station. Assume that the velocity of the satellite is $\boldsymbol{v}_s$ in the ECI frame, the velocity of the sensing station is $\boldsymbol{v}_o^{(e)}$ in the ECEF frame, and the position vector of the sensing station is $\boldsymbol{r}_o^{(e)}$ in the ECEF frame. Then, the linear velocity of the sensing station in the ECI frame is given by the formula

$$\boldsymbol{v}_o^{(c)} = \frac{\boldsymbol{R}_{ce}\boldsymbol{v}_o^{(e)} + \boldsymbol{\omega}_{ce}^{(e)} \times \left(\boldsymbol{R}_{ce}\boldsymbol{r}_o^{(e)}\right)}{1 + \beta_{o,1}\beta_{o,2}} \tag{243}$$

where '$\times$' is the cross-product operation between two vectors[15] , $\beta_{o,1} = |\boldsymbol{R}_{ce}\boldsymbol{v}_o^{(e)}|/c$ and $\beta_{o,1} = |\boldsymbol{\omega}_{ce}^{(e)} \times \left(\boldsymbol{R}_{ce}\boldsymbol{r}_o^{(e)}\right)|/c$ account for the effect of special relativity, $\boldsymbol{v}_o^{(c)}$ is a function of time t due to $\boldsymbol{R}_{ce}$'s dependence on time, $\boldsymbol{v}_o^{(e)}$ may also be time-dependent.

In most cases, both Earth's rotating speed and the moving speeds of objects on or near Earth's surface - even aircraft for example - are significantly smaller than the speed of light c. Then, (243) can be closely approximated by [62]

$$\boldsymbol{v}_o^{(c)} = \boldsymbol{R}_{ce}\boldsymbol{v}_o^{(e)} + \boldsymbol{\omega}_{ce}^{(e)} \times \left(\boldsymbol{R}_{ce}\boldsymbol{r}_o^{(e)}\right) \tag{244}$$

However, in some other cases, such as, when the Doppler shift between two satellites

[15] The cross-produce of two 3D vectors $\boldsymbol{a}$ and $\boldsymbol{b}$ can be calculated as $\boldsymbol{a} \times \boldsymbol{b} = \begin{vmatrix} i & j & k \\ a_1 & a_2 & a_3 \\ b_1 & b_2 & b_3 \end{vmatrix}$, or $\boldsymbol{a} \times \boldsymbol{b} = |\boldsymbol{a}||\boldsymbol{b}| \sin(\theta)\boldsymbol{n}$, where θ is the angle between $\boldsymbol{a}$ and $\boldsymbol{b}$ in the plane containing them and $\boldsymbol{n}$ is a unit vector perpendicular to the plane containing $\boldsymbol{a}$ and $\boldsymbol{b}$, with directions of $\boldsymbol{a}$, $\boldsymbol{b}$ and $\boldsymbol{n}$ following the righthand rule.

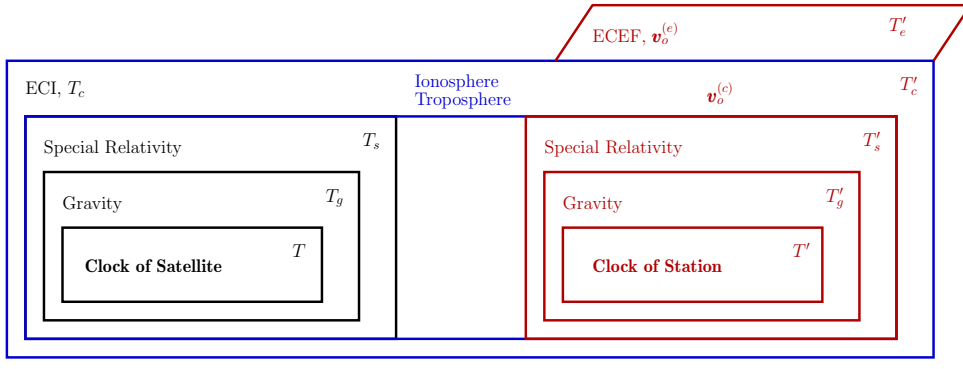

Figure 20: Illustration of reference frames at satellite and sensing station, and physical factors affecting the measurement of Doppler effect at sensing station.

or between a satellite and a flying rocket is estimated, ignoring the effect of the factor $1/(1+\beta_{o,1}\beta_{o,2})$ may result in noticeable errors. Hence, the formula of (243) needs to be used. For simplicity, the analysis below is based on (244).

When only velocity is considered, based on (244), in satellite-aided sensing/navigation of a sensing station, the objective is to derive $\boldsymbol{v}_o^{(e)}$ in the ECEF frame via, firstly, estimating the velocity $\boldsymbol{v}_o^{(c)}$ in the ECI frame, by making use of its relationship with the Doppler shift measured at the sensing station. Once $\boldsymbol{v}_o^{(c)}$ in the ECI frame is obtained, (244) can be inverted to obtain $\boldsymbol{v}_o^{(e)}$ as

$$\boldsymbol{v}_o^{(e)} = \boldsymbol{R}_{ce}^T \left[\boldsymbol{v}_o^{(c)} - \boldsymbol{\omega}_{ce}^{(e)} \times \left(\boldsymbol{R}_{ce}\boldsymbol{r}_o^{(e)}\right)\right] \tag{245}$$

when assuming that $\boldsymbol{r}_o^{(e)}$ is a priori.

Let press the linear velocity of a satellite as $\boldsymbol{v}_s^{(c)}$, which is known when the satellite's orbit is known. Express a unit line vector in parallel with the slant path from the sensing station to the satellite as $\hat{\boldsymbol{r}}_{o\to s}$, which can be assumed to be known when the satellite is fixed at a point on its orbit and the position vector of sensing station is known. Then, it would be desirable that an ideal formula as

$$f_D = -\frac{f(\boldsymbol{v}_s^{(c)} \cdot \hat{\boldsymbol{r}}_{o\to s} - \boldsymbol{v}_o^{(c)} \cdot \hat{\boldsymbol{r}}_{o\to s})}{c} \tag{246}$$

can be used. In practice, however, obtaining a measurement that strictly adheres to (246) is challenging due to several physical and technical limitations. Below the primary factors that interfere with the measured Doppler shift are analyzed.

Fig. 20 shows the reference frames involved with the satellite and sensing station.

As seen, the satellite and sensing station only share the ECI frame. Let us analyze the physical factors on the Dopper effect measured at the sensing station in the ECI frame, one-by-one from the most inner square to the biggest square representing the ECI frame.

First, assume that T is the period of the signal sent by the satellite, which is recorded by a clock carried by the satellite. Correspondingly, assume that T' is the period of the signal received by the sensing station, which is recorded by a clock carried by the sensing station. Since both satellite and sensing station lie in the Earth's gravity field, we can write the concerned Doppler effect as

$$\frac{f'}{f} = \frac{T}{T'} = \frac{T_g}{T'_g} \tag{247}$$

where T_g and T'_g are used to explicitly indicate that the recorded periods are under the effect of Earth's gravity.

Second, corresponding to T_g, assume that T_s is the period measured by a clock in the satellite's frame but free of gravity. Similarly, corresponding to T'_g, assume that T'_s is the period measured by a clock in the sensing station's frame free of gravity. Furthermore, for simplicity, assume that, relative to the center of the Earth, $\boldsymbol{r}^{(s)}$ and $\boldsymbol{r}^{(e)}$ are the position vectors of satellite and sensing station in all reference frames[16]. Hence, $|\boldsymbol{r}^{(s)}|$ and $|\boldsymbol{r}^{(e)}|$ are, respectively, the distances of satellite and sensing station from the Earth's center. Then, according to (189) in Section 0.5.3, relative to the gravity potential Φ_0 at the geoid, we have

$$\frac{f'}{f} = \frac{T_g}{T'_g} = \frac{\sqrt{1+\frac{2(\Phi(|\boldsymbol{r}^{(s)}|)-\Phi_0)}{c^2}}}{\sqrt{1+\frac{2(\Phi(|\boldsymbol{r}^{(e)}|)-\Phi_0)}{c^2}}} \times \left(\frac{T_s}{T'_s}\right) \tag{248}$$

Third, corresponding to T_s, assume that T_c is the period of satellite's transmitted signal measured by a clock in the ECI frame. Accordingly, corresponding to T'_s, assume that T'_c is the period of received signal measured by a clock also in the ECI frame. Since in the ECI frame, the satellite moves at velocity $\boldsymbol{v}_s^{(c)}$ and the sensing

[16]Otherwise, the Lorentz transformation can be applied to transform $\boldsymbol{r}$ in one reference frame to $\boldsymbol{r}'$ in a new reference as $\boldsymbol{r}' = \boldsymbol{r}_\perp + \gamma(\boldsymbol{r}_\parallel - \boldsymbol{v}t)$, where $\boldsymbol{r}_\perp$ and $\boldsymbol{r}_\parallel$ are the parallel and perpendicular components to the velocity vector $\boldsymbol{v}$, and γ is the Lorentz factor.

station moves at velocity $\boldsymbol{v}_o^{(c)}$. Hence, (248) evolves to the ECI frame as

$$\begin{aligned}\frac{f'}{f} =& \frac{\sqrt{1+\frac{2(\Phi(|\boldsymbol{r}^{(s)}|)-\Phi_0)}{c^2}}}{\sqrt{1+\frac{2(\Phi(|\boldsymbol{r}^{(e)}|)-\Phi_0)}{c^2}}} \times \left(\frac{T_s}{T_s'}\right) \\ =& \frac{\sqrt{1+\frac{2(\Phi(|\boldsymbol{r}^{(s)}|)-\Phi_0)}{c^2}}}{\sqrt{1+\frac{2(\Phi(|\boldsymbol{r}^{(e)}|)-\Phi_0)}{c^2}}} \times \frac{\sqrt{1-|\boldsymbol{v}_s^{(c)}|^2/c^2}}{\sqrt{1-|\boldsymbol{v}_o^{(c)}|^2/c^2}} \times \left(\frac{T_c}{T_c'}\right) \end{aligned} \tag{249}$$

Before going further to consider T_c/T_c' in the ECI frame, let us apply some approximation on the final equation in (249). Assume that $2(\Phi(|\boldsymbol{r}^{(e)}|)-\Phi_0)/c^2 << 1$ and $|\boldsymbol{v}_o^{(c)}|^2/c^2 << 1$. Then, (249) can be approximated as

$$\begin{aligned}\frac{f'}{f} \approx& \sqrt{\left(1+\frac{2(\Phi(|\boldsymbol{r}^{(s)}|)-\Phi_0)}{c^2}\right)\left(1-\frac{2(\Phi(|\boldsymbol{r}^{(e)}|)-\Phi_0)}{c^2}\right)} \\ & \times \sqrt{\left(1-\frac{|\boldsymbol{v}_s^{(c)}|^2}{c^2}\right)\left(1+\frac{|\boldsymbol{v}_o^{(c)}|^2}{c^2}\right)} \times \left(\frac{T_c}{T_c'}\right) \\ \approx& \sqrt{1+\frac{2[\Phi(|\boldsymbol{r}^{(s)}|)-\Phi(|\boldsymbol{r}^{(e)}|)]}{c^2}} \times \sqrt{1-\frac{|\boldsymbol{v}_s^{(c)}|^2}{c^2}+\frac{|\boldsymbol{v}_o^{(c)}|^2}{c^2}} \times \left(\frac{T_c}{T_c'}\right) \end{aligned} \tag{250}$$

where from the first to second equation, the $1/c^4$-related terms were ignored. Now, expanding the two square-roots and keeping only the linearly dependent terms, we obtain

$$\begin{aligned}\frac{f'}{f} \approx& \left[1+\frac{\Phi(|\boldsymbol{r}^{(s)}|)-\Phi(|\boldsymbol{r}^{(e)}|)}{c^2}+\frac{|\boldsymbol{v}_o^{(c)}|^2-|\boldsymbol{v}_s^{(c)}|^2}{2c^2}\right] \times \left(\frac{T_c}{T_c'}\right) \\ =& [1+I_G+I_S] \times \left(\frac{T_c}{T_c'}\right) \end{aligned} \tag{251}$$

where, by definition,

$$\begin{aligned} I_G =& \frac{\Phi(|\boldsymbol{r}^{(s)}|)-\Phi(|\boldsymbol{r}^{(e)}|)}{c^2} \\ I_S =& \frac{|\boldsymbol{v}_o^{(c)}|^2-|\boldsymbol{v}_s^{(c)}|^2}{2c^2} \end{aligned} \tag{252}$$

through which the gravity and the special relativity related dynamics generate interference on the measurement of the Dopper effect. As seen in (252), once the orbit of

Table 1: Basic data for GNSS, as well as MEO and LEO systems, where signal delay is one-way delay.

Type	Orbit Altitude	Orbit Speed	Signal Delay
Global Navigation Satellite Systems (GNSS)	20,000 km ∼ 26,000 km	3.4 km/s ∼ 3.9 km/s	60 ms ∼ 90 ms
Medium Earth Orbit (MEO) System	2,000 km ∼ 35,786 km	3 km/s ∼ 7 km/s	65 ms ∼ 140 ms
Low Earth Orbit (LEO) System	160 km ∼ 2,000 km	7.5 km/s ∼ 7.8 km/s	1.5 ms ∼ 7 ms

the satellite and the position of the sensing station are known, both $|\boldsymbol{r}^{(s)}|$ and $|\boldsymbol{r}^{(e)}|$ are known and hence, the effect of I_G can be effectively removed. Similarly, once the orbit of the satellite is known, $|\boldsymbol{v}_s^{(c)}|$ is known, whose interference on the Doppler measurement can also removed. However, $|\boldsymbol{v}_o^{(c)}|$ is the magnitude of the velocity to be measured in ECI frame, it may need to stay for very accurate sensing/navigation. However, when the speed of sensing station in the ECEF frame is small, $|\boldsymbol{v}_o^{(c)}|$ may be approximated by the Earth's rotating speed. In this case, both I_G and I_S are known, forming the systematic errors that can be removed from the measurement of Doppler effect.

Now let us forward to analyze the classic Doppler effect of T_c/T_c' in the ECI frame. While focusing on this, let us leave (251) for the moment. Table 1 lists some basic data for the GNSS as well as MEO and LEO systems.

Since both satellite rotates and sensing station moves circularly in the ECI frame, it seems that this is the case of general moving source and observer analyzed in Section 0.4.1.3. However, even such a general model may not be accurate enough for analyzing the Doppler effect experienced by a signal transmitted between satellite and sensing station. In the model used in Section 0.4.1.3, it was assumed that there is a fixed point that approximately lies on the lines between source and observer, when they transmit/receive the first and second crests of a wave. However, in satellite systems, as seen in Table 1, satellite moves fast, Earth is rotating, and the signal delay from transmitter to receiver is significant. Consequently, as shown in Fig. 21, even without considering the effect of the dynamics of atmosphere, the geometric signal propagation path $\mathcal{G}_1$, i.e., slant path, of the first wave crest may be significantly different from the path $\mathcal{G}_2$ conveying the second wave crest from satellite to sensing station, generating the so-called Sagnac effect [64]. In satellite-based sensing/navigation, the Sagnac effect should be taken into account to improve accuracy.

In the ECI frame, the effect of atmosphere also needs to be addressed, as phys-

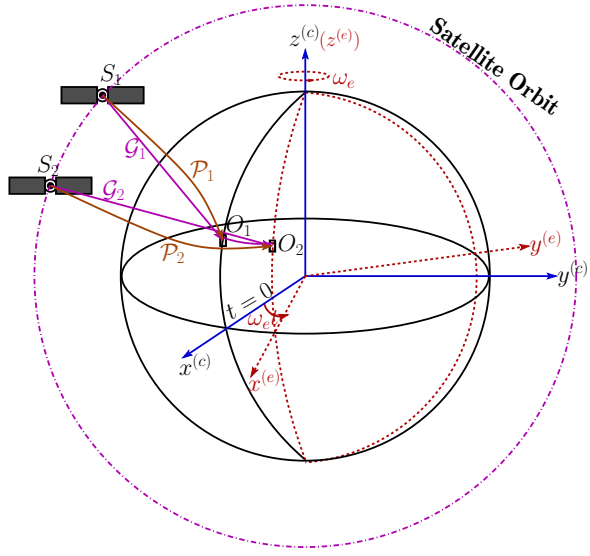

Figure 21: Illustration shows the effect of rotating Earth and circularly moving satellite, where $\mathcal{G}_1$ and $\mathcal{G}_2$ are slant paths and $\mathcal{P}_1$ and $\mathcal{P}_2$ are bended optical (physical propagation) path. The drawings are not to scale, but for conceptual purposes only.

ically, radio signals in atmosphere do not propagate along slant paths, but along the bended optical paths, as shown by $\mathcal{P}_1$ and $\mathcal{P}_2$ in Fig. 21. We have analyzed this issue in Section 0.6. However, the analysis there is on $d(Path)/dt$, considering one-path only. Therefore, to obtain the analytical results of high accuracy, in satellite signal based sensing/navigation, the two paths conveying two adjacent wave crests need to be separately analyzed, to jointly address the Sagnac effect and atmospheric effect. The analysis below abides this requirement.

Assume that satellite sends two adjacent wave crests at $t_1 = t_0$ and $t_2 = t_0 + T_c$. Correspondingly, the position vectors are $\boldsymbol{r}^{(s)}(t_1)$ and $\boldsymbol{r}^{(s)}(t_2)$, and velocities are $\boldsymbol{v}_s^{(c)}(t_1) = \boldsymbol{\omega}_s \times \boldsymbol{r}^{(s)}(t_1)$ and $\boldsymbol{v}_s^{(c)}(t_2) = \boldsymbol{\omega}_s \times \boldsymbol{r}^{(s)}(t_2)$, where $\boldsymbol{\omega}_s$ is satellite's orbital angular velocity. These two crests follow two *physical paths*, $\mathcal{P}_1$ and $\mathcal{P}_2$, to sensing station. Correspondingly, the slant paths (or LoS paths) between sensing station and satellite are $\mathcal{G}_1$ and $\mathcal{G}_2$. For sensing/navigation, t_1 and t_2, and $\boldsymbol{r}^{(s)}(t_1)$ and $\boldsymbol{r}^{(s)}(t_2)$ (hence, $\boldsymbol{v}_s^{(c)}(t_1)$ and $\boldsymbol{v}_s^{(c)}(t_2)$) are assumed a-priori information.

Corresponding to the satellite, at sensing station, assume that the time of receiving the first crest is $t_1' = t_0'$, and the time of receiving the second crest is $t_2' = t_0' + T_c'$. Accordingly, the position vectors are $\boldsymbol{r}_o^{(e)}(t_1')$ and $\boldsymbol{r}_o^{(e)}(t_2')$. The corresponding velocities of sensing station are $\boldsymbol{v}_o^{(c)}(t_1')$ and $\boldsymbol{v}_o^{(c)}(t_2)$, whose relations with the Earth's

rotational velocity $\boldsymbol{\omega}_{ce}^{(e)}$ and the sensing station's velocity $\boldsymbol{v}_o^{(e)}$ are given in (244).

Based on the above settings, the following relationships can be built:

$$t_1' = t_0 + \frac{1}{c}\int_{\mathcal{P}_1} n(p,t)dp \tag{253a}$$

$$t_2' = t_0 + T_c + \frac{1}{c}\int_{\mathcal{P}_2} n(p,t)dp \tag{253b}$$

where $n(p,t)$ is the refraction index of atmosphere along an integration path, and t is explicitly used to indicate the time-varying nature of refraction index in atmosphere. In general, $n(p,t) = n(p,t_0)$ can be assumed over a short interval of such as T_c. Hence, the period of received signal in the ECI frame is

$$\begin{aligned} T_c' = t_2' - t_1' =& T_c + \frac{1}{c}\int_{\mathcal{P}_2} n(p,t)dp - \frac{1}{c}\int_{\mathcal{P}_1} n(p,t)dp \\ =& T_c\left(1 + \frac{1}{cT_c}\left[\int_{\mathcal{P}_2} n(p,t)dp - \int_{\mathcal{P}_1} n(p,t)dp\right]\right) \end{aligned} \tag{254}$$

giving

$$\frac{T_c}{T_c'} = \left(1 + \frac{1}{cT_c}\left[\int_{\mathcal{P}_2} n(p,t)dp - \int_{\mathcal{P}_1} n(p,t)dp\right]\right)^{-1} \tag{255}$$

Let us introduce the slant paths $\mathcal{G}_1$ and $\mathcal{G}_2$ to the above formula. Then, (255) can be modified to the form of

$$\begin{aligned} \frac{T_c}{T_c'} =& \left(1 + \frac{1}{cT_c}\left[\int_{\mathcal{G}_2} dp - \int_{\mathcal{G}_1} dp\right] + \frac{1}{cT_c}\left[\int_{\mathcal{P}_2} n(p,t)dp - \int_{\mathcal{G}_2} dp\right]\right. \\ & \left. - \frac{1}{cT_c}\left[\int_{\mathcal{P}_1} n(p,t)dp - \int_{\mathcal{G}_1} dp\right]\right)^{-1} \\ =& \left(1 + \frac{d_2 - d_1}{cT_c}\right. \\ & \left. + \frac{1}{cT_c}\left[\left(\int_{\mathcal{P}_2} n(p,t)dp - \int_{\mathcal{G}_2} dp\right) - \left(\int_{\mathcal{P}_1} n(p,t)dp - \int_{\mathcal{G}_1} dp\right)\right]\right)^{-1} \\ =& \left(1 + \frac{d_2 - d_1}{cT_c} - I_{Atmo}\right)^{-1} \\ \approx& 1 - \frac{d_2 - d_1}{cT_c} + I_{Atmo} \end{aligned} \tag{256}$$

where d_1 and d_2 are the distances of the first and second slant paths. Hence, $(d_2 - d_1)/T_c$ is the average relative speed between satellite and sensing station dur-

ing t_0 (satellite starts transmission) and t_2' (sensing station receives the second crest). In (256),

$$I_{Atmo} = -\frac{1}{cT_c}\left[\left(\int_{\mathcal{P}_2} n(p,t)dp - \int_{\mathcal{G}_2} dp\right) - \left(\int_{\mathcal{P}_1} n(p,t)dp - \int_{\mathcal{G}_1} dp\right)\right] \quad (257)$$

is the interference generated by the atmosphere, including both the ionosphere and troposphere, as analyzed in Sections 0.6.1 and 0.6.1, respectively. The last approximation in (256) is obtained by neglecting the $1/c^2$-related terms.

Now, we substitute (256) back into (251), obtaining

$$\begin{aligned}\frac{f'}{f} =& (1 + I_G + I_S) \times \left(1 - \frac{d_2 - d_1}{cT_c} + I_{Atmo}\right) \\ \approx& 1 - \frac{d_2 - d_1}{cT_c} + I_G + I_S + I_{Atmo}\end{aligned} \quad (258)$$

where the approximation is due to the ignorance of the second-order terms. Finally, from (258) the Doppler shift measured by the sensing station in the ECI frame can be obtained, which is

$$f_D = -\frac{f(d_2 - d_1)}{cT_c} + I_G' + I_S' + I_{Atmo}' \quad (259)$$

where $I_G' = fI_G$, $I_S' = fI_S$ and $I_{Atmo}' = fI_{Atmo}$.

Remark 7. *So far, all the approximations imposed in the Doppler effect analysis are very accurate for the satellite sensing/navigation applications considered. This can be convinced, as the approximation in* (251) *is ignoring the* $1/c^4$*-related terms, that in* (256) *is ignoring the* $1/c^2$*-related terms and that in* (258) *is ignoring the second-order terms, which are proportional to* $1/c^2$ *at least.*

Associated with (251), we have analyzed that the interference of I_G (and hence I_G') can be near-ideally removed, the interference of I_S (and hence I_S') can be near-fully removed for most applications where the receiver's local velocity $\boldsymbol{v}_o^{(e)}$ is well-characterized or negligible compared to the tangential rotational velocity of the Earth. The interference by atmosphere is more complicated, which includes both the predictable component, generating systematic error, and the random component, generating spread Doppler spectrum and random error. Hence, to attain more accurate sensing/navigation, the predictable component should be mitigated to the minimum level. Below we analyze the interference by atmosphere.

Let express

$$I_{Atmo}' = I_I' + I_T' \quad (260)$$

where I'_T and I'_I are respectively the contributions from the troposphere and ionosphere, which, based on (257), are expressed as

$$I'_T = -\frac{f}{cT_c}\left[\left(\int_{\mathcal{P}_{2,T}} n(p,t)dp - \int_{\mathcal{G}_{2,T}} dp\right) - \left(\int_{\mathcal{P}_{1,T}} n(p,t)dp - \int_{\mathcal{G}_{1,T}} dp\right)\right] \tag{261a}$$

$$I'_I = -\frac{f}{cT_c}\left[\left(\int_{\mathcal{P}_{2,I}} n(p,t)dp - \int_{\mathcal{G}_{2,I}} dp\right) - \left(\int_{\mathcal{P}_{1,I}} n(p,t)dp - \int_{\mathcal{G}_{1,I}} dp\right)\right] \tag{261b}$$

where $\mathcal{P}_{2,T}$, $\mathcal{P}_{1,T}$, $\mathcal{G}_{2,T}$, $\mathcal{G}_{1,T}$ are the portions of paths in the troposphere, while $\mathcal{P}_{2,I}$, $\mathcal{P}_{1,I}$, $\mathcal{G}_{2,I}$, $\mathcal{G}_{1,I}$ are the corresponding potions of paths in the ionosphere.

In (261a), I'_T is the Doppler effect by the medium in the troposphere. When assuming that the troposphere is sufficiently stable during the passing interval of satellite, following the analysis in Section 0.6.2, I'_T can be approximated as

$$\bar{I}'_T \approx -\frac{f}{c}\frac{d}{dt}\int_{\mathcal{G}_T}(n(p,t)-1)dp \tag{262}$$

which, accordingly, has the expression of (217). Then, with the modeling of $N(r)$ and information about the satellite, $\bar{I}'_T$ in (262) can be evaluated, as detailed in Section 0.6.2. Consequently, the interference I'_T can be cancelled, leaving the randomly distributed residue expressed as

$$\Delta I'_T = I'_T - \bar{I}'_T \tag{263}$$

In the context of the interference I'_I in (261b) by the ionosphere, using the fact that signal from satellite to sensing station is not much bended by the ionosphere, $\mathcal{P}_{2,I} = \mathcal{G}_{2,I}$ and $\mathcal{P}_{1,I} = \mathcal{G}_{1,I}$ can be assumed. Hence, (261b) can be re-written as

$$\bar{I}'_I = -\frac{f}{cT_c}\left[\int_{\mathcal{G}_{2,I}}(n(p,t)-1)dp - \int_{\mathcal{G}_{1,I}}(n(p,t)-1)dp\right] \tag{264}$$

As analyzed in Section 0.6.1, the refractive index $n(p,t)$ is primarily determined by the local electron density and distribution, and is frequency dependent. Specifically, in satellite-based systems, the refractive index can be closely approximated as that in (199). Let in (199) $X = f_N^2/f^2$, where f_N is the plasma frequency. Then, with the

aid of the series approximation, $n(p,t)$ can be expressed as

$$n(p,t) \approx \sqrt{1-\frac{f_N^2}{f^2}} = 1 - \frac{f_N^2}{2f^2} + \mathcal{O}\left(\frac{1}{f^4}\right) \tag{265}$$

Applying it into (264) gives

$$\bar{I}_I' = \frac{1}{c}\left[\frac{\alpha_2}{f} - \frac{\alpha_1}{f} + \mathcal{O}\left(\frac{1}{f^3}\right)\right] \tag{266}$$

where $\alpha_i = 0.5T_c^{-1} f_N^2 \int_{\mathcal{G}_{i,I}} dp$ for $i = 1$ and 2.

Based on (266), a dual-frequency method [50] can be introduced to mitigate the first-order effect from the ionosphere. In detail, using (266), (259) can be re-written as

$$\begin{aligned} f_D =& f_D' + \bar{I}_I' \\ =& f_D' + \frac{1}{c}\left[\frac{\alpha_2}{f} - \frac{\alpha_1}{f} + \mathcal{O}\left(\frac{1}{f^3}\right)\right] \end{aligned} \tag{267}$$

where f_D' contains the Doppler shift by all other factors, except that by the ionosphere. Then, assume that two signals with frequencies of f_1 and f_2 are simultaneously transmitted by satellite. Correspondingly, the sensing station measures the Doppler shifts of

$$\begin{aligned} f_{D,f_1} =& f_{D,f_1}' + \frac{1}{c}\left[\frac{\alpha_2}{f_1} - \frac{\alpha_1}{f_1} + \mathcal{O}\left(\frac{1}{f_1^3}\right)\right] \\ f_{D,f_2} =& f_{D,f_2}' + \frac{1}{c}\left[\frac{\alpha_2}{f_2} - \frac{\alpha_1}{f_2} + \mathcal{O}\left(\frac{1}{f_2^3}\right)\right] \end{aligned} \tag{268}$$

where f_{D,f_2} and f_{D,f_2}' mean that they are frequency-dependent. Then, the sensing station calculates

$$f_2 f_{D,f_2} - f_1 f_{D,f_1} = (f_2 f_{D,f_2}' - f_1 f_{D,f_1}') + \mathcal{O}\left(\frac{1}{f_{1,2}^2}\right) \tag{269}$$

showing that the first-order interference by the ionosphere is ideally cancelled, and the motion information of the sensing station is embedded in $(f_2 f_{D,f_2}' - f_1 f_{D,f_1}')$. Hence, if the other interferences have been cancelled before the operation in (269), the velocity of the sensing station in ECI frame can be directly derived from $f_2 f_{D,f_2} - f_1 f_{D,f_1}$ by treating the remaining $\mathcal{O}\left(1/f_{1,2}^2\right)$ and the other possible residues as random interference.

To this point, let us assume that the systematic errors contributed by gravity, spe-

cial relativity, troposphere and ionosphere are all corrected, leaving only the random errors. Then, (259) can be modified to

$$f_D = -\frac{f(d_2 - d_1)}{cT_c} + \varepsilon \tag{270}$$

where ε accounts for the above-mentioned random errors, and f_D is kept using for simplicity. By making use of (246) but replacing the involved velocities by their averaging ones, it becomes

$$\bar{f}_D = -\frac{f(\bar{\boldsymbol{v}}_s^{(c)} \cdot \hat{\boldsymbol{r}}_{o\to s} - \bar{\boldsymbol{v}}_o^{(c)} \cdot \hat{\boldsymbol{r}}_{o\to s})}{c} \tag{271}$$

Based on this formula, once $\bar{f}_D$ is known, and since $\bar{\boldsymbol{v}}_s^{(c)}$ and $\hat{\boldsymbol{r}}_{o\to s}$ can be assumed the a-priori, there is only one variable $\bar{\boldsymbol{v}}_o^{(c)}$ of the average velocity of the sensing station in the ECI frame. Using (271) to modify (270), yielding

$$\begin{aligned} f_D =& \bar{f}_D - \left(\bar{f}_D + \frac{f(d_2 - d_1)}{cT_c}\right) + \varepsilon \\ =& \bar{f}_D + I_{Sag} + \varepsilon \end{aligned} \tag{272}$$

where $I_{Sag} = -\left(\bar{f}_D + f(d_2 - d_1)/cT_c\right)$ accounts for the change in the geometry during the signal's transmission time. In the ECI frame, this is the manifestation of the Sagnac effect [64], representing the fact that the receiver moves while the signal is in flight. This can be precisely estimated using the known Earth rotation $\boldsymbol{\omega}_{ce}^{(e)}$ and the satellite ephemeris [65].

Finally, it is worth noting that while the primary factors contributing to Doppler shift errors along the slant path have been addressed, further improvements in sensing/navigation accuracy may require the consideration of higher-order effects and subtle relativistic corrections, such as those detailed in [44].

0.8 Doppler Effect of Acoustic Waves

In the previous sections, although EM-waves were mainly assumed, the analyses having considered the effect of medium, including Sections 0.3.3 and 0.4.2, can be applied for the acoustic wave scenarios, directly or after slight modification by, such as, neglecting the relativistic effect. Hence, this section emphasizes the difference of the Doppler effect with acoustic waves from that of the Doppler effect with EM-waves.

To carry out the analysis, the following definitions are used:

- $\hat{\boldsymbol{r}}_{s\to o}$: Unit vector in parallel with the line connecting source and observer and

pointing in the direction from source to observer.

- $\boldsymbol{v}_s$: Velocity of moving source. Hence, the moving velocity of source in the direction of $\hat{\boldsymbol{r}}_{s\to o}$ is $v_s = \boldsymbol{v}_s \cdot \hat{\boldsymbol{r}}_{s\to o}$.
- $\boldsymbol{v}'_m$: Velocity of moving medium. Hence, the moving velocity of medium in the direction of $\hat{\boldsymbol{r}}_{s\to o}$ is $v'_m = \boldsymbol{v}'_m \cdot \hat{\boldsymbol{r}}_{s\to o}$.
- $\boldsymbol{v}_o$: Velocity of moving observer. Hence, the moving velocity of observer in the direction of $\hat{\boldsymbol{r}}_{s\to o}$ is $v_o = \boldsymbol{v}_o \cdot \hat{\boldsymbol{r}}_{s\to o}$.
- v: Speed of acoustic wave in stationary medium. Hence, the wave propagation speed in the direction of $\hat{\boldsymbol{r}}_{s\to o}$ is $v_w = v + v'_m$.
- $f,\ T,\ \lambda$: Frequency, period and wavelength of source acoustic wave.
- $f',\ T',\ \lambda'$: Frequency, period and wavelength of observed acoustic wave.

Based on the above definitions, the analysis below can simply assume motions along the line connecting source and observer. In the other cases, corresponding formulas can be obtained by replacing v_s, v_o, v_w accordingly using the above definitions.

Assume that source emits two adjacent crests at time $t_1 = t_0$ and $t_2 = t_0 + T$. Accordingly, the time instants of receiving these two crests are $t'_1 = t'_0$ and $t'_2 = t'_0 + T'$. Based on the above definitions, the relation of

$$T' = T + \frac{-v_s T}{v_w} + \frac{v_o T'}{v_w} \tag{273}$$

holds, which gives

$$f' = f\left(\frac{v_w - v_o}{v_w - v_s}\right) \tag{274}$$

If $v_o = 0$ and source is moving with speed v_s, there is

$$f_w = \frac{f}{1 - v_s/v_w} \tag{275}$$

which is the frequency of the acoustic wave in medium. Correspondingly, using the formula $v_w = f_w \lambda_w$, the wavelength of the acoustic wave in medium is

$$\lambda_w = \frac{v_w - v_s}{f} \tag{276}$$

The following analysis focuses on specific situations that differentiate acoustic waves from EM-waves. In relativistic scenarios, no object with mass can travel faster

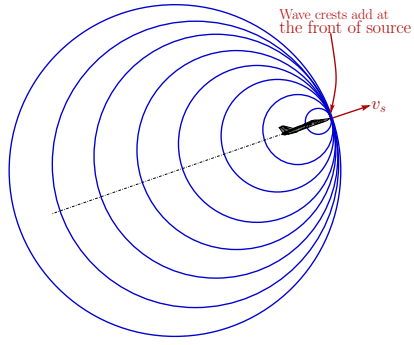

Figure 22: When the velocity of source is close to the propagation speed of acoustic signals, wave crests add in the front of source, forming sound barrier.

than c of the speed of light in a vacuum. In stark contrast, acoustic waves propagate with a much lower, medium-dependent speed. Consequently, the wave source, observer, and even the medium itself may move at a speed higher than the acoustic wave's propagation speed, leading to phenomena like shock waves (e.g., sonic booms), as analyzed below.

First, when a medium moves at a supersonic velocity relative to its stationary propagation speed, i.e., $|v'_m| \geq v$, acoustic signals become unable to propagate against the flow. In such cases, all sound energy is swept downstream, as the medium's speed exceeds the wave's ability to travel upstream. However, it is worth noting that v_w will never be negative. Mathematically, the actual propagation speed v_w in/against the direction of the flow is more accurately represented as $v_w = \max\{0, v + v'_m\}$.

Second, when a stationary source emits signals and an observer moves away at a speed $v_o \geq v_w$, the observer will never receive the acoustic signals according to (274). Mathematically, $v_o > v_w$ results in an observed frequency $f' < 0$, which is physically meaningless for a traveling wave. Thus, (274) is subject to the physical constraint of $v_o \leq v_w$.

Third, according to (274), as $v_s \to v_w$, $f' \to \infty$ and hence $\lambda' \to 0$ due to $f'\lambda' = (v_m - v_s)$. This physically means that all emitted waves by source are constructively added at the head of the source, as shown in Fig. 22. The "bunching up" of wave crests creates the extremely compressed medium in the front of the source. By Newton's third law, the medium will generate an equal force (referred to as drag force) on the source. This phenomenon is known as the "sound barrier". In the case of $v_s \to v_w$, an observer in front of the source hears nothing until the source arrives, at which point the observer experiences a near-instantaneous pressure discontinuity (like a thump), known as a "shock wave".

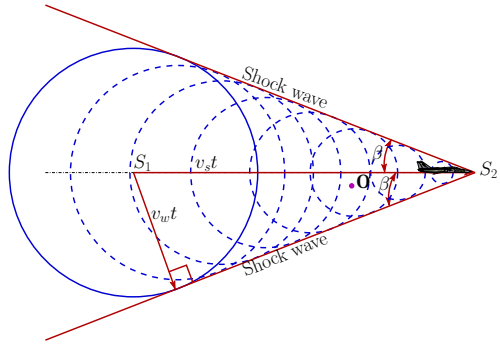

Figure 23: When the velocity of source is larger than the propagation speed of acoustic signals, source's sound generates a shock wave cone.

Fourht, in the supersonic regime of $v_s > v_w$, the formula of (274) no longer describes the Doppler effect in front of the source, as the denominator of (274) becomes negative. In this regime, the source "outruns" its own emitted waves, leading to the formation of a so-called Mach-cone, as shown in Fig. 23. On the surface of the Mach-cone, wave crests are constructively added, forming shock waves. As this cone passes a stationary observer, it experiences a *sonic boom*. After the sonic boom and when the observer enters inside the Mach-cone, it measures a sudden frequency dropping and finally a minimum frequency of $f' = f v_w/(v_w + |v_s|)$, when the observer reaches the rotational symmetric axis of the Mach-cone.

According to the geometry illustrated in Fig. 23,

$$\sin\beta = \frac{v_w}{v_s} \tag{277}$$

Hence, $(\sin\beta)^{-1}$ is equal to the *Mach number* that is defined as $M = v_s/v_w$.

Finally, in the supersonic regime of $v_s > v_w$, as seen in Fig. 23, for the signals that the source emits before its passing of the observer, the observer receives these signals reversely, i.e., the signals emitted later are received earlier than the signals emitted earlier. Analogously, if the source counts '1, 2, 3, ..., 10' before passing the observer, the observer, once inside the Mach cone, will hear '10, 9, 8,..., 1' with each individual number also played in reverse. For the signals that the source emits after its passing of the observer, these signals are received in the normal order with a time-varying frequency f', until it converges to the frequency $f' = f v_w/(v_w + |v_s|)$, when the observer arrives at the rotational symmetric axis of the Mach-cone. Furthermore, the signals emitted by the source before and after its passing of the observer interfere with each other at the observer.

0.9 Concluding Remarks

The analyses of the Doppler effect in previous sections assumed a single, pure sinusoidal frequency. However, real-world wireless systems are operated under specific bandwidth constraints. In particular, signals in narrowband, wideband, and ultra-wideband wireless systems are distributed over a frequency range. Because the Doppler shift is proportional to the operating frequency, different frequency components of a transmitted signal experience distinct frequency shifts. This results in a frequency-varying Doppler effect where the received signal exhibits a Doppler spectrum rather than a single frequency offset, introducing complex distortions, such as, inter-carrier interference in multi-carrier signaling systems.

While Section 0.6 analyzed the Doppler effect in the atmosphere, it focused on time-varying propagation paths rather than the direct Doppler shifts from random atmospheric events, including the fluctuation of air temperature, pressure and humidity in the troposphere, and the variation of electron density in the ionosphere due to the various environment changes. Instead, only the Doppler effect by the time-varying propagation paths was addressed. In addition to the random events in the atmosphere, in practical wireless systems, there are many other physical phenomena, including refraction, reflection, diffraction, scattering by various types of environmental objects, which result in multiple propagation paths from transmitter to receiver. In these systems, different propagation paths may be associated with different Doppler shifts, resulting in Doppler spread. Therefore, even when a single-tone signal is transmitted, the received signal may contain many frequency components around the emitted frequency, forming a Doppler spectrum.

In wireless sensing and communications systems, Doppler spread presents significant design challenges but can also be exploited to improve performance. In wireless communications, Doppler spread results in time-selective fading channels, which can be exploited via appropriate design of signalling and channel coding [59, 66–68], to attain the time-domain diversity gain and, hence, improve systems' performance. On the other hand, in wireless sensing, if the knowledge about the Doppler effect, such as its first-, second-order statistics, is available, this knowledge can be exploited to improve the accuracy of sensing. This constitutes an important research issue, in particular, in the regime of integrated sensing and communications (ISAC), whereas most existing research works assume the Doppler effect without spread [69–72].

Bibliography

[1] T. S. Rappaport, *Wireless Communications Principles and Practice*. New York: Prentice Hall, Inc, 2 ed., 2002.

[2] J. D. Parsons, *The Mobile Radio Propagation Channel*. John Wiley & Sons LtD., 2 ed., 2001.

[3] R. Steele and L. Hanzo, *Mobile Radio Communications*. London: IEEE Press, and John Wiley & Sons, 2nd ed., 1999.

[4] G. L. Stuber, *Principles of Mobile Communication*. Kluwer Academic Publishers, 2 ed., 2000.

[5] A. Goldsmith, *Wireless Communications*. Cambridge University Press, 2005.

[6] J. G. Proakis, *Digital Communications*. McGraw Hill, 5 ed., 2007.

[7] H. L. Bertoni, *Radio Propagation for Modern Wireless Systems*. Prentice Hall PTR, 2000.

[8] A. F. Molisch, *Relaying, MultiHop, and Cooperative Communications*, pp. 521–563. 2011.

[9] W. C. Y. Lee, *Mobile Communications Engineering*. New York: McGraw-Hill, 2nd ed., 1998.

[10] Y. Xiao and et al, "Space-air-ground integrated wireless networks for 6G: Basics, key technologies, and future trends," *IEEE Journal on Selected Areas in Communications*, vol. 42, no. 12, pp. 3327–3354, 2024.

[11] J. Liu and et al, "Space-air-ground integrated network: A survey," *IEEE Communications Surveys & Tutorials*, vol. 20, no. 4, pp. 2714–2741, 2018.

[12] T. Hong and et al, "Space-air-ground IoT network and related key technologies," *IEEE Wireless Communications*, vol. 27, no. 2, pp. 96–104, 2020.

[13] L. Fleischmann, "A graphic method for the Doppler effect," *American Journal of Physics*, vol. 13, pp. 418–419, 12 1945.

[14] V. Slusarenko and C. H. Wörner, "Graphical representation of the classical Doppler effect," *The Physics Teacher*, vol. 27, pp. 171–172, 03 1989.

[15] R. Rojas and G. Fuster, "Graphical representation of the Doppler shift: Classical and relativistic," *The Physics Teacher*, vol. 45, pp. 306–309, 05 2007.

[16] C. H. Worner and R. Rojas, "Classical doppler effect in some accelerated systems," *The Physics Teacher*, vol. 59, pp. 239–242, 04 2021.

[17] C. H. Wörner and R. Rojas, "An elementary approach to the gravitational Doppler shift," *European Journal of Physics*, vol. 38, p. 015604, nov 2016.

[18] A. Einstein, *Relativity: The Special & The General Theory - 100th Anniversary Edition (Translation: Robert W. Lawson)*. BN Publishing, 2010.

[19] H. D. Young and R. A. Freedman, *University Physics with Modern Physics*. Essex, UK: Pearson, 15 ed., 2019.

[20] K. Krane, *Modern Physics*. Hoboken, USA: John Wiley & Sons, 3 ed., 2012.

[21] F. Zanchini, "A general derivation of the classical Doppler effect in 3D space," *European Journal of Physics*, vol. 45, p. 025003, feb 2024.

[22] F. Zanchini and E. Zanchini, "A simple derivation of the relativistic Doppler effect in accelerated systems," *European Journal of Physics*, vol. 46, p. 035601, mar 2025.

[23] E. Zanchini, "Correct interpretation of two experiments on the transverse Doppler shift," *Physica Scripta*, vol. 86, p. 015004, jun 2012.

[24] X.-L. Chen, L. An, X.-B. Huang, C.-B. Yu, and L. Xu, "Comment on 'correct interpretation of two experiments on the transverse Doppler shift'," *Physica Scripta*, vol. 89, p. 067004, apr 2014.

[25] A. L. Kholmetskii, T. Yarman, O. Yarman, and M. Arik, "Analyses of Mossbauer experiments in a rotating system: Proper and improper approaches," *Annals of Physics*, vol. 418, p. 168191, 2020.

[26] R. A. Bachman, "Generalized relativistic Doppler effect," *American Journal of Physics*, vol. 54, pp. 717–719, 08 1986.

[27] R. Ferraro, *Einstein's Space-Time: An Introduction to Special and General Relativity*. New York, USA: Springer, 2007.

[28] M. Sands, R. Feynman, and R. Leighton, *The Feynman Lectures on Physics, Vol. II*. New York City, USA: Basic Books, new millennium ed. ed., 2011.

[29] S. Quattrini, "Longitudinal doppler for observers in uniform acceleration," *Qeios*, 2024.

[30] C. Semay, "Observer with a constant proper acceleration," *European Journal of Physics*, vol. 27, p. 1157, July 2006.

[31] D. Koks, "Does a clock's acceleration affect its timing rate?," *Physics FAQ*, 1998,2015.

[32] C. G. Bohmer, *Introduction to General Relativity and Cosmology*. Singapore: World Scientific Publishing Europe Ltd, 2017.

[33] J. Brandes, J. Czerniawski, and L. Neidhard, *Special and General Relativity for Physicists and Philosophers*. Carlsbad, Germany: VRI, 2023.

[34] W. Kündig, "Measurement of the transverse doppler effect in an accelerated system," *Phys. Rev.*, vol. 129, pp. 2371–2375, Mar 1963.

[35] A. L. Kholmetskii, T. Yarman, and O. V. Missevitch, "Kündig's experiment on the transverse Doppler shift re-analyzed," *Physica Scripta*, vol. 77, p. 035302, feb 2008.

[36] E. Caianiello, "Maximal acceleration as a consequence of heisenberg's uncertainty relations.," *Lettere Al Nuovo Cimento*, vol. 41, pp. 370–372, November 1984.

[37] Y. Friedman, "The maximal acceleration, extended relativistic dynamics and Doppler type shift for an accelerated source," *Annalen der Physik*, vol. 523, p. 408–416, Mar. 2011.

[38] W. Potzel, "Clock hypothesis of relativity theory, maximal acceleration, and mossbauer spectroscopy," *Hyperfine Interactions*, vol. 237, no. 1, 2016.

[39] A. L. Kholmetskii, T. Yarman, O. V. Missevitch, and B. I. Rogozev, "A mossbauer experiment in a rotating system on the second-order doppler shift: confirmation of the corrected result by kündig," *Physica Scripta*, vol. 79, p. 065007, may 2009.

[40] A. Kholmetskii, T. Yarman, and O. Missevitch, "Mossbauer experiments in a rotating system on the time dilation effect," *International Journal of Physical Sciences*, vol. 6, no. 1, pp. 84–92, 2011.

[41] A. L. Kholmetskii, T. Yarman, M. Arik, and O. Missevitch, "Novel mossbauer experiment in a rotating system: Extra energy shift confirmed," *AIP Conference Proceedings*, vol. 1648, p. 510011, 03 2015.

[42] T. Yarman, A. L. Kholmetskii, M. Arik, B. Akkuş, Y. Öktem, L. A. Susam, and O. V. Missevitch, "Novel Mossbauer experiment in a rotating system and the extra-energy shift between emission and absorption lines," *Canadian Journal of Physics*, vol. 94, pp. 780–789, Aug 2016.

[43] S. M. Carroll, *Spacetime and Geometry: An Introduction to General Relativity*. Cambridge, UK: Cambridge University Press, 2019.

[44] N. Ashby, "Relativity in the global positioning system," *Living Reviews in Relativity*, vol. 6, no. 1, p. 1, 2003.

[45] C. Zhang, Q. Li, C. Xu, L.-L. Yang, and L. Hanzo, "Space-air-ground integrated networks: Their channel model and performance analysis," *IEEE Open Journal of Vehicular Technology*, vol. 6, pp. 1501–1523, 2025.

[46] K. G. Budden, *The Propagation of Radio Waves: The Theory of Radio Waves of Low Power in the Ionosphere and Magnetosphere*. Cambridge University Press, 1988.

[47] U. Sezen, F. Arikan, and O. Arikan, "NVIS HF signal propagation in ionosphere using calculus of variations," *Geodesy and Geodynamics*, vol. 10, no. 1, pp. 72–76, 2019.

[48] C. Scotto and A. Settimi, "The calculation of ionospheric absorption with modern computers," *Advances in Space Research*, vol. 54, no. 8, pp. 1642–1650, 2014.

[49] L. J. Nickisch, M. A. Hausman, and S. V. Fridman, "Range rate-Doppler correlation for HF propagation in traveling ionospheric disturbance environments," *Radio Science*, vol. 41, no. 5, 2006.

[50] W. H. Guier and G. C. Weiffenbach, "A satellite Doppler navigation system," *Proceedings of the IRE*, vol. 48, no. 4, pp. 507–516, 1960.

[51] B. R. Bean and G. D. Thayer, "Models of the atmospheric radio refractive index," *Proceedings of the IRE*, vol. 47, no. 5, pp. 740–755, 1959.

[52] S. Chapman, "The absorption and dissociative or ionizing effect of monochromatic radiation in an atmosphere on a rotating earth," *Proceedings of the Physical Society*, vol. 43, p. 26, jan 1931.

[53] S. Chapman, "The absorption and dissociative or ionizing effect of monochromatic radiation in an atmosphere on a rotating earth part ii. grazing incidence," *Proceedings of the Physical Society*, vol. 43, p. 483, sep 1931.

[54] J. K. Hargreaves, *The Solar-Terrestrial Environment: An Introduction to Geospace - the Science of the Terrestrial Upper Atmosphere, Ionosphere, and Magnetosphere*. Cambridge Atmospheric and Space Science Series, Cambridge University Press, 1992.

[55] X. Huo, Y. Long, H. Liu, and et al., "A novel ionospheric tec mapping function with azimuth parameters and its application to the chinese region," *Journal of Geodesy*, vol. 98, no. 13, 2024.

[56] H. S. Hopfield, "The effect of tropospheric refraction on the Doppler shift of a satellite signal," *Journal of Geophysical Research (1896-1977)*, vol. 68, no. 18, pp. 5157–5168, 1963.

[57] E. K. Smith and S. Weintraub, "The constants in the equation for atmospheric refractive index at radio frequencies," *Proceedings of the IRE*, vol. 41, no. 8, pp. 1035–1037, 1953.

[58] H. S. Hopfield, "Two-quartic tropospheric refractivity profile for correcting satellite data," *Journal of Geophysical Research (1896-1977)*, vol. 74, no. 18, pp. 4487–4499, 1969.

[59] L.-L. Yang, J. Shi, K.-T. Feng, L.-H. Shen, S.-H. Wu, and T.-S. Lee, *Resource Optimization in Wireless Communications: Fundamentals, Algorithms and Applications*. London, United Kingdom: Academic Press, 2025.

[60] K. Wu, J. Pegoraro, and et al, "Sensing in bistatic ISAC systems with clock asynchronism: A signal processing perspective," *IEEE Signal Processing Magazine*, vol. 41, no. 5, pp. 31–43, 2024.

[61] C. Sturm and W. Wiesbeck, "Waveform design and signal processing aspects for fusion of wireless communications and radar sensing," *Proceedings of the IEEE*, vol. 99, no. 7, pp. 1236–1259, 2011.

[62] A. Noureldin, T. B. Karamat, and J. Georgy, *Fundamentals of Inertial Navigation, Satellite-based Positioning and their Integration*. Berlin, Germany: Springer Berlin, Heidelberg, 2013.

[63] M. S. Grewal, L. R. Weill, and A. P. Andrews, *Global Positioning Systems, Inertial Navigation, and Integration*. Hoboken, New Jersey: John Wiley & Sons, 2nd ed., 2007.

[64] N. Ashby, *The Sagnac Effect in the Global Positioning System*, pp. 11–28. Dordrecht: Springer Netherlands, 2004.

[65] W. Hu and J. A. Farrell, "Derivation of the Sagnac (Earth-rotation) correction and analysis of its accuracy for GNSS applications," *Journal of Geodesy*, vol. 98, Nov 2024. Open Access.

[66] L.-L. Yang, *Multicarrier Communications*. Chichester, United Kingdom: John Wiley, 2009.

[67] M. K. Simon and M.-S. Alouini, *Digital Communication over Fading Channels*. New York: John Wiley & Sons, 2 ed., 2005.

[68] W. E. Ryan and S. Lin, *Channel Codes: Classical and Modern*. New York: Cambridge University Press, 2009.

[69] K. Meng and et al, "Cooperative ISAC networks: Opportunities and challenges," *IEEE Wireless Communications*, vol. 32, no. 3, pp. 212–219, 2025.

[70] A. Liu and et al, "A survey on fundamental limits of integrated sensing and communication," *IEEE Communications Surveys & Tutorials*, vol. 24, no. 2, pp. 994–1034, 2022.

[71] J. A. Zhang and et al, "Enabling joint communication and radar sensing in mobile networks-a survey," *IEEE Communications Surveys & Tutorials*, vol. 24, no. 1, pp. 306–345, 2022.

[72] W. Zhou and et al, "Integrated sensing and communication waveform design: A survey," *IEEE Open Journal of the Communications Society*, vol. 3, pp. 1930–1949, 2022.